Mononuclear and Multinuclear Palladacycles as Catalyst Precursors

by

Andrew John Swarts

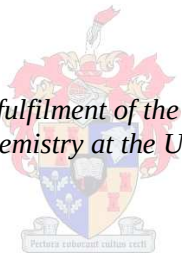

Thesis presented in partial fulfilment of the requirements for the degree Master of Science in Chemistry at the University of Stellenbosch

Supervisor: Prof. Selwyn Frank Mapolie
Faculty of Science
Department of Chemistry and Polymer Science

March 2011

DECLARATION

By submitting this thesis/dissertation electronically, I declare that the entirety of the work contained therein is my own, original work, that I am the sole author thereof (save to the extent explicitly otherwise stated), that reproduction and publication thereof by Stellenbosch University will not infringe any third party rights and that I have not previously in its entirety or in part submitted it for obtaining any qualification.

March 2011

Copyright © 2011 University of Stellenbosch

All rights reserved

DEDICATION

This Master's Dissertation is dedicated to the loving memory of a dear friend and brother, Lyle Williams. Your legacy remains a source of inspiration and joy to us.

ACKNOWLEDGEMENTS

All thanks and praise goes to our Heavenly Father, who through His grace and mercy has carried me thus far and allowed me to complete this degree. His preservation is absolute and His mercy is all-encompassing. Thank you to the ministers in the congregation for their prayers and words of upliftment.

To my supervisor, Professor Selwyn F. Mapolie, I express my sincere gratitude for his guidance and mentorship throughout this research project. I look forward to working with you into the future.

A special thank you to my family: Andre Swarts, Roseline Swarts, Clara Simpson, Justin and Jason Swarts. Your love and support during this time is appreciated and my gratitude to you lives in my soul.

To my friends: Marco, Morph, Lyle, Paul, Roy, Wesley, Ludwig, Dean, Elroy, Hoosain, Robin, Marlin, Angelique, Candice, Rene, Leanne, Nicole, Tracey, thank you for all your support and understanding throughout this degree. I love you guys!!

To the Organometallic Research Group at Stellenbosch University, Rehana Malgas-Enus, Jane Mugo, Hennie Kotze, Wallace Manning, Danie van Niekerk, Drs. Gangadhar Bagihalli and Douglas Onyancha, thank you for making the slaving in the lab a more pleasurable experience. Also, thank you for putting up with my stress-relief mechanism, singing and whistling very loudly.

I would like to thank Elsa Malherbe and Dr. Jan Gertenbach, for their assistance with NMR and SCD analyses.

A special thank you to my good friend Rehana Malgas-Enus, not only for your friendship, but also for proof-reading this thesis and providing constructive criticism throughout the writing process.

To my girlfriend, Megan Samantha Birch: You've carried me and supported me even when I thought that there was no light at the end of the tunnel. I thank you from the bottom of my heart for your love and encouragement. You are an angel in my life.

CONFERENCE CONTRIBUTIONS

Andrew Swarts and Selwyn Mapolie

Known and Novel Palladacycles as Catalyst Precursors: Attempts at 1-Hexene Oligomerisation. CATSA Annual Conference, Goudini Spa, Rawsonville, South Africa, 2009.

Andrew Swarts and Selwyn Mapolie

The Application of Known and Novel Palladacycles as Catalyst Precursors in the Isomerisation of α-Olefins. International Symposium on Homogeneous Catalysis (ISHC 17), Poznan, Poland, 2010.

Andrew Swarts and Selwyn Mapolie

Palladacycles as Catalyst Precursors in the Transformation of α-Olefins. CATSA Annual Conference, Bains Game Lodge, Bloemfontein, South Africa, 2010.

ABSTRACT

Compounds benzylidene-2,6-diisopropylphenylamine (**L1**), 2-chlorobenzylidene-2,6-diisopropylphenylamine (**L2**), 2-bromobenzylidene-2,6-diispropylphenylamine (**L3**) and 4-methylbenzylidene-2,6-diisopropylphenylamine (**L4**) were prepared by Schiff base condensation of 2,6-diisopropylaniline and the respective aldehydes in a 1:1 molar ratio. The ligands were characterised by FT-IR, ^{1}H NMR spectroscopy, and in the case of ligand **L4**, by ^{13}C NMR spectroscopy, ESI-MS and microanalysis. Dinuclear μ-Cl palladacycles (**C1-C4**) of the type $[PdCl(R\text{-}C_6H_3)CH{=}N\text{-}\{2,6\text{-}^{i}Pr_2\text{-}C_6H_3\}]_2$ were prepared by electrophilic C-H activation, starting from the respective ligands and reacting them with $(MeCN)_2PdCl_2$ in the presence of NaOAc which demonstrated the slightly distorted square planar geometry around the palladium centre. Complexes **C1-C4** were reacted with triphenylphosphine and trimethylphosphine in 1:1 molar ratio to isolate mononuclear palladacycles of the type $[Pd(PR'_3)Cl(R\text{-}C_6H_4)CH{=}N\{2,6\text{-}^{i}Pr_2\text{-}C_6H_3\}Cl]$ (**C5-C11**). Treatment of complex **C3** and **C4** with excess trimethylphosphine led to the formation of non-cylometallated complexes (**C12-C13**) bearing trimethylphosphine ligands in a *trans* arrangement. All complexes were fully characterised by FT-IR, ^{1}H, ^{13}C, $^{31}P\{^{1}H\}$ NMR spectroscopy, ESI-MS, microanalyses and in the case of complex **C8** by SCD analysis. The dinuclear μ-Cl palladacycles were also subjected to bridge-splitting reactions with bidentate tertiary phosphines, bis(diphenylphosphino)methane and 1,2-bis(diphenylphosphino)ethane, to yield dinuclear μ-phosphine palladacycles (**C14-C20**) of the type $[\{PdCl(R\text{-}C_6H_3)CH{=}N(2,6\text{-}^{i}Pr\text{-}C_6H_3)\}_2(\mu\text{-}Ph_2P(CH_2)_nPPh_2)]$ (where n = 1 for dppm, and n = 2 for dppe). These novel complexes were fully characterised by FT-IR, ^{1}H, ^{13}C and $^{31}P\{^{1}H\}$ NMR spectroscopy, ESI-MS and microanalyses.

Commercially available 1st generation DAB-PPI dendrimer was peripherally modified via Schiff base condensation with benzaldehyde (**DL1**), 2-chlorobenzaldehyde (**DL2**), 2-bromobenzaldehyde (**DL3**) and *p*-tolualdehyde (**DL4**). Dendrimer ligands of the type DAB-[N=CH-(R-C_6H_4)]$_4$ were isolated and fully characterised by FT-IR, ^{1}H and ^{13}C NMR spectroscopy, ESI-MS and microanalyses. Attempts to prepare analogous dendritic complexes to **C1-C4** were unsuccessful, instead benzylaldiminato Pd(II) metallodendrimers, **DC1-DC4**, of the type *cis*-[PdX_2L_2] (where X = Cl and L constitutes one arm of the dendrimer) were isolated and fully characterised by FT-IR, ^{1}H and ^{13}C NMR spectroscopy, ESI-MS and microanalyses.

The mononuclear palladacycles, **C5-C8**, and 1st generation Pd(II) metallodendrimers, **DC1-DC4**, were efficient catalysts in the Heck coupling of iodobenzene and 1-octene. The metallodendrimers displayed greater catalytic efficiency than the palladacycles, both in activity and selectivity. In both cases the catalytically active species was postulated to be palladium nanoparticles, with the dendrimer ligands (**DL1-DL4**) conferring greater stability on the nanoparticles than the monofunctional ligands (**L1-L4**).

The mononuclear palladacycles demonstrated the ability to isomerise 1-hexene, in the presence of methyl aluminoxane (MAO) as co-catalyst. The complexes showed moderate activity in converting 1-hexene to 2-hexene and displayed high selectivity for the formation of *E*-2-hexene. The difference in catalytic activity between the complexes was attributed to differences in the stability of the active species. The selectivity was observed to be the same for all the catalysts evaluated and the catalytically active species was postulated as a Pd(II)-hydride species.

OPSOMMING

Verbindings bensilideen-2,6-diisopropielfenielamien (**L1**), 2-chloorbensilideen-2,6-diisopropielfenielamien (**L2**), 2-broombensilideen-2,6-diispropielfenielamien (**L3**) and 4-metielbensilideen-2,6-diisopropielfenielamien (**L4**) is deur middel van Schiff basis kondensasie van 2,6-diisopropielanilien en verskeie aldehiede in 'n 1:1 molêre verhouding berei. Die ligande is volledig deur FT-IR, ^{1}H en ^{13}C KMR spektroskopie, ESI-massa spektrometrie en mikroanalise gekarakteriseer. Tweekern μ-Cl palladasikliese verbindings (**C1-C4**), van die tipe, $[PdCl(R\text{-}C_6H_3)CH{=}N\text{-}\{2,6\text{-}^{i}Pr\text{-}C_6H_3\}]_2$, is deur elektrofiliese C-H aktivering berei deur die toepaslike ligand en $(MeCN)_2PdCl_2$ in die teenswoordigheid van NaOAc te reageer. Die verbindings is volledig gekarakteriseer, en in die geval van verbinding **C2**, deur Enkel Kristaal X-straal Diffraksie geanaliseer. Die kompleks neem n verwringde vierkant vlak geometrie om die metaal aan. Verbindings **C1-C4** was met trifenielfosfien en trimetielfosfien in 'n 1:1 molêre verhouding gereageer en mononuklêre palladasikliese verbindings (**C5-C11**) is geisoleerd. Wanneer 'n oormaat trimetielfosfien gebruik is, word nie-palladasikliese verbindings (**C12-C13**) geisoleer waarin die twee trimetielfosfien ligande *trans* teenoor mekaar is. Al die verbindings was volledig deur FT-IR, ^{1}H, ^{13}C en $^{31}P\{^{1}H\}$ KMR spektroskopie, ESI-massa spektrometrie, mikroanalise en in die geval van kompleks **C8**, met X-straal diffraksie gekarakteriseer. Die tweekern palladasikliese verbindings is ook met bis(difenielfosfino)metaan en 1,2-bis(difenielfosfino)etaan gereageer om μ-fosfien palladasikliese verbindings (**C14-C20**) te vorm. Hierdie komplekse is volledig deur middel van die bogenoemde analitiese tegnieke gekarakteriseer.

Kommersiëel beskikbare eerste generasie DAB-PPI dendrimere was perifereel gemodifiseer deur middel van Schiff basis kondensasie met bensaldehied (**DL1**), 2-chloorbensaldehied (**DL2**), 2-broombensaldehied (**DL3**) en *p*-tolualdehied (**DL4**).

Dendritiese ligande van die soort DAB-[N=CH-(R-C_6H_4)]$_4$ is geisoleerd en volledig deur FT-IR, ^{1}H, ^{13}C en ^{31}P{^{1}H} KMR specktroskopie, ESI-massa spektrometrie en mikroanalise gekarakeriseer. Alle pogings om dendrimeer-gedraagde palladasikliese verbindings te isoleer was onsuksesvol. Instede daarvan is bensilaldiminato Pd(II) metalodendrimere (**DC1-DC4**) van die tipe, *cis*-[PdX_2L_2] (waar X = Cl and L een arm van die dendrimer is), geisoleer en ten volle gekarakteriseer.

Die monokern palladasikliese verbindings, **C5-C8**, en die generasie een Pd(II) metalodendrimere, **DC1-DC4**, was as katalisators in die Heck-koppeling van iodobenseen en 1-okteen toegepas. Beide verbinding-tipes kon hierdie transformasie kataliseer. Die metalodendrimere vertoon beter katalitiese aktiwiteit en selektiwiteit en vir beide kompleks-tipes was die katalities-aktiewe spesies as nanodeeltjies voorgestel. Daar is waargeneem dat die dendrimeer ligande beter stabilitet aan die katalities-aktiewe deeltjies verskaf.

Die monokern komplekse, **C5-C8**, toon die vermoë om 1-hekseen na 2-hekseen te isomeriseer, in die teenswoordigheid van ’n ko-katalisator, metiel aluminoksaan (MAO). Die komplekse toon matige aktiwiteite vir hierdie katalitiese proses met hoë selektiwiteit vir *E*-2-hekseen. Die tendens ten opsigte van aktiwiteit van die komplekse is as gevolg van verskille in stabiliteit van die aktiewe spesies. Die selektiwiteit was dieselfde vir al die geëvalueerde komplekse en ’n Pd(II)-hidried spesies word as die katalities-aktiewe spesies voorgestel.

Table of Contents

List of Figures

List of Schemes

Chapter 1: Fundamentals and Catalytic Applications of Palladacycles.

Chapter 4: Catalytic Applications of Mononuclear Palladacycles and Pd(II) Metallodendrimers.

List of Tables

List of Abbreviations

Å	Angstrom
MeCN	Acetonitrile
OAc	Acetate
br.	broad
δ	chemical shift
$CDCl_3$	deuterated chloroform
COD	1,5-cyclooctadiene
d	doublet
dd	doublet of doublets
dt	doublet of triplets
DAB	diaminobutane
dba	dibenzylideneacetone
DMSO	dimethylsulphoxide
DCM	dichloromethane
DMSO-d_6	deuterated dimethylsulphoxide
ESI-MS	Electron Spray Ionisation Mass Spectrometry
FT-IR	Fourier Transform Infra Red
GC-FID	Gas Chromatography Flame Ionisation Detector
hr(s)	hour(s)
Hz	hertz
^{i}Pr	*iso*-propyl
J	coupling constant

KIE	kinetic isotope effect
m	multiplet
M.p.	melting point
min	minutes
m/z	mass to charge ratio
ml	millilitres
mmol	millimole
Me	methyl
MHz	megahertz
NHC	N-heterocyclic carbene
NMR	Nuclear Magnetic Resonance
OMe	methoxy
Ph	C_6H_5
PPI	polypropyleneimine
ppm	parts per million
SCD	Single Crystal X-Ray Diffraction

Chapter 1: Fundamentals and Catalytic Applications of Palladacycles

1.1. Introduction.

The field of organometallic chemistry, particularly of the late transition metals, has witnessed phenomenal growth over the past number of years. In particular, the area of organopalladium compounds has witnessed advances in both synthetic aspects as well as a range of applications. These compounds tend to be easily prepared and handled and are found to be stable both in the solid state and in solution. The rich chemistry of organopalladium compounds may be attributed to the fact that the metal-centre undergoes redox-interchange between the stable Pd(II)/Pd(0) oxidation states readily. Organopalladium compounds containing a metal-carbon σ-bond which is intramolecularly stabilised by a $2e^-$-donor atom (N, P, S etc.) are referred to as cylopalladated compounds, or palladacycles.[1] Since the initial synthesis and characterisation of palladacycles in the 1960's[2] the field has seen tremendous growth in synthetic aspects as well as in their application in catalysis and as advanced materials.[3-4] This chapter will review the literature pertaining to the synthetic and structural aspects of palladacycles and their application in catalytic processes.

1.2. Types of palladacycles.

Palladacycles may be divided into two types based on their basic structural features: four-electron or six-electron donors. These types may be abbreviated as CD or DCD (where D denotes the $2e^-$-donor atom. The former may exist as halogen- or acetate-bridged dimers and may adopt one of two geometries: the *cisoid* conformation, in which the C-atoms (and the donor atoms) are *cis* with respect to one another; and the *transoid* conformation, in which the C-atoms (and donor atoms) are *trans* to one another. CD-palladacycles may be isolated as dimeric or monomeric complexes, and may be neutral, anionic or cationic in nature. The exact nature of the palladacycle is dependent on the type of ligands occupying the

coordination sphere of the metal-centre. The metallated carbon atom is most commonly an aromatic sp^2-hybridised C-atom, but may also be a sp^3-hybridised (aliphatic or benzylic) or a vinylic sp^2-hybridised C-atom. The most common donor atom found in palladacycles is nitrogen, and occurs in a variety of ligand systems. These include, but are not limited to, imines, azobenzenes, pyridines and amides. Other donor atoms include P, S, O and As. The most common palladacycles are those derived from imine- and tertiary amine-containing ligand systems, with a propensity for the formation of five- and, to a lesser extent, six-membered rings. DCD-palladacycles, also known as pincer-type palladacycles, usually exist as symmetrical complexes, with a propensity for the formation of five-membered rings, or as unsymmetrical complexes, with mixed five- and six-membered rings.

1.3. The nature of the carbon atom, C.

The first reports regarding cyclopalladation involved the activation of a $C_{sp}{}^2$-H bond resulting in the formation of a M-$C_{sp}{}^2$ σ-bond.[2] Since then, many examples have appeared in the literature where aromatic C-H activation predominates. The greater bond strength of M-$C_{sp}{}^2$ over M-$C_{sp}{}^3$ bonds have been proposed as an explanation for this preference.[5] Seminal work in the 1970's demonstrated that the C-H bonds of alkanes may undergo oxidative addition to transition metal complexes.[6] Thermodynamic and kinetic studies on the intermolecular activation of arene C-H bonds by [(C_5Me_5)Rh(PMe_3)] demonstrated a slight preference for the activation of arene C-H bonds over alkane C-H bonds, and that the lack of examples in the literature of metal complexes that activate $C_{sp}{}^3$-H bonds was not due to an inherent difference in the kinetics of arene and alkane activation.[7] In the context of cyclopalladation the question of aromatic versus aliphatic C-H activation has been in the foreground since initial palladacycle synthesis.[8]

Albert *et. al.* studied the factors governing cyclopalladation, specifically the preferential activation of aromatic C-H bonds.[9-10] They studied the cyclopalladation of *N*-mesitylbenzylideneamines with $Pd(OAc)_2$. The ligands not only allowed for the isolation of either *exo* (where the C=N bond is outside the metallacycle) or *endo* (where the C=N bond is inside the metallacycle) isomers (Fig. 1.1) but also provided a means to evaluate the metallation tendency of aromatic or aliphatic C-H bonds, thereby observing the importance of ring size of the metallacycle formed.

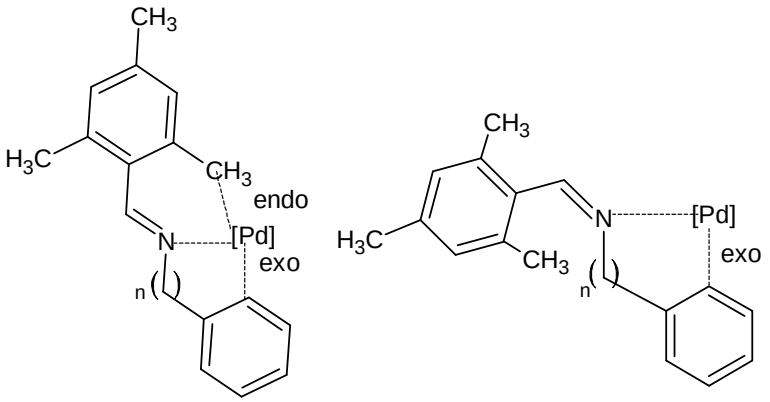

Fig. 1.1 Possible isomers formed in the cyclometallation reaction.[9-10]

It was found that the reaction conditions employed has a marked effect on whether *exo* or *endo* isomers are isolated as well as whether aromatic or aliphatic C-H bond activation occurred (Scheme 1.1). Also, an isomerisation process was observed when *exo*-5-membered species was refluxed in AcOH resulting in the formation of *endo*-6-membered palladacycles.

The process was found to occur only in acidic medium. The thermodynamic driving force for the reaction was attributed to the formation of the *endo* metallacycle, even if it resulted in the formation of 6-membered palladacycles. Another aspect of the study evaluated the steric effect on the cyclopalladation reaction. Blocking of the 5-position of the ligand by *Me*-groups resulted in the exclusive formation of *endo*-6-membered palladacycles in which aliphatic C-H bonds were activated.

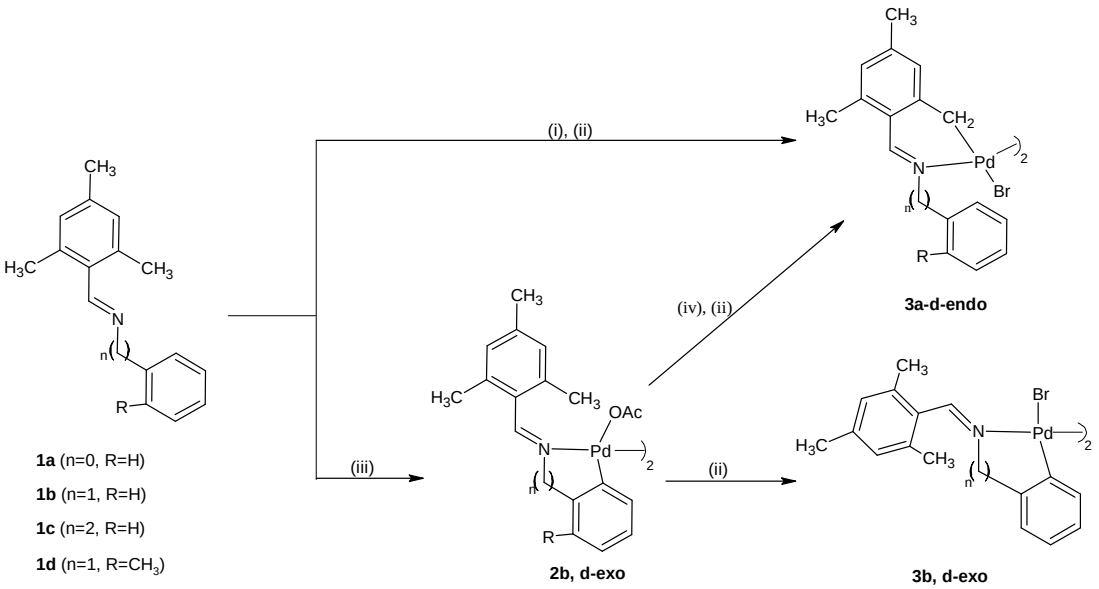

Scheme 1.1 Synthetic procedures for the regioselective synthesis of cyclopalladated mesitylbenzylideneamines**.**[9]

Here it is shown how the regioselectivity of cyclopalladation may be governed by thermodynamic control.

Regioselective cyclopalladation is further exemplified by the work of Alsters *et. al.*[11] They prepared C,N,N', aryl, benzyl and alkyl ligand systems and evaluated these in cyclopalladation by reaction with $Pd(OAc)_2$ and in some cases with $Pd(dba)_2$

(dba = dibenzylideneacetone). In most cases, preferential aromatic C-H activation was observed. An interesting observation was made when comparing the cyclopalladation behaviour of two analogous ligands (Fig. 1.2). Although **4a** could undergo either aromatic or aliphatic C-H bond activation, only aromatic C-H bond activation was observed which led to the formation of 5-membered ring-systems. In the case of **4b**, aliphatic (benzylic) C-H activation was observed which resulted in the exclusive formation of 6-membered ring-systems even though aromatic C-H activation, which would result in the formation of 5-membered ring-systems, was possible. To gain insight into the mechanism of cyclopalladation and specifically into the regioselectivity observed, coordination adducts were prepared and their cyclopalladation behaviour studied by solution-state NMR spectroscopy.

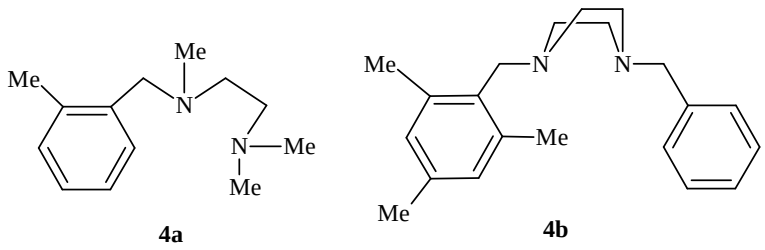

Fig. 1.2 Isomers, **4a** and **4b**.[11]

In the context of regioselectivity the NMR study demonstrated that in the coordination adducts analogous to **4a** containing mesityl-groups there is slow rotation about the Ph-CH_2 axis; whereas for coordination adducts analogous to **4b** no rotation is observed. Work on the cyclopalladation of quinolines found that axial CH-M interactions destabilise the ensuing palladacycles.[12] This effect had been observed in systems where steric constraints force the

interacting C-H bond to occupy a specific position with respect to the metal centre. No steric constraints were prevalent in the complexes under investigation thus for the cyclopalladation of **4a**, preferential aromatic metallation was attributed to the close proximity of the *ortho*-proton to the metal-centre facilitating electrophilic attack of Pd on the *ortho*-carbon atom. In **4b** the *ortho*-protons of the phenyl ring could not come into close proximity of the metal-centre (as observed for **4a**). This resulted in an increase in the activation energy for aromatic C-H activation and an alternative reaction pathway i.e. aliphatic C-H activation became operative. In this example the regioselectivity of cyclopalladation was controlled by lowering the activation energy associated with a particular activation pathway i.e. aliphatic versus aromatic C-H activation by facilitating close approach of the desired C-H bond to the metal-centre.

Kind and co-workers reported the cyclopalladation of 1'1-azonapthalene with $[Pd(hfa)_2]$ (hfa = 1,1,1,5,5,5-hexafluoropentane-2,4,-dionato-κ^2-*O,O'*) (Scheme 1.2).[13] A mixture of two isomers; the *ortho*-complex (isomer **A**) and the *peri*-complex (isomer **B**); was isolated.

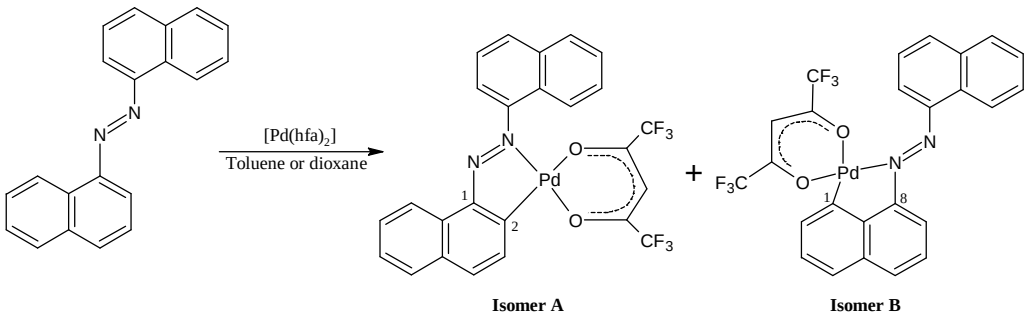

Scheme 1.2 Synthesis of isomers, **A** and **B**.[13]

It was found that the nature of the solvent as well as the reaction temperature employed had a significant impact on the product distribution. In toluene at low temperature

only trace amounts of each isomer formed whilst an increase in reaction time and temperature resulted in the formation of 59% of isomer **A** and 25% of isomer **B**. A control experiment was conducted to monitor the formation of the isomeric products which was accomplished with the aid of ^{1}H NMR spectroscopy. The ligand was reacted with the Pd precursor in d_8-toluene at 100 °C with samples withdrawn at specific time intervals and analysed by ^{1}H NMR. ^{1}H NMR analyses indicated that during the initial period of reaction the formation of isomer **B** predominated and that an increase in reaction time resulted in a preferential increase in the percentage of isomer **A**. It was also observed that refluxing this reaction mixture resulted in the exclusive formation of isomer **A**. From these results it was concluded that isomer **B** forms as the kinetic product which converts to the thermodynamically stable product, isomer **A**. The effect of solvent was evaluated by performing the reaction in dioxane. It was found that isomer **B** formed preferentially regardless of reaction time or temperature with the ratio of isomers **B:A** being 2:1. The regioselectivity observed in the system investigated was attributed to the nature of the *peri*-H atom which is more acidic than the *ortho*-H atom. The enhanced acidity facilitated the formation of the 6-membered metallacycle (isomer **B**) as the kinetic product. Also, in polar solvents this acidity is further enhanced thus explaining the predominant formation of isomer **B** in dioxane regardless of reaction time or temperature.

The above examples all examined regioselectivity between aromatic and aliphatic C-H bond activation. Valk *et.al.* reported an interesting example of regioselective cyclopalladation via C-$SiMe_3$ activation.[14] They prepared a series of silyl-substituted benzene and naphthalene ligands and evaluated these in cyclopalladation with Li_2PdCl_4 and $Pd(OAc)_2$ (Scheme 1.3). Higher product yields were obtained when employing $Pd(OAc)_2$ which was attributed to an increase in electrophilic character at the palladium centre in comparison to

Li_2PdCl_4. In all cases examined, cyclopalladation occurred via the activation of the C-Si bond even when aromatic or aliphatic C-H bond activation was possible. Here the regioselectivity of cyclopalladation is governed by the higher reactivity of the C-Si bond toward electrophilic attack of the palladium centre.

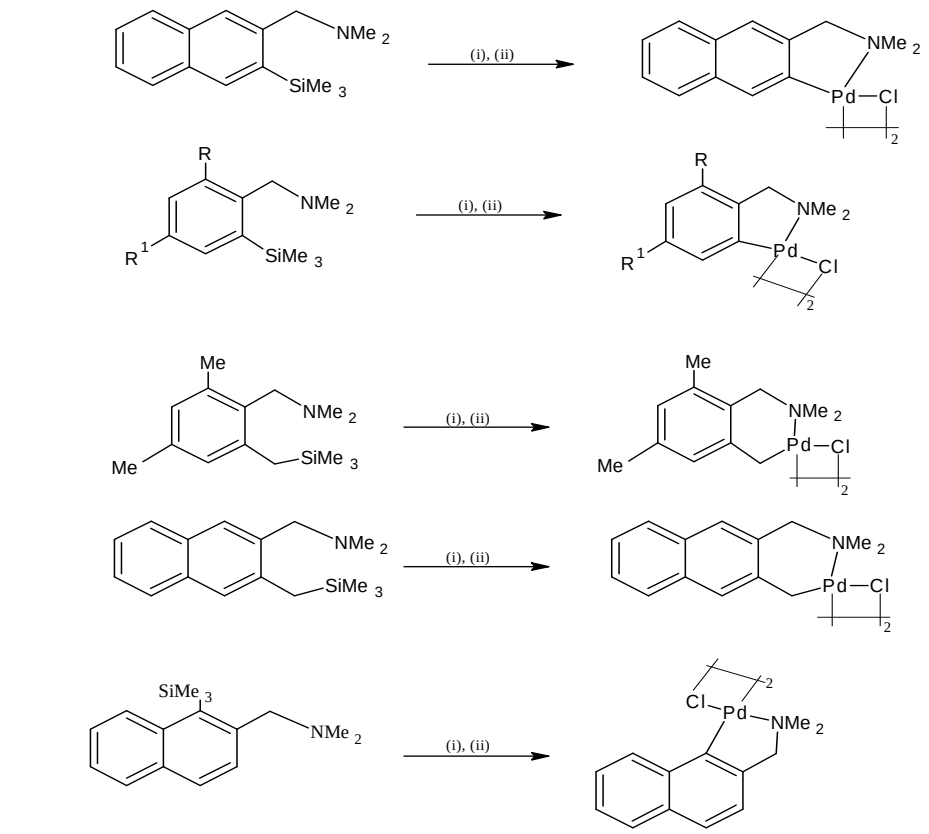

Reaction conditions: (i)$Pd(OAc)_2$, MeOH (ii) LiCl

Scheme 1.3 Reactivity of silyl-substituted benzene and naphthalene ligands.[14]

The nature of the C-atom has been shown to have a significant effect on the cyclopalladation reaction. By modulating steric and electronic effects as well as the reaction conditions employed, the regioselectivity of cyclopalladation may be directed toward a desired product.

1.4. The nature of the donor atom, D.

The cyclometallation process is initiated by the exchange of a ligand in the metal precursor for the donor site, D, in the ligand to be cyclometallated. The effect of the donor group in cyclometallation may be classified in terms of both its basicity and its steric impact. The Hard-Soft Acid-Base (HSAB) principle developed by Pearson[15] may be employed to describe the coordination behaviour between the donor atom and the metal-centre. Thus cyclometallation with early transition metals generally proceed well when the donor groups consist of O- or N-donor atoms which are regarded as hard bases. At the other end of the spectrum cyclometallation with late transition metals is observed to proceed efficiently when the donor groups consist of P- or S-donor atoms. The HSAB principle cannot be applied exclusively to predict trends in donor atom-metal centre interactions as there are exceptions. For example cyclometallation of Pd with primary amines, which may be classified as hard bases by consideration of the HSAB principle, has been observed. This will be discussed in more detail.

The work of Cope and Friedrich on the cyclopalladation of aryl-alkylamines[16] allowed the following prerequisites for the cyclometallation of amine-derived ligands to become generally accepted:[6]

- the nitrogen atom should be tertiary;
- the metallacycle formed should be a 5-membered ring and
- the aromatic ring should not be deactivated to electrophilic attack.

These prerequisites were exemplified by the reaction of N,N-dimethylbenzylamine or N,N-dimethyl-4-methoxybenzylamine with tetrachloropalladate, $[PdCl_4]^{2-}$ in 1:2 molar ratios to yield dinuclear μ-Cl *ortho*-metallated complexes whereas the reactions with benzylamine, N-methylbenzylamine, N,N-dimethyl-2-phenyl-1-ethylamine and

N,N-dimethyl-4-nitro-benzylamine resulted in the formation of coordination complexes of the type $[PdCl_2(amine)_2]$. In the ensuing years several exceptions to these 'rules' were reported. For instance, Cockburn and co-workers reported the cyclopalladation of a primary amine, triphenylmethylamine with sodium tetrachloropalladate, Na_2PdCl_4.[17] The reason for the formation of cyclometallated complexes was attributed to the presence of bulky substituents at the α-carbon which served to promote the cyclopalladation process. Avshu and co-workers reported the reaction of coordination complexes of the type $[ML_2X_2]$ where M = Pd or Pt; L = amine or phosphine and X = I, Cl or SCN with silver tetrafluoroborate ($AgBF_4$).[18] When employing EtOAc as solvent dimeric cyclopalladated μ-I complexes were isolated. Despite these reports the general consensus amongst the research community had always been that primary amines were inert toward direct C-H bond activation to yield the corresponding palladacycles.

Fuchita and co-workers reported the cyclopalladation of unsubstituted benzylamine.[19] This was accomplished by the reaction of benzylamine with $Pd(OAc)_2$ in a 1.1: 1 molar ratio in benzene at 60 °C for 24 hrs (Scheme 1.4a). ^1H NMR analysis confirmed the formation of the cyclopalladated μ-Cl complexes.

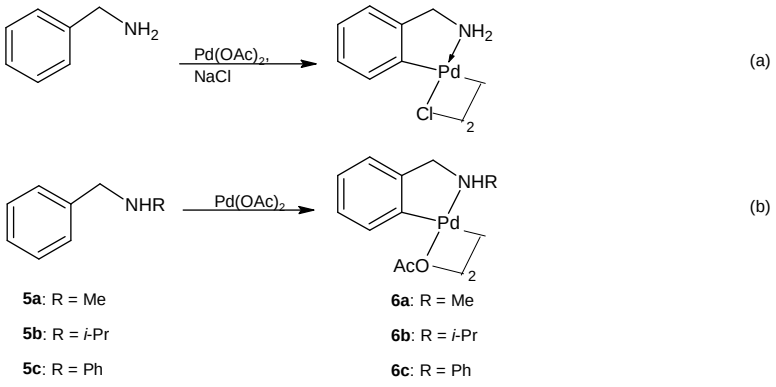

Scheme 1.4 Cyclopalladation of unsubstituted benzylamine.[19]

Further reports by the same researchers described the reactions of *N*-methyl-, *N*-isopropyl- and *N*-phenylbenzylamine with $Pd(OAc)_2$ in 1.1 :1 molar ratios in benzene at 60 °C for 24 hrs (Scheme 1.4b).[20] In all cases the cyclopalladated μ-OAc complexes could be isolated. Metathesis and bridge-splitting reactions allowed for the isolation of μ-Cl and mononuclear palladacycles respectively. These results stood in stark contrast to the work by Cope[16] as well as that reported by Vicente and co-workers.[21] The fundamental difference was in the nature of the reagents and the reaction conditions employed i.e. a change in Pd precursor from $PdCl_4^{2-}$ and $PdCl_2$ to $Pd(OAc)_2$ as well as employing benzene as reaction solvent instead of methanol and acetone.

Vicente and co-workers reported the cyclopalladation of a primary nitrobenzylamine (Scheme 1.5) and thereby demonstrated that primary amines in which the aromatic ring is deactivated to electrophilic attack may undergo the cyclometallation reaction.[22]

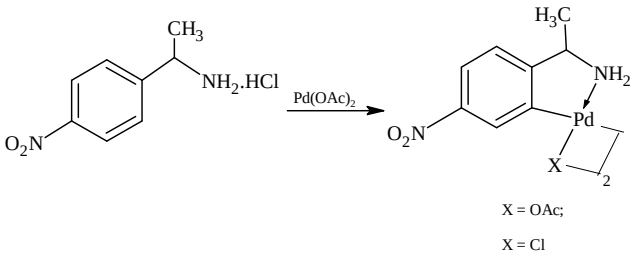

Scheme 1.5 Cyclopalladation of primary nitrobenzylamine.[22]

This was accomplished by reacting the hydrochloride salt of (S)-α-methyl-4-nitrobenzylamine with $Pd(OAc)_2$ in the presence of NaOH which resulted in the isolation of both cyclopalladated μ-OAc and μ-Cl complexes.

The limiting rules outlined by Cope and Friedrich[16] were infringed simultaneously by the work of Vicente and co-workers where they reported the cyclopalladation of primary phenethylamines.[23] For halide-substituted arylamines (X = Cl, F) the reaction with $Pd(OAc)_2$

followed by bridge-splitting with PPh_3 allowed for the isolation of the mononuclear palladacycles (Scheme 1.6a). Where the substituent on the aromatic ring was the NO_2-group, reaction of the corresponding hydrochloride salt with $Pd(OAc)_2$ followed by bridge-splitting with PPh_3 resulted in the isolation of mononuclear palladacycles consisting of a 6-membered ring; a donor group in which the N-atom was primary and where the aromatic ring was highly e^--deficient (Scheme 1.6b).

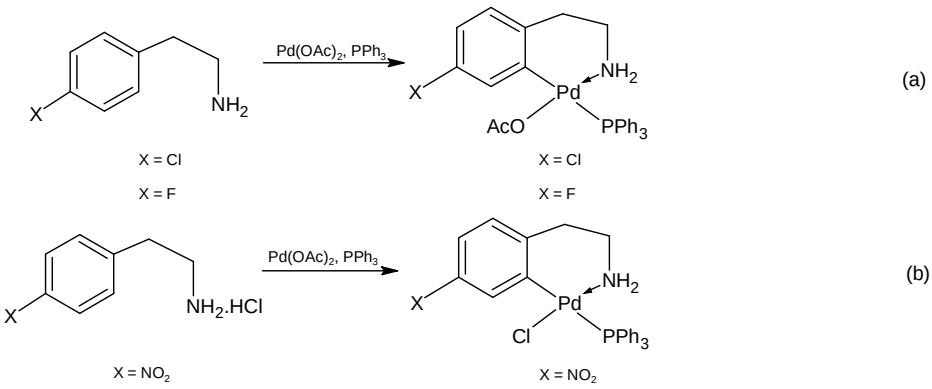

Scheme 1.6 Cyclopalladation of deactivated primary amines.[23]

The work described served to change the fundamental understanding associated with the nature of the N-atom in the context of cyclopalladation.

1.5. The mechanism of cyclopalladation.

1.5.1. Electrophilic C-H bond activation:

The discussion thus far has centred on the C-atom and the donor group in the cyclometallation reaction. A deliberate attempt has been made to avoid any mechanistic discussion up until this point.

For many years it had been known that cyclopalladation must proceed via a mechanism which involves the electrophilic aromatic substitution of Pd at the C-atom of the ligand.[24]

The first reports evaluating mechanistic details was by Takahashi and Tsuji[25] where they evaluated the carbonylation behaviour of symmetrically and asymmetrically substituted azobenzene complexes. Analysis of the carbonylation products allowed for the determination of which aryl ring was cyclometallated in the starting material. The results obtained showed that metal-carbon σ-bond formation was facilitated by e^--donating substituents (Me and OMe) on the aryl ring and that in the case of e^--withdrawing substituents, cyclometallation of the unsubstituted aryl ring would predominate. They concluded that M-C σ-bond formation proceeded via electrophilic substitution of palladium chloride on the benzene ring.

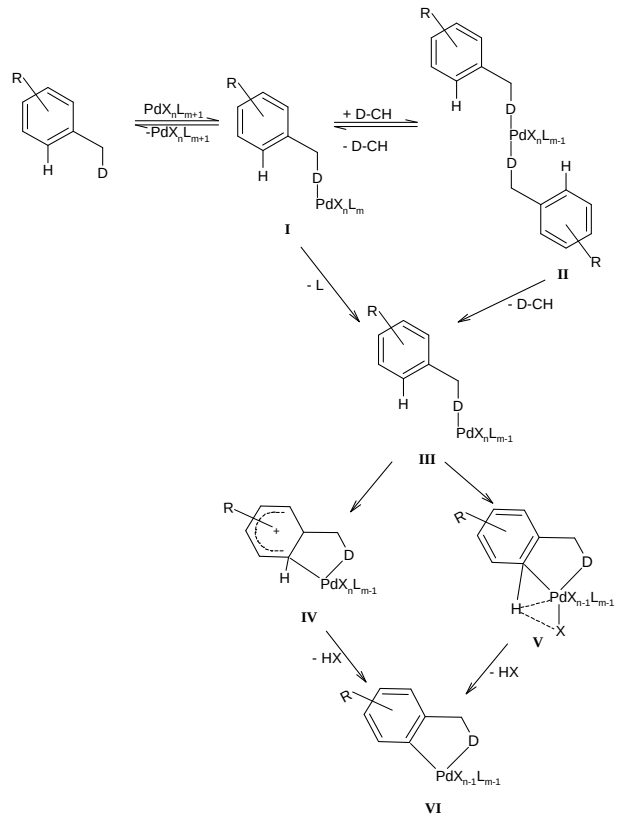

Scheme 1.7 A general reaction mechanism for cyclopalladation via electrophilic C-H activation.

Work by Bruce and co-workers[26-27] evaluated the cyclometallation behaviour of various asymmetrically substituted azobenzene ligands with manganese and palladium precursors. For 2-F, 3-F and 3-CF_3 mono-substituted azobenzene ligands, cyclopalladation afforded metal complexes where the unsubstituted aryl ring was metallated preferentially with a high selectivity (> 80%) for the formation of complexes in which the F- or CF_3-substituent was in the *para* position (Scheme 1.8). For the 4-F mono-substituted azobenzene ligand a mixture of cyclometallated products were isolated with a propensity for the formation of palladacycles where the unsubstituted aryl ring was metallated. In contrast, for 2-F, 3-F and 3-CF_3 mono-substituted azobenzene ligands cyclomanganation afforded metal complexes in which the F-substituted aryl ring was metallated preferentially with a high selectivity for the formation of metal complexes in which the F- or CF_3-substituent is *ortho* to the M-C σ-bond (Scheme 1.9). Similar results are observed for the 4-F ligand with metallation of the activated aryl ring dominating in a ratio of 3:2. Cyclopalladation of 3-OMe azobenzene afforded palladacycles in which the OMe-group is *para* to the M-C σ-bond with high regioselectivity. This was attributed to the strong resonance inducing effect of the methoxy-group.

Cyclomanganation of this ligand resulted in the isolation of two isomeric products (Fig 1.3) in a 60:40 ratio in which both the unsubstituted ring and the 2-position of the OMe-substituted ring is attacked. Isomer **2** is formed as a result of the e^--withdrawing inductive effect of the OMe-group. Interestingly, both cyclomanganation and cyclopalladation of 3-CO_2Et azobenzene afforded a metallacycle with a M-C σ-bond in the same position (*ortho* to the -CO_2Et group). This observation was attributed to an interaction between the incoming metal atom and the CO_2Et group thereby directing the attack at the position *ortho* to the substituent.

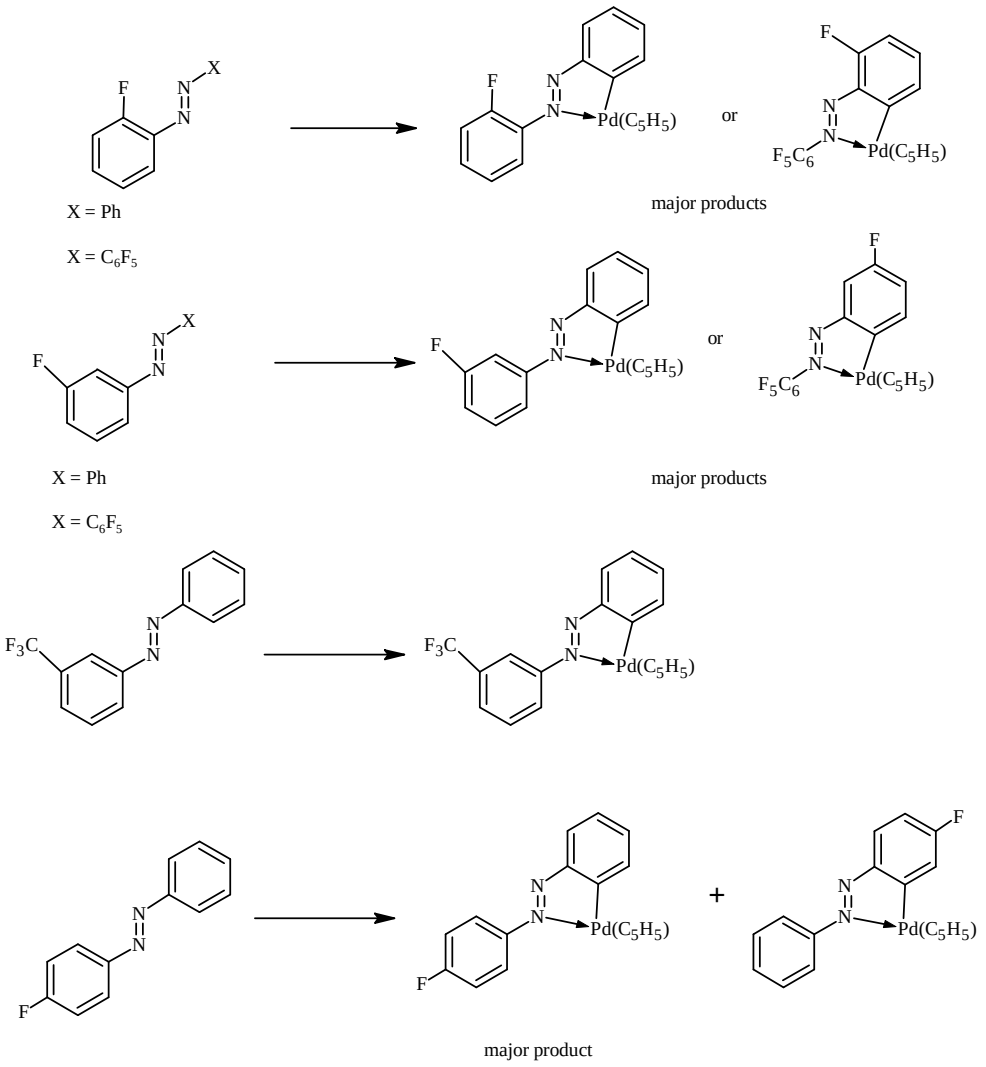

Scheme 1.8 Cyclopalladation of azobenzene ligands.[26-27]

The results indicated that e⁻-withdrawing substituents activated the ring toward nucleophilic attack by low-valent metal complexes as is the case for [$MnMe(CO)_5$], and that e⁻-donating substituents activated the ring toward electrophilic attack by electrophilic late transition-metal complexes as is the case for $PdCl_2$. The authors also postulated the formation of an arenium ion (such as **IV**, Scheme 1.7) as a key intermediate in the cyclopalladation reactions investigated.

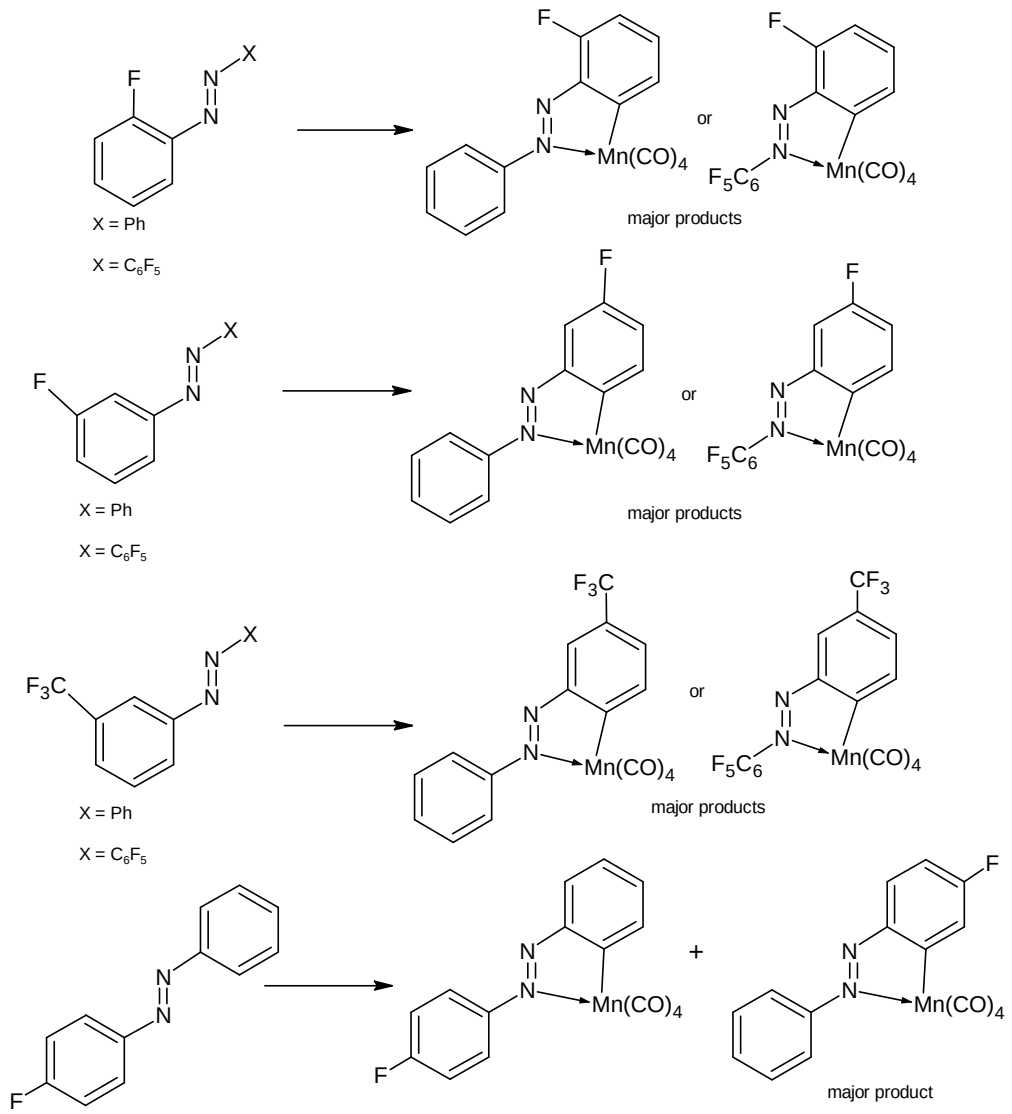

Scheme 1.9 Cyclomanganation of azobenzene ligands.[26-27]

Hiraki and co-workers[28] evaluated the reaction of $Pd(OAc)_2$ with 4-methyl-4'-nitrobenzylsulphide. Palladacycles were isolated in which the aryl ring bearing the Me-substituent was metallated indicating that cyclopalladation with $Pd(OAc)_2$ occurred via electrophilic attack on the electron-rich aryl ring.

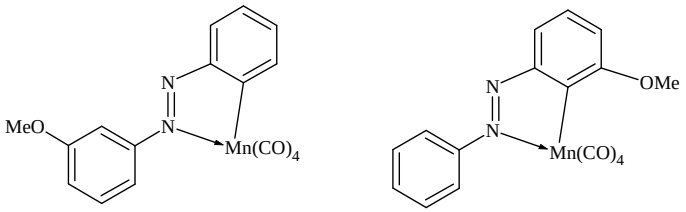

Isomer 1 **Isomer 2**

Fig. 1.3 Regioselective cyclomanganation forming isomer **1** and isomer **2**.[28]

The above discussion focussed on experimental evidence for electrophilic aromatic substitution to be the operative reaction pathway in cyclopalladation reactions.

Ryabov and co-workers evaluated the kinetics of *ortho*-palladation of various ring-substituted *N*,*N*-dimethylbenzylamines with $Pd(OAc)_2$ in acetic acid and chloroform (Scheme 1.10).[29] UV-analysis showed that the ligands existed in their protonated form in acetic acid with the equilibrium being shifted far to the left (Eq. 1).

$$[RCH_2NHMe_2]^+O_2CMe \rightleftharpoons RCH_2NHMe_2 + HO_2CMe \quad (1)$$

The kinetic data obtained for the cyclopalladation in acetic acid showed that the reaction pathway involved coordination of the amine ligand to the palladium precursor, which in acetic acid media was identified as $[Pd_3(O_2CMe)_6]$. This was followed by the rate-limiting step which was identified as slow cleavage of Pd-OAc bridges. The rate-limiting step was then proceeded by rapid cyclisation to form the cyclopalladated complex.

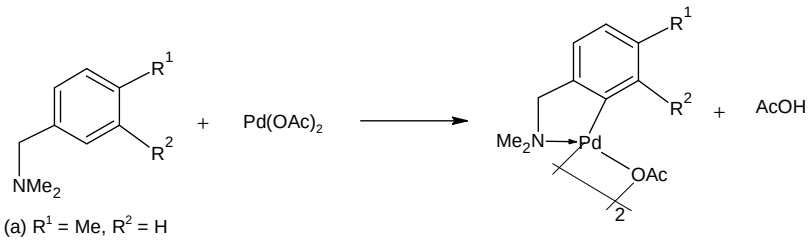

(a) R^1 = Me, R^2 = H

(b) R^1 = R^2 = OMe

(c) R^1 = R^2 = H

(d) R^1 = OMe, R^2 = H

(e) R^1 = Cl, R^2 = H

(f) R^1 = NO_2, R^2 = H

Scheme 1.10 Kinetic evaluation of cyclopalladation in acetic acid and chloroform.[29]

In contrast, kinetic data obtained for the cyclopalladation in chloroform showed that the reaction pathway involved ligand dissociation to form a three-coordinate intermediate which resulted in subsequent cleavage of the C-H σ-bond. C-H σ-bond cleavage was identified as the rate-limiting step. The authors proposed a mechanism which proceeded via **I**→ **II** → **III** → **VI** (Scheme 1.7), in which **III** is a three-coordinate intermediate and the rate-limiting step being the cleavage of the C-H σ-bond. The thermodynamic parameters obtained for the cyclopalladation via a 'dissociative' pathway suggested a highly ordered transition state, and the authors suggested an arenium ion (**IV**, Scheme 1.7) as the key intermediate in the cyclopalladation reaction.

Gomez and co-workers conducted kinetic studies on the cyclopalladation of imine ligands in aprotic and protic solvents.[30-31] The observed rate constants and thermodynamic parameters obtained in both solvent systems were found to be in agreement with data reported for the C-H bond activation via an electrophilic substitution pathway.[29, 32-34] The observed rate constant in acetic acid was found to be faster than that for the reaction in toluene which was indicative of the transition state in the acid-mediated process being more

similar to the final cyclometallated product. A similar observation had been made for the C-H bond activation in dirhodium(II) core complexes.[32-34] From the thermal activation parameters obtained in toluene and acetic acid as solvents the transition state was postulated to proceed via a four-membered species in which proton abstraction is facilitated by an interaction between the proton to be abstracted and a terminal acetate group (Fig. 1.4).

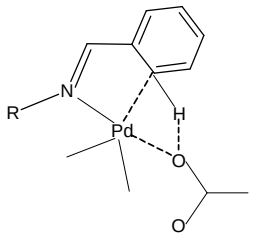

Fig. 1.4 The four-membered transition state postulated by Gomez and co-workers.[30-31]

It was thus concluded that the cyclopalladation of imine ligands proceeded via an initial fast step which is the formation of the imine-palladium coordination complex. This was followed by the rate-determining step which involved the formation of a highly-ordered 4-membered transition state. The formation of this transition state was observed to be favoured in protic media, via the formation of the $MeCO_2H_2^+$ leaving group which facilitated the formation of the cyclometallated product.

Davies and co-workers evaluated the cyclometallation of dimethylbenzylamine (DMBA-H) with $Pd(OAc)_2$ by employing density functional theory (DFT) calculations.[35] Work by Ryabov *et. al.* identified the monomeric square-planar complex, $Pd(OAc_2)$(DMBA-H), as a key intermediate in this particular reaction thus this species was employed as the starting point for all subsequent calculations. The complex was calculated to

have both η^2- and η^1-acetate ligands. The first step in the cyclometallation reaction was calculated to proceed with the displacement of one arm of the η^2-acetate ligand by one *ortho* C-H bond. This step was found to have an energy of + 13 kcal/mol and resulted in the formation of an agostic intermediate with a calculated energy of + 11.0 kcal/mol. The agostic intermediate also exhibited an H-bonding interaction between the *ortho*-H atom and the displaced acetate arm. The molecule was thus ideally set for H-transfer to occur and this step was calculated to proceed via a minimal activation barrier of + 11.1 kcal/mol. The H-acceptor acetate arm was found to twist away from the newly formed Pd-C bond and donate the transferred H-atom to the second acetate ligand. The formation of the cyclometallated product was calculated to have an associated energy of - 13.2 kcal/mol. The formation of the cyclometallated product was found to be both thermodynamically favourable and kinetically accessible. An overall activation barrier relative to the starting complex was calculated as being only 13.0 kcal/mol.

H-transfer via a four-membered transition state and oxidative addition pathways were evaluated as alternative C-H activation pathways. Both processes were found to be far more energy-intensive with calculated activation barriers of + 34.3 and + 25.7 kcal/mol for the respective pathways. A key feature that was observed for both processes is that during C-H bond cleavage the *ortho*-H atom and the displaced acetate arm are on opposite sides of the Pd coordination plane. This makes it more difficult for H-transfer to take place in these processes. The computed activation barrier for the H-transfer pathway via a six-membered transition state (**V**, + 13.0 kcal/mol) was found to compare well with experimental values reported for other palladium acetate promoted cyclometallation reactions.[8, 29] Furthermore, a small value for the H/D KIE could be computed and the substituent effect observed in the Hammett plot could be qualitatively reproduced.

A short Pd···H contact of 1.91 Å and an elongated C-H distance of 1.15 Å were observed for the agostic complex. Also, significant changes in the calculated natural atomic charges were only observed at the activated C-H bond, when going from $Pd(OAc)_2$(DMBA-H) to the agostic intermediate. This is in contrast to what would be observed for a transition state which consisted of a Wheland intermediate. The formation of the agostic species was calculated to be the rate-determining step in the cyclometallation process, with formation of the cyclometallated product being dependant on deprotonation occurring. The acetate ligand is appropriately positioned to abstract the H-atom in the six-membered transition state. The cyclometallated product is thus formed with little distortion in the transition state and virtually no activation barrier. In contrast, significant lengthening of the Pd-O bond is required in the four-membered transition state which results in a much higher activation energy.

It was concluded that the cyclometallation of DMBA-H with $Pd(OAc)_2$ proceed via an agostic C-H complex which then undergoes intramolecular H-transfer via a six-membered transition state to the coordinated acetate ligand. Thus palladium acetate has the dual function of facilitating the electrophilic C-H activation of the ligand and acting as an intramolecular base for deprotonation to occur.

1.5.2. Transcyclometallation.

Transcyclometallation involves the exchange of one cyclometallated ligand for another. This C-H activation process involves both M-C σ-bond rupture and formation and depending on which occurs first may proceed via two intermediates. If M-C bond formation

is preceded by M-C' bond formation then an inorganic intermediate is generated whereas a diorgano metal complex intermediate is generated when M-C' bond formation occurs first.[36]

Ryabov evaluated the mechanistic aspects of transcyclometallation by studying the thermodynamics and kinetics of a series of OAc-bridged palladacycles in the presence of free ligand.[37] (Scheme 1.11)

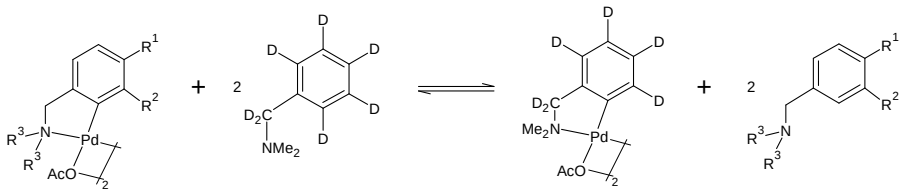

	R^1	R^2	R^3
7a	MeO	MeO	MeO
7**b**	Me	H	Me
7**c**	H	H	Me
7**d**	MeO	H	Me
7**e**	Cl	H	Me
7**f**	NO_2	H	Me
7**g**	H	H	Et

Scheme 1.11 A general scheme of the reactions employed to evaluate the transcyclometallation process.[37]

^{1}H NMR analysis of the equilibrium showed that the equilibrium process was reversible.[38-39] The equilibrium constants obtained indicated that in acetic acid media the equilibrium was shifted to the left for e$^-$-deficient substrates. This nucleophilic behaviour has been observed previously when employing $Pd(OAc)_2$ as palladating agent in acidic media.[29] Orthopalladation of e$^-$-deficient ligands thus appeared to be under thermodynamic control. A benzylamine containing both e$^-$-rich and deficient aromatic rings was reacted with $Pd(OAc)_2$ in acetic acid and chloroform (Scheme 1.12).

Two isomers (Scheme 1.12, isomer **IA** and **IB**) were obtained which upon heating in acetic acid demonstrated a thermodynamic preference for isomer **IB** i.e. the e^--deficient aromatic ring. Comparison of the equilibrium constants for **7c** and **7g** (Scheme 1.11) demonstrated the preferential cyclometallation of less sterically hindered amines.[16, 40]

The kinetics of transcyclometallation was studied by evaluating the ligand exchange between **7c** and phenylpyridine and azobenzene respectively (Scheme 1.13).

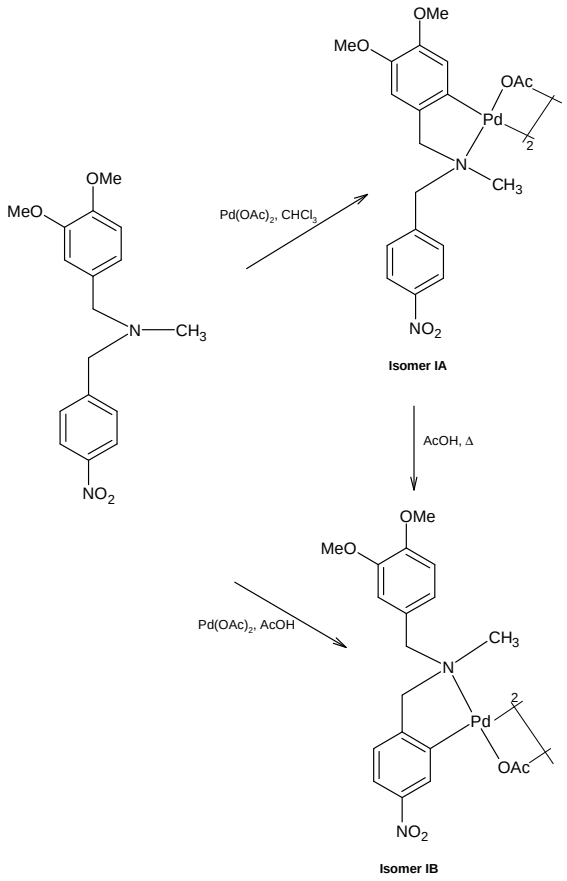

Scheme 1.12 Reaction scheme demonstrating the thermodynamic preference for the formation of isomer **IB**.[37]

The results obtained were indicative of a dissociative mechanism in which dissociation of the amine ligand occurred. This was followed by protolytic cleavage of the

Pd-C bond in the presence of AcOH. The result was the formation of an inorganic intermediate which could then undergo cyclometallation with either phenylpyridine or azobenzene.

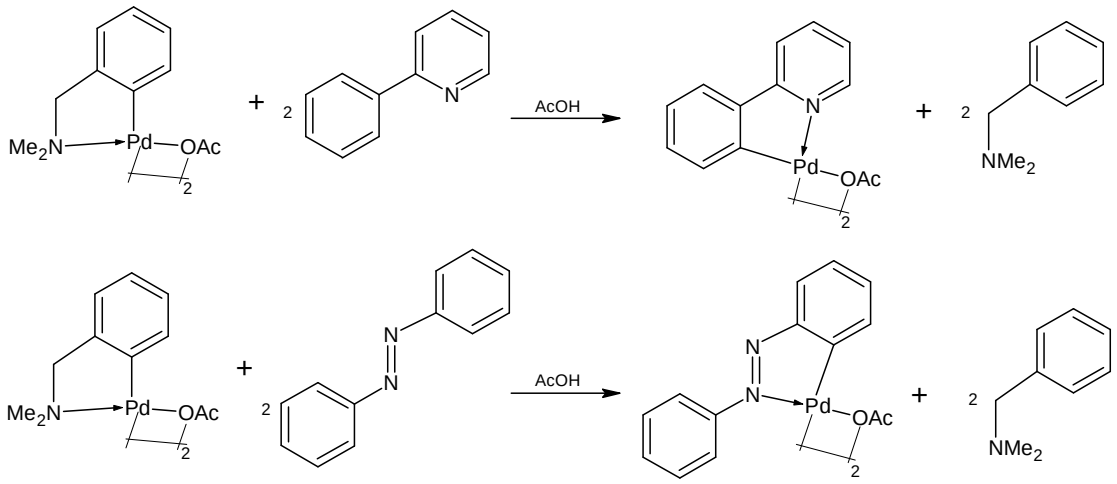

Scheme 1.13 Ligand exchange between **7c** and phenylpyridine (top) and azobenzene (bottom).[37]

These mechanistic concepts have found widespread acceptance and have allowed insight into cyclopalladation as a reaction with widespread applicability.

1.6 The application of palladacycles in C-C coupling reactions.

Although the literature is flooded with reports on the synthesis and characterisation of palladacycles the first reports of their application in catalysis only appeared in the 1980's.[41-42] Palladium and its complexes occupy an enviable position in organic synthesis as a catalyst for organic transformation and palladacycles are no exception. This is evidenced by numerous publications and review articles describing the application of these complexes in C-C bond

formation.[3, 43-45] These coupling reactions have recently occupied centre stage as a result of Heck, Suzuki and Negishi being awarded the 2010 Nobel Prize in Chemistry.

1.6.1 The Heck coupling reaction.

The Heck-coupling reaction involves the catalytic arylation and alkenylation of olefinic substrates. This reaction was discovered independently by Mizoroki[46] and Heck (Scheme 1.14).[47]

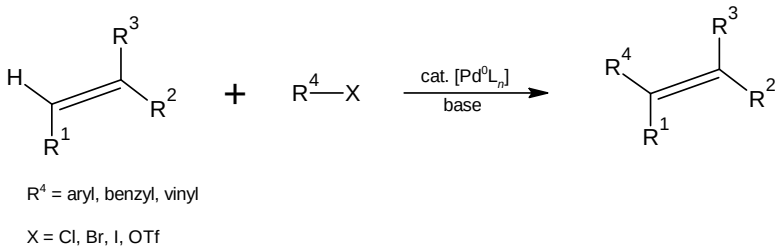

Scheme 1.14 A general scheme for the Heck reaction**.**

The first report of palladacycles as catalysts in Heck coupling was by Beller and co-workers (Fig1.5).[48]

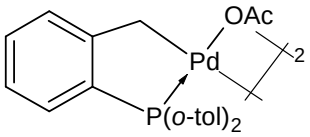

Fig. 1.5 Herrmann-Beller palladacycle.[49]

The complex in Figure 1.5 was found to exhibit high activity and thermal stability. This discovery sparked wide-spread interest in the application of palladacycles in Heck

coupling and numerous palladacycles of all classes have been shown to catalyse the Heck reaction. However, it should be noted that even trace amounts of palladium in the system would catalyse the Heck coupling of iodo- and bromoarenes under conventional reaction conditions.[50]

Mechanistically the reaction has been postulated to proceed via the classical Pd(0)/Pd(II) catalytic cycle as observed for other Pd-catalysed organic transformations.[51-52] The palladacycles thus serve as a reservoir for the active Pd(0) species. Activity differences observed when employing different palladacyclic catalyst precursors have been attributed to varying degrees of catalyst preactivation.[43] The key step in Heck coupling has been proposed to involve the slow release of low-ligated Pd(0) species which is active in the catalytic process. Catalytically efficient palladacycles are those in which the release of the Pd(0) species is neither too fast or too slow. The former is characteristic of palladacycles with poor thermal stability while the latter is observed for thermally robust palladacycles.[3, 44]

The Heck reaction involving chloroarenes catalysed by palladacycles remains a challenge. This is due to the lower reactivity of chloroarenes and the fact that higher temperatures (> 150°C) are required with no significant improvement in yield or turnover numbers (TON's) being observed. Schnyder *et. al.* evaluated a series of mononuclear palladacycles in the Heck-coupling of 4-chloroanisole with *n*-butyl acrylate.[53] These complexes were prepared *in situ* by mixing the μ-OAc palladacycles with sterically demanding e^--rich secondary phosphines. The complexes exhibited activities comparable or higher than the most active systems reported in literature.[54-55] Other examples in the literature describe the application of a cyclopalladated oxime complex as well as a carbene-derived palladacycle.[56]

The temperature-dependence of the Heck coupling reaction is a constant feature in the literature with elevated temperature being a prerequisite to facilitate the catalytic transformation. Consorti and co-workers reported the application of μ-Cl palladacycles derived from propargyl amine in the Heck coupling of aryl chlorides, bromides and iodides with *n*-butyl acrylate and styrene (Scheme 1.15).[57]

The catalytic reaction was observed to proceed at room temperature with high TON's. The palladacycle was observed to function as a reservoir of catalytically active Pd(0) species.

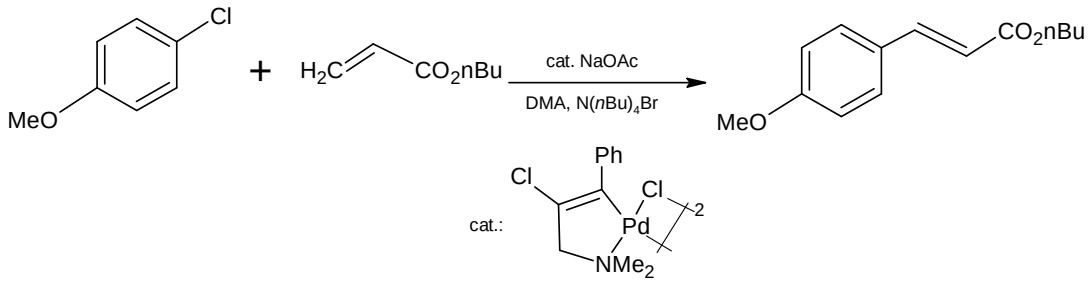

Scheme 1.15 The Heck coupling of *p*-chloroanisole and *n*-butyl acrylate.[57]

The major drawbacks in homogeneous catalysis remain catalyst separation and recyclability. Numerous attempts to circumvent these problems have been reported and have also been applied to palladacycles in catalysis. Examples include the work by Gomez in which an oxime palladacycle was derivatised with imidazolium moieties which could be immobilised in imidazolium-based ionic liquids.[58] A significant amount of catalytic activity was attributed to leaching of Pd from the support into the reaction medium. Bergbreiter and co-workers demonstrated the immobilisation of tridentate SCS-palladacycles onto a poly-ethylene glycol (PEG) polymer and evaluated these complexes in the Heck coupling of aryl iodides and various activated alkenes (Fig. 1.6).[59-60]

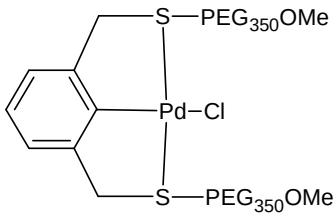

Fig. 1.6 PEG-supported SCS palladacycle evaluated in Heck coupling of aryl iodides and alkenes.[59-60]

The immobilised complexes catalysed the reaction with high activity and displayed recyclability. Mechanistic investigations found that the immobilised SCS-palladacycles serve as reservoirs of catalytically active Pd(0) species.[61] Palladacycles have also been immobilised on MCM-41[62-63] and other Si-based materials.[64]

The application of palladacycles in Heck coupling has been extended to encompass more complex substrates.[65-66] They have been successfully applied in the total synthesis of natural products and their chemistry in these catalytic transformations have been intensively investigated as outlined by a number of outstanding reviews.[3, 43, 67-68]

1.6.2 The Suzuki coupling reaction

The Suzuki- or Suzuki-Miyaura coupling reactions involves the Pd-catalysed reaction of arylboronic acids and organohalides in the presence of base (Scheme 1.16).

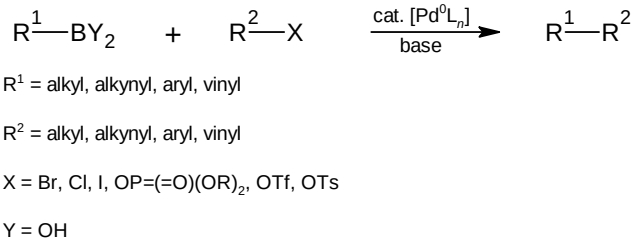

Scheme 1.16 A general scheme for the Suzuki reaction.

This C-C cross-coupling reaction was developed and outlined in a series of articles by Suzuki and Miyaura in the 1980's.[69-72] The catalyst employed in these reactions were typically Pd(II)-phosphine complexes in the presence of inorganic bases. The first report of the application of palladacycles in Suzuki-coupling was by Herrmann, employing the catalyst precursor in Figure 1.5.[49]

This sparked a revival in this particular area of catalysis with a tremendous increase in the number of reports highlighting the application of palladacycles in the Suzuki-coupling reaction.[3, 45, 73] As is the case for the Heck coupling reaction, trace amounts of palladium present in the system would catalyse the reaction. Furthermore, activated arylhalides would undergo the Suzuki-coupling in the presence of a palladium salt even at room temperature.[74]

Much research efforts have been devoted to the development of catalyst systems which allow the coupling of deactivated aryl chlorides and bromides.

Bedford employed a CN-palladacycle, with tricyclohexylphosphine (PCy_3) as an ancillary ligand, formed *in situ* as a catalyst precursor in the Suzuki coupling of aryl chlorides and phenylboronic acid (Fig 1.7).[75]

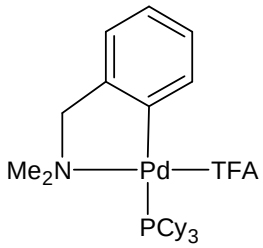

Fig. 1.7 Bedford CN-palladacycle employed in the Suzuki coupling of aryl chlorides and phenylboronic acid.[75]

Quantitative conversions and TON's exceeding the most active reported catalyst system previously reported were obtained.[76-78]

Schnyder *et. al.* demonstrated the ability of isolated mononuclear CN-palladacycles bearing secondary phosphane ligands to catalyse the Suzuki coupling of aryl chlorides, with activities comparable to that reported by Bedford.[53]

Nolan employed NHC-bearing palladacycles in the Suzuki-Miyaura coupling of activated and deactivated aryl chlorides with phenylboronic acid in the presence of NaO^tBu (Scheme 1.17).[79]

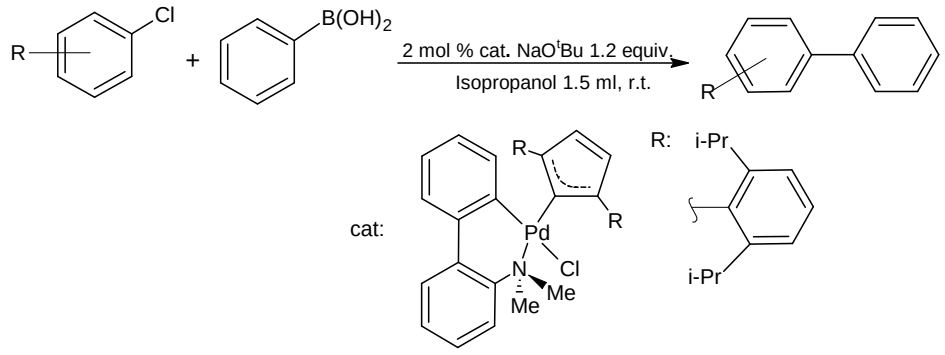

Scheme 1.17 The application of NHC-palladacycles in Suzuki-Miyaura coupling.[79]

The catalytic reaction proceeded at room temperature and required short reaction times to go to almost quantitative conversion. The catalytic system facilitated the reaction of sterically hindered coupling partners, which had always been a stumbling block when developing C-C coupling catalysts.[80]

The Bedford group have also demonstrated the ability of polystyrene-immobilised palladacycles to facilitate the Suzuki coupling of activated, non-activated and deactivated aryl chlorides (Fig. 1.8, **I** and **II**).[81]

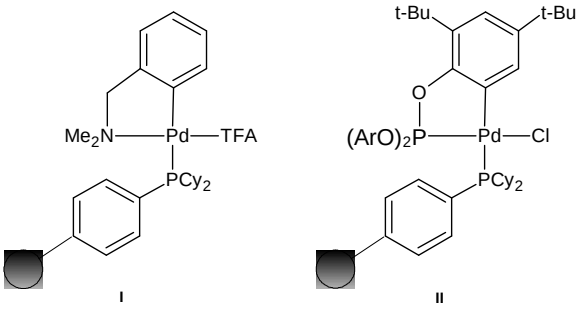

Fig. 1.8 Bedford PS-immobilised palladacycles, **I** and **II**.[81]

The immobilised palladacycles showed higher activity in some instances than their homogeneous analogues, despite the fact that the catalyst systems were non-recyclable. Minimal leaching of palladium from the support was an added advantage observed for this catalyst system, contrary to what had been observed for other immobilised palladacycle catalysts.[58]

1.6.3 Other cross-coupling reactions

Palladacycles have also been successfully employed as precatalysts in other C-C and C-X (where X = N or P) coupling reactions. Examples are in the Ullman,[82] Stille,[83] Sonogashira [84] and Buchwald-Hartwig amination reactions.[76-77]

de Meijere employed a Stille-Heck coupling sequence as a key step in the synthesis of steroidal δ-amino acids.[85] This transformation was effected by employing the Hermann-Beller palladacycle in Figure 1.5 with various substituents on the P-atom, in the presence of 1,4-bis(diphenylphosphino)butane (dppb) as co-ligand. The addition of co-ligand allowed for lower catalyst loadings and imparted greater stability to the catalytically active species present in the reaction medium.

Trzeciak and co-workers evaluated dinuclear triarylphosphito-derived palladacycles and their non-cyclometallated analogues in ionic liquids as solvent in the Sonogashira reaction of iodobenzene and phenyl acetylene (Scheme 1.18).[86]

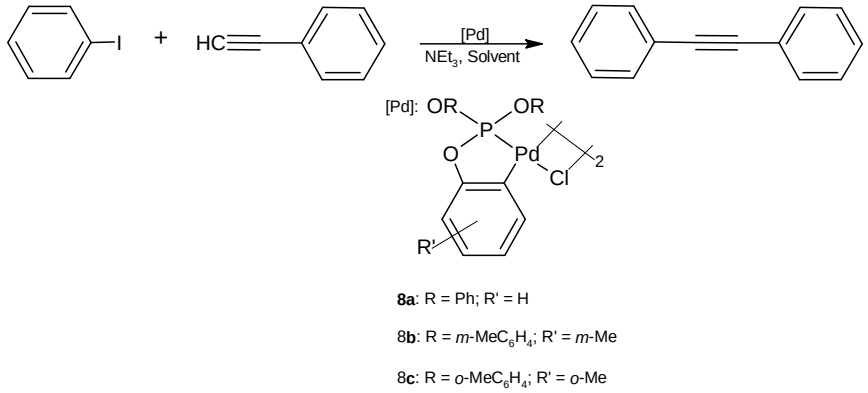

Scheme 1.18 Triarylphosphito palladacycles in the Sonogashira reaction.[86]

Complex **8b** with [bmim][PF_6] (bmim = 1-butyl-3-methylimidazolium cation) as solvent was found to be the most active catalyst with almost quantitative conversion of substrate. Ionic liquids as solvents were found to enhance the activity of the catalyst systems in comparison to employing traditional organic solvents as reaction medium.

The Nolan group recently demonstrated the applicability of CN-palladacycles bearing NHC-ligands in the Buchwald-Hartwig amination reaction.[87] The palladacycle (Fig. 1.9) promoted the amination of activated, neutral and deactivated aryl chlorides in the presence of KO^{t}Bu with remarkably high activity. The catalyst system also showed tolerability toward carboxylic acid and amide functionalities present in the substrates employed.

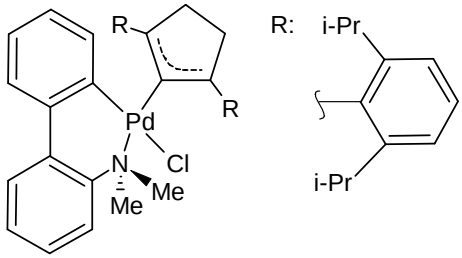

Fig. 1.9 NHC-palladacycle employed in the Buchwald-Hartwig amination reaction.[87]

1.7. Objectives of the study

The applicability of palladacycles as well-defined, air- and thermally-stable catalyst precursors has undergone tremendous growth over the past years. They exhibit exceptionally high activity and as outlined in the previous sections have been shown to catalyse the transformation of traditionally unreactive substrates.

Recent developments in our research group have implicated CN-palladacycles derived from imine ligands as active catalysts in the oligomerisation of ethylene, when activated with modified methyl aluminoxane (MMAO).[88] The complexes exhibited moderate activity in the oligomerisation reaction whilst high selectivity for C_8-oligomers was observed.

With this precedent in mind, the objective of the study was two-fold. Firstly, it was to prepare and characterise known and novel palladacycles and evaluate these complexes in the transformation of α-olefins to value-added products. The palladacycles were thus evaluated as catalyst precursors in the Heck coupling of iodobenzene and 1-octene as well as in the isomerisation of 1-hexene.

Secondly, it was to develop novel immobilised palladacycles. The Mapolie group has extensive experience in the immobilisation of catalysts on dendrimer supports.[89-91] The immobilised palladacycles would be evaluated in the catalytic transformation of α-olefins and their activity compared to their mononuclear analogues. It was further envisaged that the dendritic palladacycles could be recovered and recycled, mitigating the traditional limitations of homogenous catalyst systems.

Thus **Chapter 1** discusses the literature pertaining to the fundamental aspects of palladacycles, including mechanistic details. Also, their application in catalysis, particularly C-C coupling reactions, is discussed briefly.

Chapter 2 details the synthesis and characterisation of monofunctional ligands and their cyclopalladated derivatives, via C-H bond activation. The reactivity of these μ-Cl palladacycles toward mono- and bidentate tertiary phosphines were also investigated.

In **Chapter 3** the synthetic studies toward the preparation of dendrimer-supported palladacycles are described. The synthetic attempts led to the isolation of non-cyclometallated palladium metallodendrimers and their synthesis and characterisation is discussed.

Chapter 4 details a comparative study of the application of mononuclear palladacycles and palladium metallodendrimers as catalysts in the Heck coupling of

iodobenzene and 1-octene. Also, this chapter describes the evaluation of mononuclear palladacycles as efficient catalysts in the isomerisation of 1-hexene, with methyl aluminoxane (MAO) as a co-catalyst

References

1. I. Omae, *Chem. Rev*., 1979, **79**, 287-321.
2. A. C. Cope and R. Siekman, W., *J. Am. Chem. Soc.*, 1965, **87**, 3272-3273.
3. J. Dupont, C. S. Consorti and J. Spencer, *Chem. Rev.*, 2005, **105**, 2527-2572.
4. M. Ghedini, I. Aiello, A. Crispini, A. Golemme, M. La Deda and D. Pucci, *Coord. Chem. Rev*., 2006, **250**, 1373-1390.
5. W. D. Jones and F. J. Feher, *Acc. Chem. Res.*, 1989, **22**, 91-100.
6. R. H. Crabtree, J. M. Mihelcic and J. M. Quirk, *J. Am. Chem. Soc.*, 1979, **101**, 7738-7740.
7. W. D. Jones and F. J. Feher, *J. Am. Chem. Soc.*, 1985, **107**, 620-631.
8. A. D. Ryabov, *Chem. Rev*., 1990, **90**, 403-424.
9. J. Albert, R. M. Ceder, M. Gomez, J. Granell and J. Sales, *Organometallics*, 1992, **11**, 1536-1541.
10. J. Albert, J. Granell, J. Sales, X. Solans and M. Font-Altaba, *Organometallics*, 1986, **5**, 2567-2568.
11. P. L. Alsters, P. F. Engel, M. P. Hogerheide, M. Copijn, A. L. Spek and G. van Koten, *Organometallics*, 1993, **12**, 1831-1844.
12. A. J. Deeming and I. P. Rothwell, *J. Organomet. Chem.*, 1981, **205**, 117-131.
13. L. Kind, A. J. Klaus, P. Rys and V. Gramlich, *Helv. Chim. Acta*, 1998, **81**, 307-316.
14. J.-M. Valk, J. Boersma and G. van Koten, *J. Organomet. Chem.*, 1994, **483**, 213-216.

15. R. G. Pearson, *J. Am. Chem. Soc.*, 1963, **85**, 3533-3539.

16. A. C. Cope and E. C. Friedrich, *J. Am. Chem. Soc.*, 1968, **90**, 909-913.

17. B. N. Cockburn, D. V. Howe, T. Keating, B. F. G. Johnson and J. Lewis, *J. Chem. Soc., Dalton Trans.*, 1973, 404-410.

18. A. Avshu, R. D. O'Sullivan, A. W. Parkins, N. W. Alcock and R. M. Countryman, *J. Chem. Soc., Dalton Trans.*, 1983, 1619-1624.

19. Y. Fuchita and H. Tsuchiya, *Polyhedron*, 1993, **12**, 2079-2080.

20. Y. Fuchita, H. Tsuchiya and A. Miyafuji, *Inorg. Chim. Acta*, 1995, **233**, 91-96.

21. J. Vicente, I. Saura-Llamas and P. G. Jones, *J. Chem. Soc., Dalton Trans.*, 1993, 3619-3624.

22. J. Vicente, I. Saura-Llamas, M. G. Palin and P. G. Jones, *J. Chem. Soc., Dalton Trans.*, 1995, 2535-2539.

23. J. Vicente, I. Saura-Llamas, J. Cuadrado and M. C. Ramirez de Arellano, *Organometallics*, 2003, **22**, 5513-5517.

24. G. W. Parshall, *Acc. Chem. Res.*, 1970, **3**, 139-144.

25. H. Takahashi and J. Tsuji, *J. Organomet. Chem.*, 1967, **10**, 511-517.

26. M. I. Bruce, B. L. Goodall and F. G. A. Stone, *J. Chem. Soc., Dalton Trans.*, 1973, 558-559.

27. M. I. Bruce, B. L. Goodall and F. G. A. Stone, *J. Chem. Soc., Dalton Trans.*, 1978, 687-694.

28. K. Hiraki, Y. Fuchita and Y. Kage, *J. Chem. Soc., Dalton Trans.*, 1984, 99-101.

29. A. D. Ryabov, I. K. Sakodinskaya and A. K. Yatsimirsky, *J. Chem. Soc., Dalton Trans.*, 1985, 2629-2638.

30. M. Gomez, J. Granell and M. Martinez, *Organometallics*, 1997, **16**, 2539-2546.

31. M. Gomez, J. Granell and M. Martinez, *J. Chem. Soc., Dalton Trans.*, 1998, 37-43.

32. F. Estevan, P. Lahuerta, E. Peris, M. Angeles Ubeda, S. García-Granda, F. Gómez-Beltrán, E. Pérez-Carreño, G. González and M. Martínez, *Inorg. Chim. Acta*, 1994, **218**, 189-193.

33. G. Gonzalez, P. Lahuerta, M. Martinez, E. Peris and M. Sanau, *J. Chem. Soc., Dalton Trans.*, 1994, 545-550.

34. F. Estevan, G. Gonzalez, P. Lahuerta, M. Martinez, E. Peris and R. van Eldik, *J. Chem. Soc., Dalton Trans.*, 1996, 1045-1050.

35. D. L. Davies, S. M. A. Donald and S. A. Macgregor, *J. Am. Chem. Soc.*, 2005, **127**, 13754-13755.

36. M. Albrecht, *Chem. Rev.*, 2010, **110**, 576-623.

37. A. D. Ryabov, *Inorg. Chem.*, 1987, **26**, 1252-1260.

38. A. D. Ryabov and A. K. Yatsimirskii, *Inorg. Chem.*, 1984, **23**, 789-790.

39. J. K.-P. Ng, S. Chen, Y. Li, G.-K. Tan, L.-L. Koh and P.-H. Leung, *Inorg. Chem.*, 2007, **46**, 5100-5109.

40. G. Van Koten, *Pure and Applied Chemistry*, 1989, **61**, 1681-1694.

41. P. K. Santra and C. R. Saha, *J. Mol. Catal.*, 1987, **39**, 279-292.

42. A. Bose and C. R. Saha, *J. Mol. Catal.*, 1989, **49**, 271-283.

43. I. P. Beletskaya and A. V. Cheprakov, *Chem. Rev.*, 2000, **100**, 3009-3066.

44. I. P. Beletskaya and A. V. Cheprakov, *J. Organomet. Chem.*, 2004, **689**, 4055-4082.

45. J. Dupont, M. Pfeffer and J. Spencer, *Eur. J. Inorg. Chem.*, 2001, 1917-1927.

46. T. Mizoroki, K. Mori and A. Ozaki, *Bull. Chem. Soc. Jpn.*, 1971, **44**, 581-581.

47. R. F. Heck and J. P. Nolley, *J. Org. Chem.*, 1972, **37**, 2320-2322.

48. W. A. Herrmann, C. Brossmer, K. Öfele, C.-P. Reisinger, T. Priermeier, M. Beller and H. Fischer, *Angew. Chem. Int. Ed. Engl.*, 1995, **34**, 1844-1848.

49. M. Beller, H. Fischer, W. A. Herrmann, K. Öfele and C. Brossmer, *Angew. Chem. Int. Ed. Engl.*, 1995, **34**, 1848-1849.

50. A. S. Gruber, D. Pozebon, A. L. Monteiro and J. Dupont, *Tetrahedron Lett.*, 2001, **42**, 7345-7348.

51. A. H. M. de Vries, J. M. C. A. Mulders, J. H. M. Mommers, H. J. W. Henderickx and J. G. de Vries, *Organic Letters*, 2003, **5**, 3285-3288.

52. M. T. Reetz and J. G. de Vries, *Chem. Commun.*, 2004, 1559-1563.

53. A. Schnyder, A. F. Indolese, M. Studer and H.-U. Blaser, *Angew. Chem. Int. Ed.*, 2002, **41**, 3668-3671.

54. A. Ehrentraut, A. Zapf and M. Beller, *Synlett*, 2000, 1589-1592.

55. A. Schnyder, T. Aemmer, Adriano F. Indolese, U. Pittelkow and M. Studer, *Adv. Synth. Catal.*, 2002, **344**, 495-498.

56. S. Iyer and A. Jayanthi, *Synlett*, 2003, 1125-1128.

57. C. S. Consorti, M. L. Zanini, S. Leal, G. Ebeling and J. Dupont, *Organic Letters*, 2003, **5**, 983-986.

58. A. Corma, H. García and A. Leyva, *Tetrahedron*, 2004, **60**, 8553-8560.

59. D. E. Bergbreiter, P. L. Osburn and Y.-S. Liu, *J. Am. Chem. Soc.*, 1999, **121**, 9531-9538.

60. D. E. Bergbreiter and S. Furyk, *Green Chem.*, 2004, **6**, 280-285.

61. D. E. Bergbreiter, P. L. Osburn and J. D. Frels, *Adv. Synth. Catal.*, 2005, **347**, 172-184.

62. C. Venkatesan and A. P. Singh, *Catal. Lett.*, 2003, **88**, 193-197.

63. C. Venkatesan and A. P. Singh, *J. Catal.*, 2004, **227**, 148-163.

64. K. Yu, W. Sommer, M. Weck and C. W. Jones, *J. Catal.*, 2004, **226**, 101-110.

65. B. D. Dangel, K. Godula, S. W. Youn, B. Sezen and D. Sames, *J. Am. Chem. Soc.*, 2002, **124**, 11856-11857.

66. B. Sezen, R. Franz and D. Sames, *J. Am. Chem. Soc.*, 2002, **124**, 13372-13373.

67. A. B. Dounay and L. E. Overman, *Chem. Rev.*, 2003, **103**, 2945-2964.

68. L. F. Tietze, H. Ila and H. P. Bell, *Chem. Rev.*, 2004, **104**, 3453-3516.

69. N. Miyaura, T. Yanagi and A. Suzuki, *Synth. Commun.*, 1981, **11**, 513 - 519.

70. N. Miyaura, K. Yamada, H. Suginome and A. Suzuki, *J. Am. Chem. Soc.*, 1985, **107**, 972-980.

71. N. Miyaura, T. Ishiyama, M. Ishikawa and A. Suzuki, *Tetrahedron Lett.*, 1986, **27**, 6369-6372.

72. N. Miyaura, T. Ishiyama, H. Sasaki, M. Ishikawa, M. Sato and A. Suzuki, *J. Am. Chem. Soc.*, 1989, **111**, 314-321.

73. J. Dupont, C. S. Consorti and J. Spencer, in *The Chemistry of Pincer Compounds*, Elsevier Science B.V., Amsterdam, 2007, pp. 1-24.

74. D. Zim, A. L. Monteiro and J. Dupont, *Tetrahedron Lett.*, 2000, **41**, 8199-8202.

75. R. B. Bedford and C. S. J. Cazin, *Chem. Commun.*, 2001, 1540-1541.

76. D. W. Old, J. P. Wolfe and S. L. Buchwald, *J. Am. Chem. Soc.*, 1998, **120**, 9722-9723.

77. J. P. Wolfe and S. L. Buchwald, *Angew. Chem. Int. Ed.*, 1999, **38**, 2413-2416.

78. J. P. Wolfe, R. A. Singer, B. H. Yang and S. L. Buchwald, *J. Am. Chem. Soc.*, 1999, **121**, 9550-9561.

79. O. Navarro, R. A. Kelly and S. P. Nolan, *J. Am. Chem. Soc.*, 2003, **125**, 16194-16195.

80. G. Altenhoff, R. Goddard, C. W. Lehmann and F. Glorius, *Angew. Chem. Int. Ed.*, 2003, **42**, 3690-3693.

81. R. B. Bedford, S. J. Coles, M. B. Hursthouse and V. J. M. Scordia, *Dalton. Trans.*, 2005, 991-995.

82. D. A. Alonso, L. Botella, C. Nájera and M. C. Pacheco, *Synthesis*, 2004, 1713-1718.

83. W. A. Herrmann, K. Öfele, D. v. Preysing and S. K. Schneider, *J. Organomet. Chem.*, 2003, **687**, 229-248.

84. R. Chinchilla and C. Nájera, *Chem. Rev.*, 2007, **107**, 874-922.

85. H. W. Sünnemann, A. Hofmeister, J. Magull and A. d. Meijere, *Chem, Eur. J.*, 2006, **12**, 8336-8344.

86. I. Błaszczyk, A. Trzeciak and J. Ziółkowski, *Catal. Lett.*, 2009, **133**, 262-266.

87. J. Broggi, H. Clavier and S. P. Nolan, *Organometallics*, 2008, **27**, 5525-5531.

88. N. Mungwe, M.Sc. Thesis University of the Western Cape, **2007**.

89. G. Smith, R. Chen and S. Mapolie, *J. Organomet. Chem.*, 2003, **673**, 111-115.

90. R. Malgas-Enus, S. F. Mapolie and G. S. Smith, *J. Organomet. Chem.*, 2008, **693**, 2279-2286.

91. J. N. Mugo, S. F. Mapolie and J. L. van Wyk, *Inorg. Chim. Acta*, 2010, **363**, 2643-2651.

Chapter 2: Synthesis and Reactivity of Palladacycles derived from Imine Ligands

2.1 Introduction

2.1.1 Schiff base ligands.

The reaction between a carbonyl compound and an amine was first observed by Hugo Schiff,[1] the product of which was termed a Schiff base (Scheme 2.1).

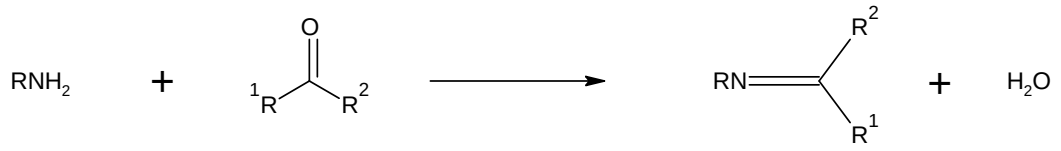

R: alkyl, aryl etc. R^1: alkyl, aryl etc.

R^2: alkyl, aryl etc

Scheme 2.1 General Schiff base condensation reaction.

Their ease of synthesis, the ability to coordinate to virtually all types of metals regardless of oxidation state and the enhanced stability imparted to the ensuing metal complexes have elevated Schiff base ligands to the status of "privileged ligands".[2] Their design allows for the incorporation of various steric and electronically modulating functional groups as well as chiral elements thereby facilitating the synthesis of ligand-metal systems with unique physical and chemical properties. The literature is flooded with reports detailing the synthesis and application of metal complexes bearing Schiff base ligands. Examples include amongst others manganese,[3-4] vanadium, [5] cadmium, zinc, nickel and copper complexes (Fig 2.1).[4]

In the context of cyclopalladation Schiff base ligands have also proven themselves amenable to palladacycle synthesis. Careful consideration of ligand design and reaction conditions has allowed the regioselective synthesis of palladacycles. This has been

exemplified by the work of the Granell group.[6-8] Of significance was their work on the cyclopalladation of mesitylbenzylideneamines with $Pd(OAc)_2$ (see Chapter 1, Section 1.3) in which they demonstrated the thermodynamic preference for the formation of *endo* palladacycles even if it resulted in a palladacycle ring size > 5 atoms.

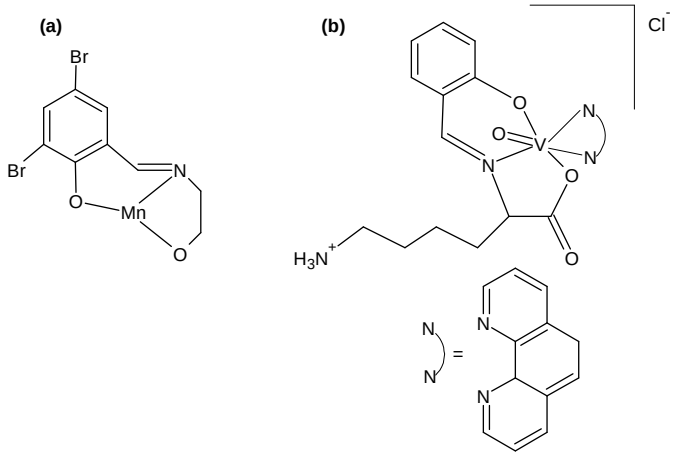

Fig. 2.1 Examples of metal complexes bearing Schiff base ligands; (a) manganese and (b) vanadium.

More recently, regioselectivity in cyclopalladation reactions was further demonstrated by work of the Vila group.[9]

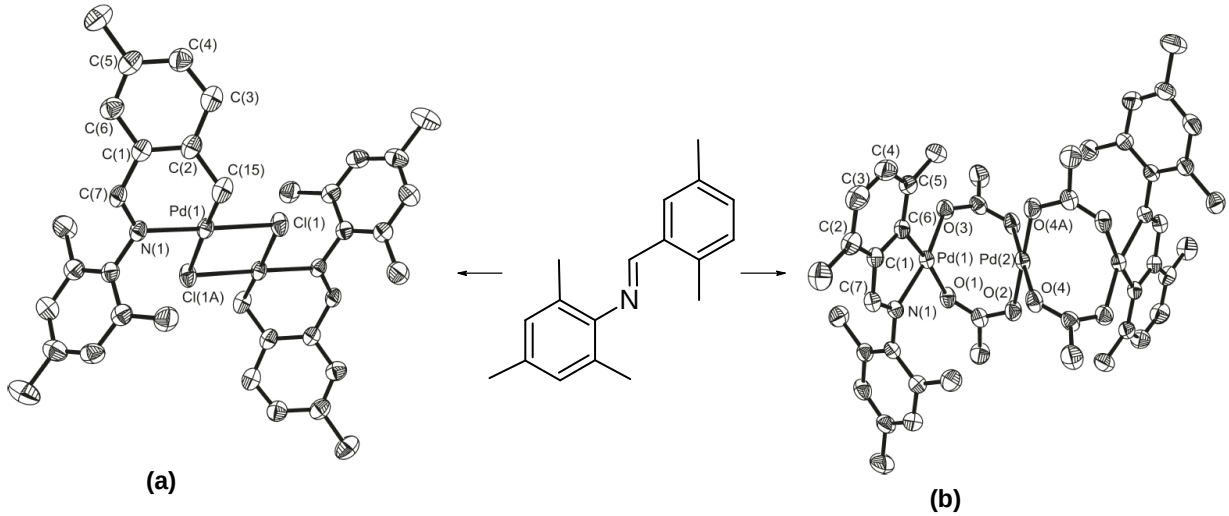

Fig. 2.2 Regioselective cyclopalladation of 2,5-dimethyl-2,4,6-trimethylphenylamine.[9]

They examined the cyclopalladation behaviour of 2,5-dimethylbenzylidene-2,4,6-trimethylphenylamine with $Pd(OAc)_2$ in toluene and acetic acid (Fig. 2.2). In toluene as solvent at ambient temperature, they isolated complexes formed by aromatic C-H activation (Fig. 2.2, **b**). In acetic acid under reflux conditions complexes formed by aliphatic C-H activation were the sole products (Fig. 2.2, **a**). In all cases, only *endo* palladacycles were isolated.

Here we report the synthesis and characterisation of monofunctional Schiff base ligands and their application as scaffolds in palladacycle synthesis.

2.2 Results and Discussion.

2.2.1 Monofunctional Schiff base ligand synthesis.

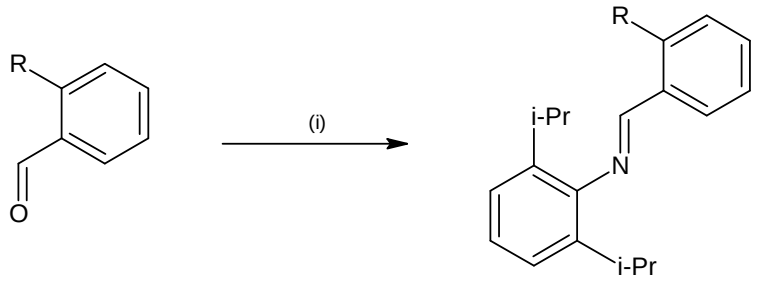

L1: R = H

L2: R = 2-Cl

L3: R = 2-Br

L4: R = 4-Me

(i) 1mol eq. 2, 6-diisopropylaniline, EtOH, r.t., 24hrs

Scheme 2.2 A general scheme for the preparation of the monofunctional ligands.

The monofunctional ligands, **L1-L4**, were prepared by Schiff base condensation of 2,6-diisopropylaniline with various mono-substituted aldehydes (Scheme 2.2) The ligands

were isolated in high yields as yellow crystalline solids and displayed solubility in polar organic solvents. The ligands were found to be stable both in solution and in the solid state. Ligands **L1**,[10] **L2**,[11] and **L3**[10] have been reported previously whereas **L4** is novel (Fig. 2.3).

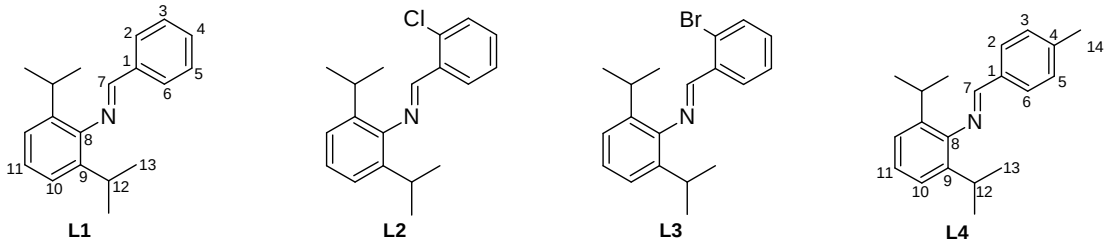

Fig. 2.3 A schematic representation of the synthesised ligands with numbering for NMR analysis.

The monofunctional ligands were characterised by a range of analytical techniques. FT-IR analysis indicated the formation of the desired condensation product as evidenced by the absence of characteristic $\upsilon_{C=O}$ bands of the aldehyde starting material and the formation of absorption bands corresponding to the $\upsilon_{C=N}$ of the imine products in the range 1620-1640 cm^{-1} (Table 2.1).

Table 2.1 Analytical data pertaining to ligand synthesis.

Ligand	FT-IR ($\upsilon_{C=N}$, cm^{-1})[a]	ESI-MS (*m/z*)[b]	Melting Point (°C)[c]
L1	1638	266	63-64
L2	1624	301	52-53
L3	1624	345	78-79
L4	1638	280	93-94

[a] Recorded as neat spectra on a ZnSe crystal, employing an ATR accessory. [b] Reported ion corresponds to the proton adduct of the molecular ion, $[M + H]^+$, [c] Melting points recorded are uncorrected.

Table 2.2 ^{1}H NMR spectral data of **L1**-**L4**.[a]

Compd.	C***H***=N	Aromatic Region	Aliphatic Region		
			(Me)$_2$C*H*	**Ar-*Me***	**CH(*Me*)$_2$**
L1	8.22 (s, 1H, H^{7})	7.94 (m, 2H, H^{2,6,3}); 7.54 (m, 3H, H^{3,4,5}); 7.17 (m, 3H, H^{10,11})	3.00 (dt, 2H, H^{12}, $^{3}J_{H-H}$ 6.82 Hz)		1.19 (d, 12H, H^{12,13}, $^{3}J_{H-H}$ 7.02 Hz)
L2	8.76 (s, 1H, H^{7})	8.37 (d, 1H, H^{3}, $^{2}J_{H-H}$ = 8.58 Hz); 7.53 (m, 3H, H^{4,5,6}); 7.24 (m, 3H, H^{10,11})	3.08 (dt, 2H, H^{12}, $^{3}J_{H-H}$ 6.82 Hz)		1.30 (d, 12H, H^{12,13}, $^{3}J_{H-H}$ 7.02 Hz)
L3	8.60 (s, 1H, H^{7})	8.28 (dd, 1H, H^{3}, $^{3}J_{H-H}$ 7.78 Hz, $^{4}J_{H-H}$ 1.91 Hz); 7.66 (dd, 1H, H^{6}, $^{3}J_{H-H}$ 7.78 Hz, $^{4}J_{H-H}$ 1.17 Hz); 7.47 (t, 1H, H^{4}, $^{3}J_{H-H}$ 7.34 Hz); 7.37 (dt, 1H, H^{5}, $^{3}J_{H-H}$ 7.92 Hz, $^{4}J_{H-H}$ 1.91 Hz); 7.19 (m, 3H, H^{10,11})	3.00 (dt, 2H, H^{12}, $^{3}J_{H-H}$ 6.82 Hz)		1.20 (d, 12H, H^{12,13}, $^{3}J_{H-H}$ 7.02 Hz)
L4	8.18 (s, 1H, H^{7})	7.83 (d, 2H, H^{2,6}); 7.34 (d, 2H, H^{3,5}, 8.07 Hz); 7.16 (m, 3H, H^{10,11})	3.00 (dt, 2H, H^{12}, $^{3}J_{H-H}$ 6.82 Hz)	2.46 (s, 3H, H^{14})	1.18 (d, 12H, H^{12,13}, $^{3}J_{H-H}$ 7.02 Hz)

[a] Spectra run in $CDCl_3$ at 25 °C. Chemical shifts reported as δ ppm values, referenced relative to the residual solvent peak. Superscripts denote protons as per numbering scheme (Fig. 2.3).

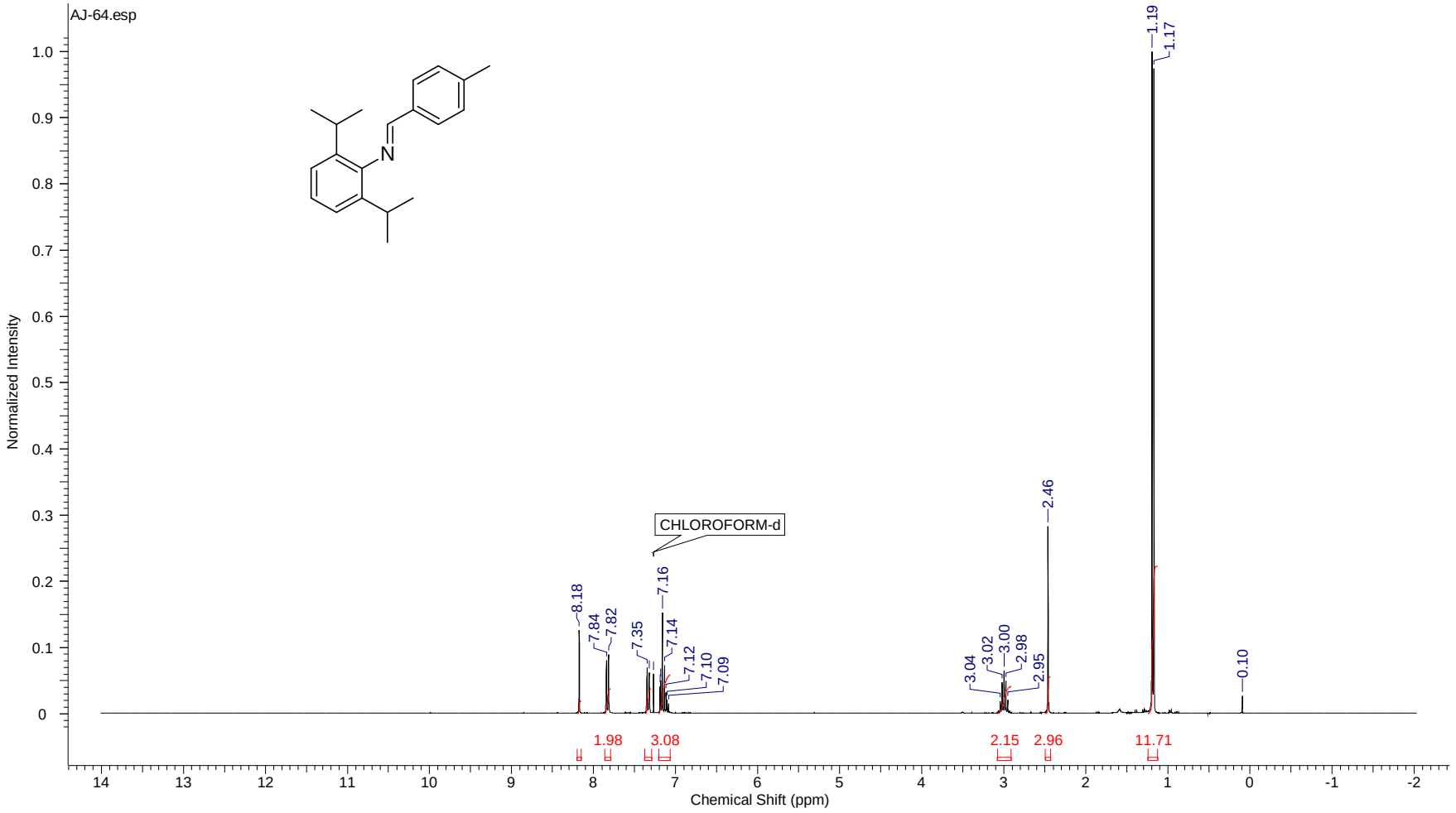

Fig. 2.4 ^{1}H NMR spectrum of 4-methylbenzylidene-2,6-diisopropylphenylamine, **L4**.

The imine proton resonances in the ^{1}H NMR spectra of the ligands were observed in the range δ 8.18-8.76 ppm (Table 2.2). For ligands **L2** and **L3** (halide substituents) the imine resonances are shifted more downfield in comparison to **L1** and **L4**. This difference may be attributed to the inductive effect of the halogen substituents.[12] The aromatic region of the ^{1}H NMR spectra showed resonances typical of either 1,2- or 1,4-disubstitution (Fig. 2.4). In the aliphatic region we observed the equivalence of the ^{i}Pr groups, observed as a doublet integrating for twelve protons, due to free rotation about the C-N single bond. In the ^{13}C NMR spectra of the ligands the imine carbon resonances were observed in the range 158-162 ppm. ESI-MS analysis showed peaks corresponding to proton adducts of the molecular ion, $[M + H]^{+}$, providing additional confirmation that the ligands were successfully prepared (Table 2.1).

2.2.2 Cyclopalladation of Schiff base ligands.

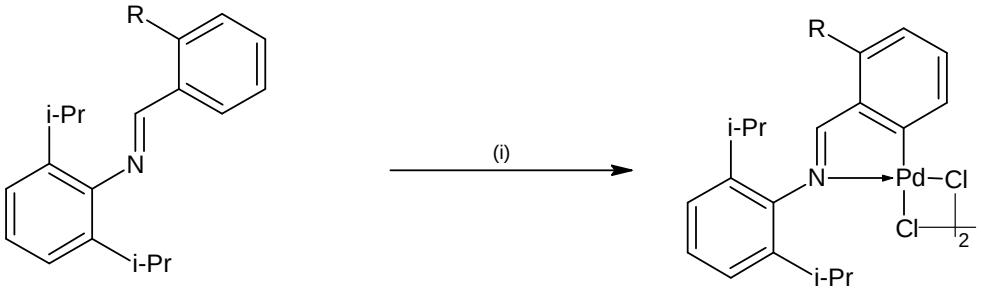

L1: R = H
L2: R = 2-Cl
L3: R = 2-Br
L4: R = 4-Me

C1: R = H
C2: R = 2-Cl
C3: R = 2-Br
C4: R = 4-Me

(i) 1 mol. eq $(MeCN)_2PdCl_2$, 2 mol eq. NaOAc, DCM, 6-21 hrs, r.t.,

Scheme 2.3 A general scheme for the synthesis of chloro-bridged palladacycles.

The chloro-bridged palladacycles, **C1-C4**, were prepared by the reaction of the palladium salt bis(acetonitrile) palladium dichloride, $(MeCN)_2PdCl_2$, with **L1-L4**, in the presence of excess NaOAc as a base at room temperature (Scheme 2.3). The cyclometallation

proceeds via electrophilic C-H activation of the aromatic ring. The presence of an intermolecular base is crucial in facilitating palladacycle formation as evidenced by the isolation of starting material in the absence of base. Davies and co-workers demonstrated the effect of $^{-}$OAc-ions when employing $Pd(OAc)_2$ as palladium precursor (see Chapter 1, Section 1.5.1) using DFT calculations.[13] Reaction time also played an important role in isolating the desired products, with too short reaction times resulting in the isolation of coordination complexes of the type $[PdCl_2(imine)_2]$. Using a previously reported synthetic approach in which MeOH was employed as solvent resulted in significant decomposition of the palladium precursor to palladium black.[11] Dichloromethane was thus employed as reaction solvent. This revised synthetic approach resulted in the isolation μ-Cl palladacycles with product yields ranging between 70-85 %. The palladacycles were isolated as yellow air-stable solids. Complexes **C1** and **C4** were found to be soluble in chlorinated organic solvents whereas **C2** and in particular **C3** displayed only partial solubility in chlorinated organic solvents.

The complexes were characterised by a range of analytical techniques. In the FT-IR spectra of the complexes the imine absorption band was observed to shift to lower wavenumbers in the range 1585-1598 cm^{-1} (Table 2.3), in comparison to that of the free ligands. This was indicative of coordination of the N-atom of the imine moiety to the metal centre which resulted in a decrease in the double bond character of the imine functionality.[14]

The ^{1}H NMR spectra of the complexes showed an upfield shift of the imine proton resonances in the range of δ 7.69-8.14 ppm, in comparison to that of the free ligands (Table 2.4).

Furthermore, in the aromatic region the resonance of the *ortho*-H atom of the benzylidene ring disappeared and a complicated series of multiplets were observed

integrating for twelve (as is the case for **C2**, **C3** and **C4**) and fourteen protons (as is the case for **C1**) respectively (Fig. 2.5).

Table 2.3 Analytical data pertaining to the chloro-bridged palladacycles.

Complex	FT-IR ($\upsilon_{C=N}$, cm^{-1})[a]	Decomposition Temperature (°C)[b]
C1	1599	240-245
C2	1585	> 320
C3	1585	> 320
C4	1598	270-275

[a] Recorded as neat spectra on a ZnSe crystal, employing an ATR accessory. [b] Melting points recorded are uncorrected. No melting prior to decomposition was observed

This was indicative of the fact that cyclopalladation took place preferentially via C-H bond activation.[15] In the aliphatic region the methine proton resonances of the isopropyl substituents were observed to shift downfield as a result of complexation of the ligand to the metal centre and the *Me*-groups of the ^{i}Pr unit was split into two doublets integrating for a total of six protons each (Fig. 2.5).

Analogous resonance shifts to those observed in the ^{1}H NMR spectra were observed when subjecting the μ-Cl complexes to ^{13}C NMR analysis. The imine carbon atom resonances shifted to the high field region upon complexation and was observed in the range δ 175-177 ppm. Also, the carbon atom bound to palladium was observed to resonate in the range δ 142-146 ppm and provided further evidence to the fact that cyclopalladation occurred.[10, 16]

Suitable crystals of complex **C2** for SCD analysis were obtained by the slow evaporation of a dichloromethane:hexane mixture. The complex crystallised as a discrete molecule with one half of the molecule in the asymmetric unit. Crystallographic data (Table 2.8) as well as selected bond lengths and angles are tabulated (Table 2.9).

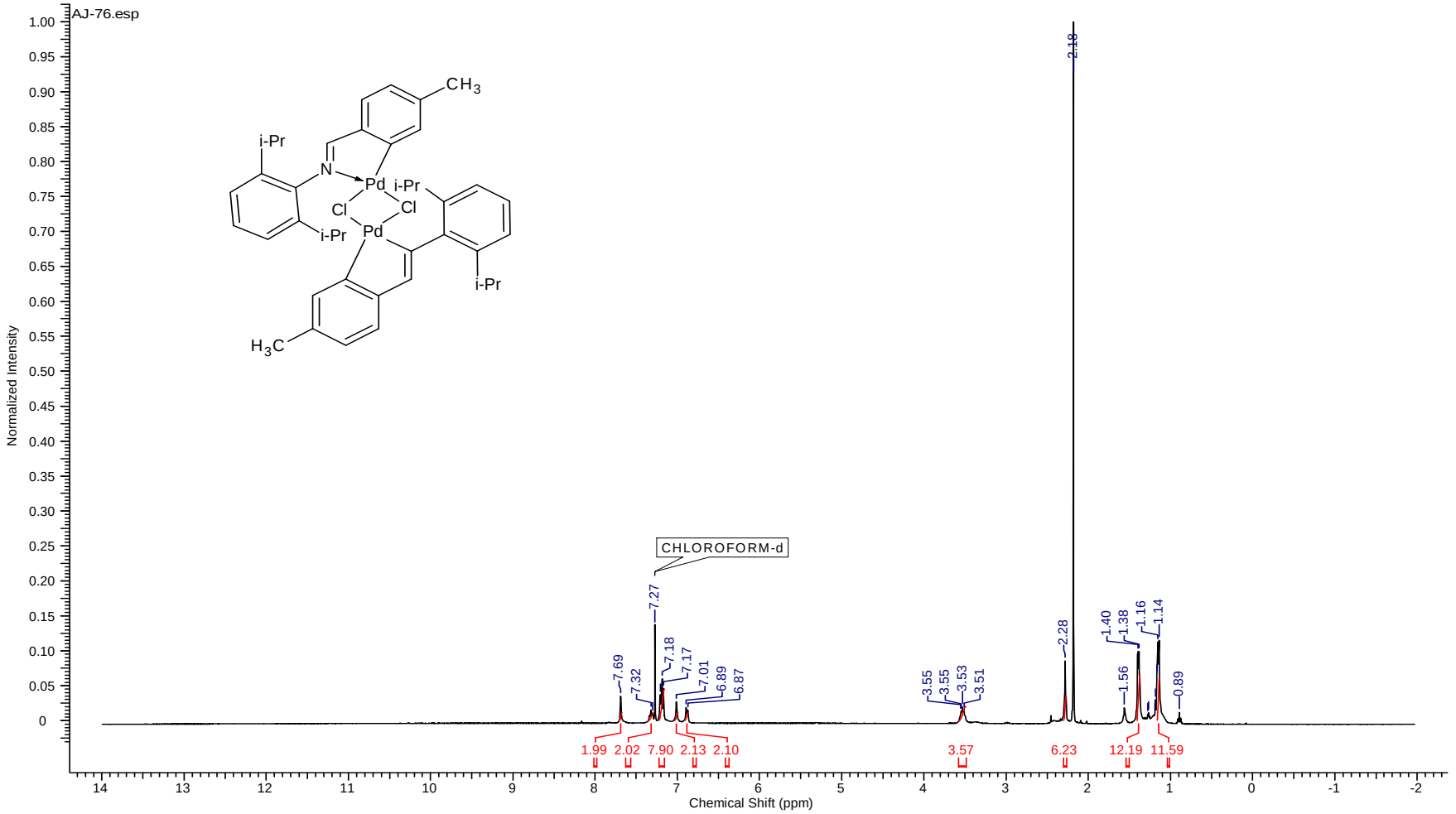

Fig. 2.5 ^{1}H NMR spectrum of complex **C4** recorded in $CDCl_3$ at 25 °C.

Table 2.4 ^{1}H NMR spectral data of complexes **C1-C4**.[a]

Compd.	C*H*=N	Aromatic Region	Aliphatic Region		
			(Me)$_2$C*H*	**Ar-*Me***	**CH(*Me*)$_2$**
C1	7.75 (s, 2H)	7,19 (m, 7H); 7.11 (m, 7H)	3.53 (dt, 4H, $^{3}J_{H-H}$ 6.63 Hz)		1.39 (d, 6H, $^{3}J_{H-H}$ 6.04 Hz); 1.14 (d, 6H, $^{3}J_{H-H}$ 6.82 Hz)
C2	8.14 (s, 2H)	7.34 (m, 2H); 7.20 (m, 4H); 7.01 (m, 6H)	3.49 (dt, 4H $^{3}J_{H-H}$ 6.43 Hz)		1.39 (d, 6H, $^{3}J_{H-H}$ 6.43 Hz); 1.19 (d, 6H, $^{3}J_{H-H}$ 6.82 Hz)
C3	8.13 (s, 2H)	7.34 (m, 2H); 7.20 (m, 8H); 6.87 (m, 2H)	3.49 (dt, 4H, $^{3}J_{H-H}$ 6.31 Hz)		1.38 (d, 6H, $^{3}J_{H-H}$ 6.60 Hz); 1.17 (d, 6H, $^{3}J_{H-H}$ 6.60 Hz)
C4	7.69 (s, 2H)	7.32 (m, 2H); 7.19 (m, 6H); 7.01 (m, 2H); 6.90 (m, 2H)	3.53 (dt, 4H, $^{3}J_{H-H}$ 6.04 Hz)	2.28 (s, 6H)	1.39 (d, 6H, $^{3}J_{H-H}$ 7.02 Hz, 1.18 (d, 12H, $^{3}J_{H-H}$ 7.02 Hz)

[a] Spectra run in $CDCl_3$ at 25 °C. Chemical shifts reported as δ ppm values, referenced relative to residual proton signals of the solvent.

The molecule consists of two palladium centres bridged by two chloride atoms. The remainder of the coordination sphere of the metal is occupied by the Schiff base ligand, coordinated through the benzylidene carbon and imine nitrogen atom to form the five-membered chelate ring (Fig. 2.6).

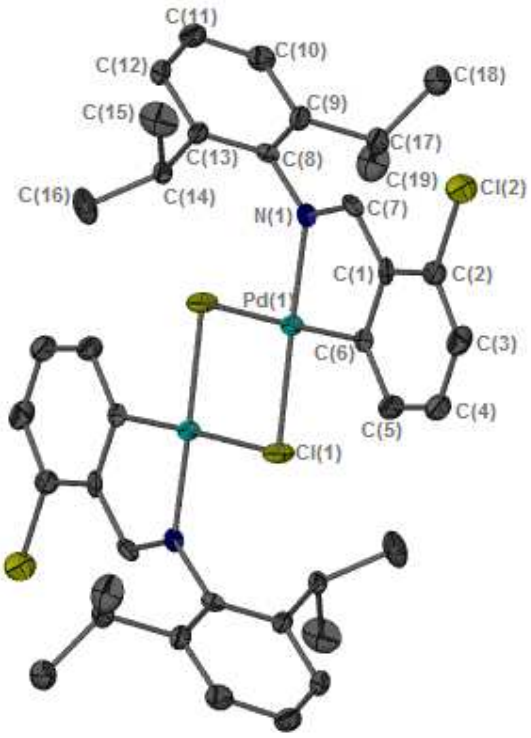

Fig. 2.6 Molecular structure of complex **C2**, drawn with 50 % probability ellipsoids. Hydrogen atoms omitted for clarity.

The geometry around the metal centre is essentially square planar as evidenced by the sum of the angles about the palladium centre. The most noticeable distortion corresponds to the C(6)-Pd-N(1) angle of the cyclometallated ring of 81.5(2) ° which is as a result of chelation of the ligand to the metal centre. The Pd-C bond length of 1.979(6) Å is somewhat shorter than the expected value based on the sum of the covalent radii whereas the Pd-N bond

length of 2.028(5) Å is longer than the expected value for the sum of the van der Waals radii.[17] This difference is due to the differing *trans* influence of the two coordinating atoms. This is further demonstrated by the difference in the Pd-Cl bond lengths. The Pd-Cl(1) bond *trans* to the N-atom of 2.447(2) Å is longer than the Pd-Cl bond *trans* to the C-atom, which has a length of 2.329(2) Å. The Pd-Pd interatomic distance of 3.477 Å precludes any Pd-Pd interaction. All bond lengths and angles fall into the range observed for analogous μ-Cl palladacycles.[10]

2.2.3 The reactivity of chloro-bridged palladacycles toward monodentate phosphines.

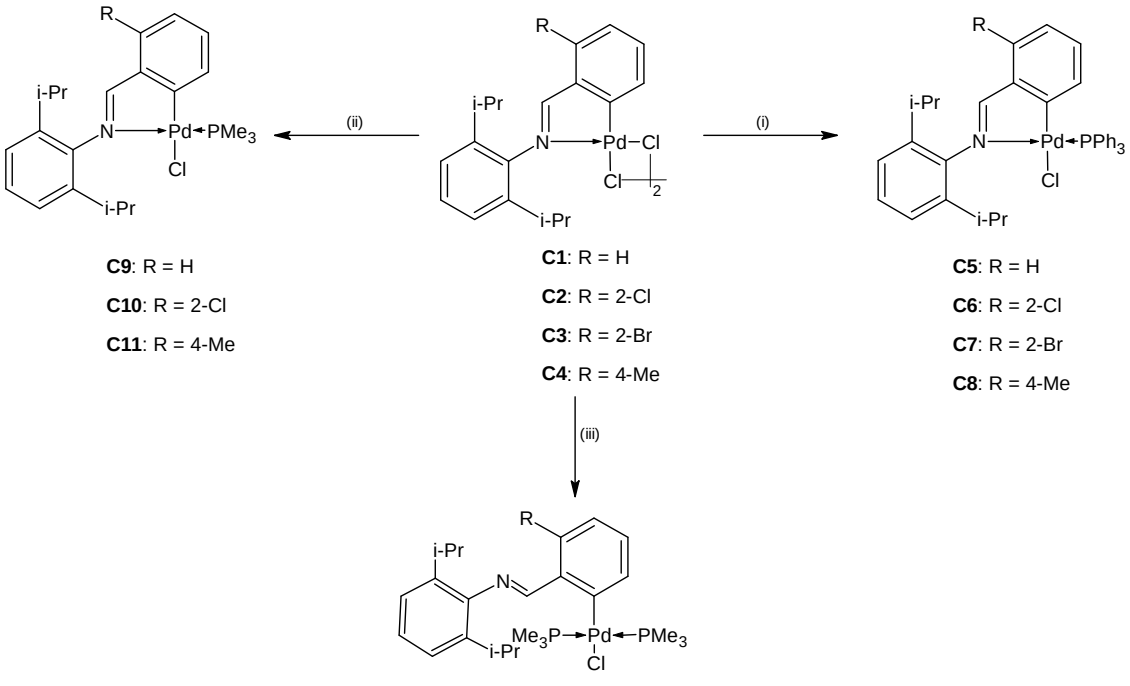

(i) 2 mol eq. PPh_3, DCM, 1hr, r.t. (ii) 2 mol eq. PMe_3, DCM, 1hr, r.t. (iii) excess PMe_3, DCM, 1hr, r.t.

Scheme 2.4 A general scheme of the reactivity of chloro-bridged palladacycles.

The chloro-bridged palladacycles, **C1-C4**, were reacted with tertiary phosphines, varying in their steric and electronic properties (Scheme 2.4). The phosphine-substituted palladacycles were isolated as pale-yellow air- and moisture-stable solids in high yields. The complexes displayed solubility in chlorinated organic solvents but were found to be insoluble in alkanes, ethers and alcohols. Due to time constraints only certain μ-Cl palladacycles were reacted with trimethylphosphine.

In the FT-IR spectrum of the mononuclear complexes, a slight shift to higher wavenumbers of the imine absorption band was observed, in comparison to the μ-Cl palladacycles (Table 2.5). This was due to the relative increase in σ-donating ability of the phosphine ligand, when compared to Cl^- as a ligand. This resulted in an increase in the double bond character of the C=N double bond. Also, strong absorption bands in the range 1430-1440 cm^{-1} and 680-690 cm^{-1} were observed in the FT-IR spectra of the complexes which were attributed to the C-P and Pd-P bond stretching vibrations respectively. These observations provided further evidence that coordination of the phosphine ligand to the metal centre had occurred.[6-8] For complexes **C12** and **C13**, the imine absorption band was observed at 1620 and 1622 cm^{-1} respectively, which was in the range observed for the free ligands. This demonstrated the fact that in these complexes the imine N-atom was no longer coordinated to the palladium metal centre but was displaced by a second phophine.[11] Also, these results demonstrated the basicity difference between triphenylphosphine and trimethylphosphine as ligands.[8]

In the ^1H NMR spectra of the mononuclear cyclometallated complexes, **C5-C11**, the imine proton resonance was observed to shift to higher field in comparison to the μ-Cl complexes, with the triphenylphosphine complexes shifting more downfield than their trimethylphosphine analogues (Table 2.6, Fig. 2.7). This was attributed to an increase in the

basicity of the trimethylphosphine ligand, which resulted in an increase in e^--density on the palladium centre. This in turn resulted in back-donation of excess e^--density onto the imine functional group thereby shielding the imine proton from the effect of the externally applied magnetic field.[12] Also, the imine proton resonance was observed to be split into a doublet integrating for one proton in the range δ 7.96-8.61 ppm. This was due to four-bond coupling ($^4J_{H\text{-}P}$) of the imine proton to the phosphorus atom of the tertiary phosphine ligand.

Table 2.5 Analytical data pertaining to the mononuclear cyclometallated and non-cyclometallated complexes.

Compound	FT-IR ($\upsilon_{C=N}$, cm^{-1})[a]	ESI-MS (*m/z*)[b]	Decomposition Temperature (°C)[c]
C5	1604	633	226-227
C6	1605	667	244-247
C7	1606	711	258-261
C8	1608	648	214-217
C9	1612	446	181-184
C10	1609	481	180-185
C11	1608	460	178-183
C12[d]	1620	602	192-196
C13[d]	1622	537	168-171

[a] Recorded as neat spectra on a ZnSe crystal, employing an ATR accessory. [b] Recorded in positive ion mode. Reported ion corresponds to $[M - Cl]^+$. [c] Melting point reported as uncorrected. For **C5-C11**, decomposition without melting occurred. [d] For **C12-C13**, melting with decomposition > 250 °C.

The bridge-splitting reaction was noted to have a remarkable effect on the proton resonances associated with the ligand backbone. The H-atom *ortho* to the metallated carbon atom was observed to be the most shielded, particularly for **C5-C8**. This was as a result of the coordination of the triphenylphosphine ligand in a *cis* fashion relative to the metallated carbon atom. The phenyl protons experience anisotropic shielding by the aromatic rings, resulting in an upfield shift of these resonances.[7, 12] This effect was also observed for the Ar-Me group in complex **C8**. The *ortho* H-atom also exhibited $^4J_{H\text{-}P}$ coupling to the P-atom

of the tertiary phosphine which provided further evidence to the *cis* geometry of the phosphine ligand. The methine protons of the ^{i}Pr groups of complexes **C5-C11** were observed to resonate in the same region as that observed for complexes **C1-C4** and as such confirmed coordination of the imine N-atom to the palladium centre. For complexes **C9-C11** (Fig. 2.8), the appearance of a doublet integrating for a total of nine protons in the range δ 1.69-1.71 ppm in comparison to a doublet at δ 1.19 ppm for the free phosphine molecule provided evidence that a single trimethylphosphine molecule was coordinated to the palladium centre. As was the case for the methine protons, no significant shift in the resonances of the methyl protons of the ^{i}Pr group was observed which was indicative of the fact that no change in the imine N-atom coordination mode took place during the bridge-splitting reaction.

Analogous resonances to those of complexes **C1-C4** were observed in the ^{13}C NMR spectra of the cleaved complexes with the imine carbon resonance observed in the range δ 175-178 ppm, while the *o*-metallated carbon resonance was observed in the range δ 145-146 ppm. For **C12** and **C13** the imine carbon resonance was observed in the range δ 161-163 ppm, analogous to that of the free ligands, demonstrating that the imine N-atom was not coordinated to the palladium centre.

In the ^{31}P{^{1}H} NMR spectra of complexes **C5-C11** only a single resonance was observed in the range δ 41-43 ppm for the PPh_3-cleaved complexes and in the range δ -4 to -3 ppm and ~ -16 ppm for the cyclo- and non-cyclometallated PMe_3-cleaved complexes respectively (Table 2.7). The coordinated tertiary phosphine was observed to be high field shifted when compared to the free phosphine ligand. This provided further confirmation that the phosphine was in fact coordinated to the metal centre.[18-20]

Table 2.6 ^{1}H NMR data of the complexes **C5**-C**13**.[a]

Compd.	C***H***=N	Aromatic Region	Aliphatic Region			
			P(*Me*)$_3$	**(Me)$_2$C*H***	**Ar-*Me***	**CH(*Me*)$_2$**
C5	8.11 (d, 1H, $^{4}J_{H-P}$ 7.78 Hz)	7,71-7.78 (m, 6H, $^{3}J_{H-H}$ 6.75 Hz); 7.33-7.43 (m, 9H, $^{3}J_{H-H}$ 6.31 Hz); 7.14-7.23 (m, 3H, $^{3}J_{H-H}$ 5.87 Hz); 7.02 (t, 1H, $^{3}J_{H-H}$ 7.34 Hz); 6.70 (t, 1H, $^{3}J_{H-H}$ 7.34 Hz); 6.50 (t, 1H, $^{3}J_{H-H}$ 7.04 Hz)	-	3.42-3.53 (m, 2H, $^{3}J_{H-H}$ 6.75 Hz)	-	1.37 (d, 6H, $^{3}J_{H-H}$ = 6.90 Hz); 1.21 (d, 6H, $^{3}J_{H-H}$ =6.90 Hz)
C6	8.61 (d, 1H, $^{4}J_{H-P}$ 7.92 Hz)	7.69-7.77 (m, 6H, $^{3}J_{H-H}$ 6.75 Hz); 7.33-7.44 (m, 9H, $^{3}J_{H-H}$ 6.31 Hz); 7.15-7.23 (m, 3H, $^{3}J_{H-H}$ 6.75 Hz); 6.92 (d, 1H, $^{3}J_{H-H}$ 7.92 Hz); 6.61 (t, 1H, $^{3}J_{H-H}$ 7.78 Hz); 6.38 (t, 1H, $^{2}J_{H-H}$ 7.04 Hz)	-	3.40-3.49 (m, 2H, $^{3}J_{H-H}$ 6.90 Hz)	-	1.37 (d, 6H, $^{3}J_{H-H}$ = 6.43 Hz); 1.23 (d, 6H, $^{3}J_{H-H}$ = 6.90 Hz)
C7	8.61 (d, 1H, $^{4}J_{H-P}$ 7.78 Hz)	7.69-7.76 (m, 6H, $^{3}J_{H-H}$ 6.75 Hz); 7.33-7.44 (m, 9H, $^{3}J_{H-H}$ 7.34 Hz); 7.15-7.24 (m, 3H, $^{3}J_{H-H}$ 6.90 Hz); 7.10 (d, 1H, $^{3}J_{H-H}$ 6.90 Hz); 6.51 (t, 1H, $^{3}J_{H-H}$ 7.19 Hz); 6.42 (t, 1H, $^{3}J_{H-H}$ 6.90 Hz)	-	3.40-3.49 (m, 2H, $^{3}J_{H-H}$ 6.90 Hz)	-	1.37 (d, 6H, $^{3}J_{H-H}$ = 6.90 Hz); 1.23 (d, 6H, $^{3}J_{H-H}$ = 6.90 Hz)

[a] Spectra run in $CDCl_3$ at 25 °C. Chemical shifts are reported as δ ppm values, reference relative to protons of the residual solvent peak.

Table 2.6 ^{1}H NMR data of complexes **C5**-**C13** (continued).[a]

Compd.	C***H***=N	Aromatic Region	Aliphatic Region			
			P(*Me*)$_3$	**(Me)$_2$C*H***	**Ar-*Me***	**CH(*Me*)$_2$**
C8	8.04 (d, 1H, $^{4}J_{H-P}$ 7.92 Hz)	7.73-7.81 (m, 6H); 7.29-7.47 (m, 9H); 7.13-7.23 (m, 3H); 6.81 (d, 1H, $^{3}J_{H-H}$ 7.34 Hz); 6.18 (d, 1H, $^{4}J_{H-P}$ 6.16 Hz)	-	3.42-3.53 (dt, 2H, $^{3}J_{H-H}$ 6.31 Hz)	1.80 (s, 3H)	1.37 (d, 6H, $^{3}J_{H-H}$ 6.90 Hz); 1.19 (d, 6H, $^{3}J_{H-H}$ 6.90 Hz)
C9	8.00 (d, 1H, $^{4}J_{H-P}$ 7.78 Hz)	7.45 (d, 1H, $^{3}J_{H-H}$ 7.19 Hz, $^{3}J_{H-H}$ 8.80 Hz); 7.34-7.38 (m, 1H); 7.24-7.31 (m, 2H); 7.16-7.22 (m, 3H)	1.71 (d, 9H, $^{2}J_{H-P}$ 10.86 Hz)	3.25-3.34 (dt, 2H, $^{3}J_{H-H}$ 6.75 Hz)	-	1.33 (d, 6H, $^{3}J_{H-H}$ 6.75 Hz); 1.13 (d, 6H, $^{3}J_{H-H}$ 6.90 Hz)
C10	8.51 (d, 1H, $^{4}J_{H-P}$ 7.81 Hz)	7.24-7.28 (m, 2H); 7.18-7.21 (m, 3H); 7.11 (d, 1H, $^{3}J_{H-H}$ 7.03 Hz)	1.69 (d, 9H, $^{2}J_{H-P}$ 10.74 Hz)	3.23-3.70 (dt, 2H, $^{3}J_{H-H}$ 6.64 Hz)		1.34 (d, 6H, $^{3}J_{H-H}$ 7.03 Hz); 1.16 (d, 6H, $^{3}J_{H-H}$ 7.23 Hz)
C11	7.96 (d, 1H, $^{4}J_{H-P}$ 7.81 Hz)	7.35 (d, 1H, $^{3}J_{H-H}$ 7.62 Hz); 7.22 (d, 1H, $^{3}J_{H-H}$ 6.64 Hz); 7.16-7.18 (m, 3H); 7.01 (d, 1H, $^{4}J_{H-P}$ 7.03 Hz)	1.71 (d, 9H, $^{2}J_{H-P}$ 10.74 Hz)	3.26-3.33 (dt, 2H, $^{3}J_{H-H}$ 6.84 Hz)	2.41 (s, 3H)	1.33 (d, 6H, $^{3}J_{H-H}$ 6.84 Hz); 1.13 (d, 6H, $^{3}J_{H-H}$ 6.84 Hz)
C12	8.75 (s, 1H)	7.46 (br. s, 1H); 7.12-7.20 (br. m, 5H)	1.16 (t, 18H, $^{2}J_{H-P}$ 7.04 Hz)	3.27-3.40 (dt, 2H, $^{3}J_{H-H}$ 6.46 Hz)	-	1.19 (d, 12H, $^{3}J_{H-H}$ 6.90 Hz)
C13	8.76 (s, 1H)	7.31-7.43 (br. m, 2H); 7.13-7.21 (m, 3H); 7.00 (t, 1H, $^{3}J_{H-H}$ 7.04 Hz)	1.18 (t, 18H, $^{2}J_{H-P}$ 7.04 Hz)	2.99-3.08 (dt, 2H, $^{3}J_{H-H}$ 6.90 Hz)	2.35 (s, 3H)	1.20 (d, 12H, $^{3}J_{H-H}$ 6.75 Hz)

[a] Spectra run in $CDCl_3$ at 25 °C. Chemical shifts are reported as δ ppm values, referenced relative to protons of the residual solvent peak.

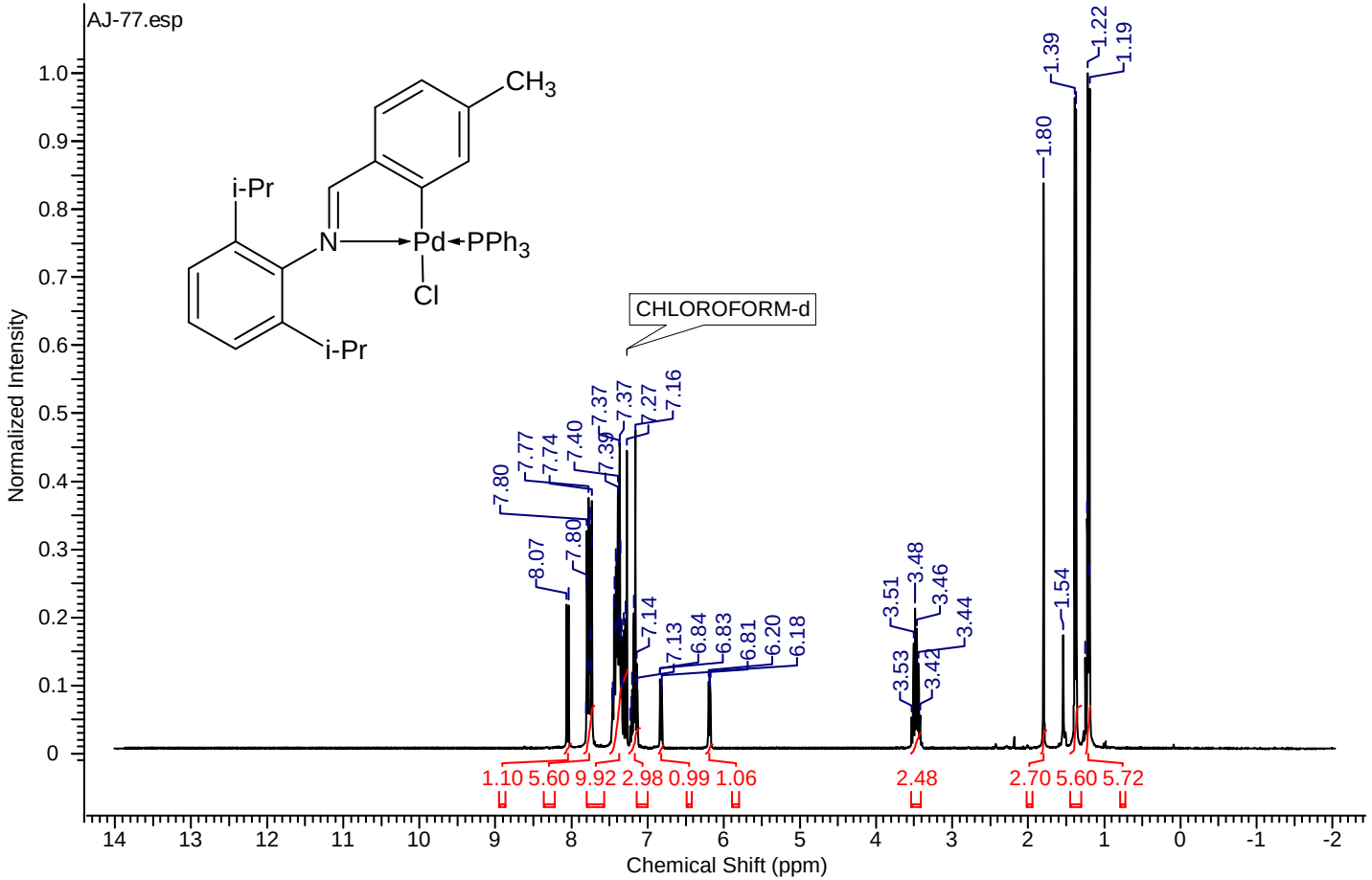

Fig. 2.7 ^{1}H NMR spectrum of complex **C8** recorded in $CDCl_3$ at 25 °C.

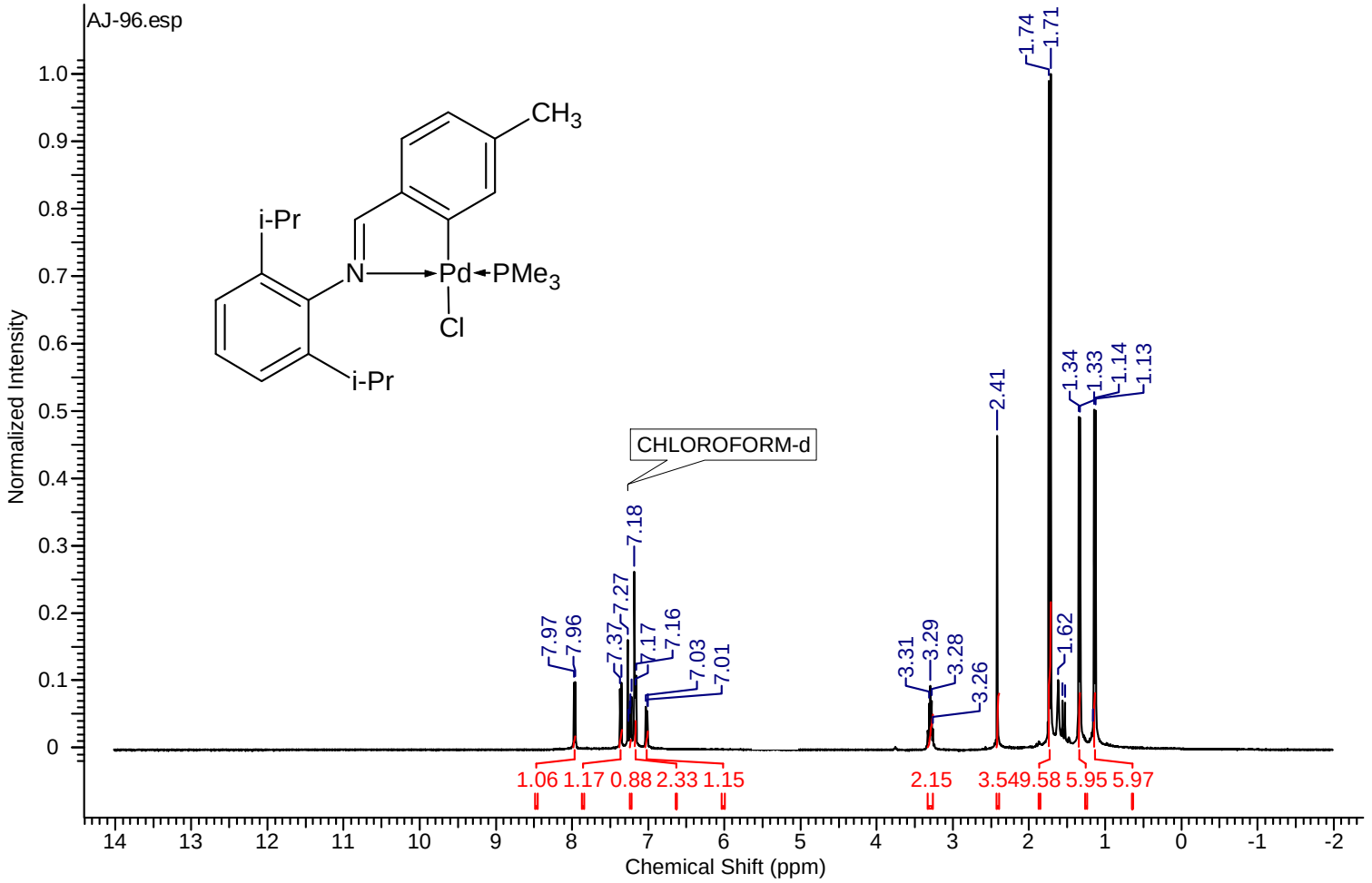

Fig. 2.8 ^{1}H NMR spectrum of complex **C11** recorded in $CDCl_3$ at 25 °C.

The phosphine-substituted palladacycles were also characterised by ESI-MS. The major fragment observed in the positive ion ESI-MS spectra of the phosphine-cleaved complexes corresponded to the fragment, $[M\text{-}Cl]^+$, in which the Cl^- ion was abstracted as a result of the ionisation process (Table 2.5, Fig. 2.9).[21-22]

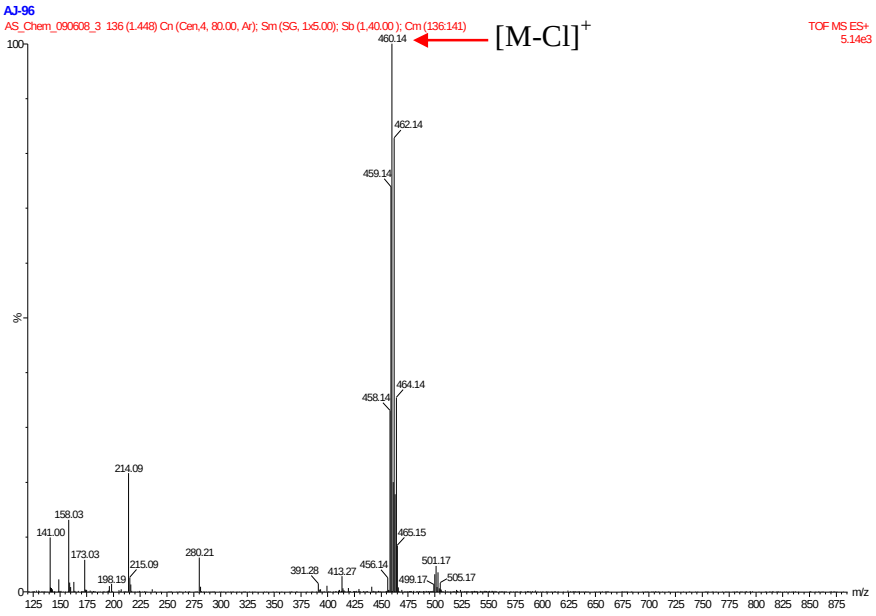

Fig. 2.9 ESI-MS spectrum of complex **C11** showing $[M\text{-}Cl]^+$ as major fragment (indicated by arrow).

Table 2.7 $^{31}P\ \{^1H\}$ NMR analytical data for cyclometallated complexes.[a]

Complex	δ (ppm)
C5	42.21
C6	41.76
C7	41.53
C8	41.64
C9	- 4.28
C10	- 4.60
C11	- 4.15
C12	- 16.15
C13	- 16.01

[a] Spectra run in $CDCl_3$, referenced relative to H_3PO_4.

Suitable crystals of complex **C8** was obtained by the slow evaporation of a 1:1 dichloromethane:hexane mixture. The crystallographic data (Table 2.8) as well as selected bond lengths (Table 2.9) are shown. The coordination sphere of the palladium centre is occupied by the N- and orthometallated C-atom of the benzylidene ligand in a *cis* arrangement, whilst the Cl- and P-atom of the phosphine ligand occupied the remaining coordination sites (Fig. 2.10). The coordination geometry around the metal centre is essentially square planar as noted by the sum of the angles about the palladium centre.

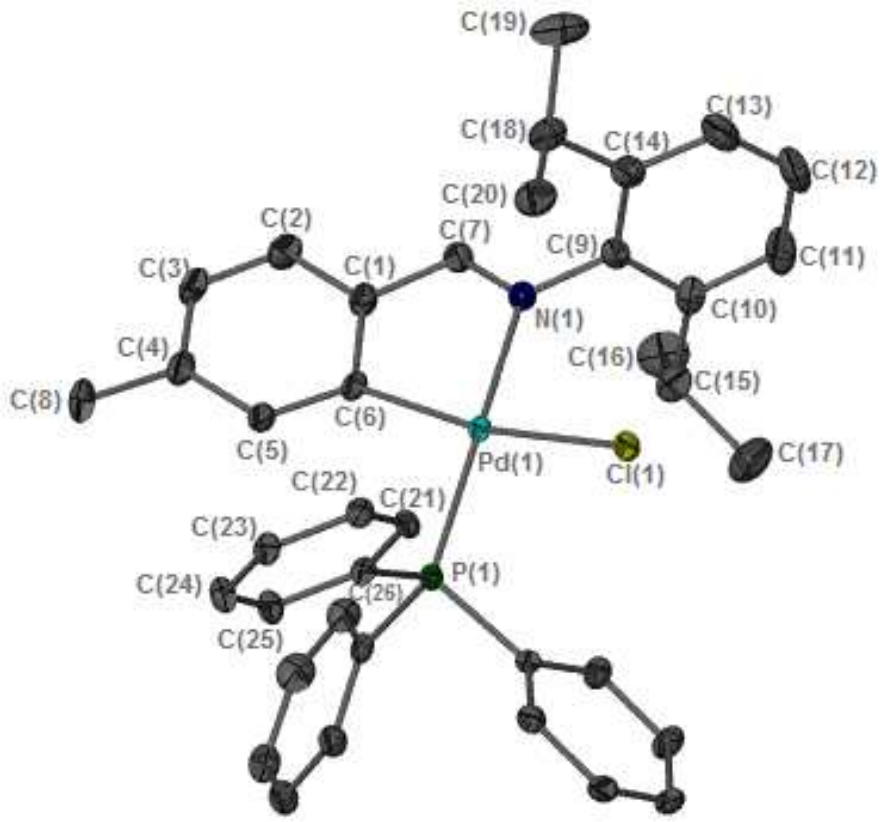

Fig. 2.10 The molecular structure of complex **C8**, drawn with 50 % probability ellipsoids. Hydrogen atoms omitted for clarity.

Table 2.8 Crystallographic data for complexes **C2** and **C8**.

Complex	**C2**	**C8**
Empirical Formula	$C_{38}H_{42}Cl_4N_2Pd_2$	$C_{38}H_{39}ClNPPd$
Temperature (K)	100(2)	100(2)
Wavelength (Å)	0.71073	0.71073
Crystal System	monoclinic	monoclinic
Space Group	$P_{21/n}$	$P_{21/n}$
***a* [Å]**	9.8189(18)	20.1626(5)
***b* [Å]**	10.0246(18)	9.3473(2)
***c* [Å]**	18.797(3)	20.5284(5)
α [°]	90.00	90.00
β [°]	91.899(2)	110.2880(10)
γ [°]	90.00	90.00
volume [Å^3]	1849.2(6)	3628.88(15)
Z	2	4
calc density [Mg/m^3]	1.583	1.249
abs. coeff [mm^{-1}]	1.291	0.654
***F*(000)**	888	1408
crystal dimensions (mm)	0.14 x 0.10x 0.04	0.34 x 0.31 x 0.12
Reflections [Fo > 4(Fo)	3159	9306
Parameters	212	384
goodness-of-fit on F^2	1.171	1.058
Final R indices [I > 2σ/(I)]	R_1 = 0.0793	R_1 = 0.0688
	wR_2 = 0.1400	wR_2 = 0.2047

The most noticeable distortion corresponds to the C(6)-Pd-N(1) angle in the cyclometallated ring of 80.7(1) ° which is as a result of C'N-chelation of the ligand to the metal.[20] The Pd-C bond length of 2.010(3) Å is somewhat shorter than the expected value

based on the sum of the covalent radii whereas the Pd-N bond length of 2.101(2) Å is longer than the expected value for the sum of their van der Waals radii.[17]

Table 2.9 Selected bond lengths (Å) and angles (°) of complexes **C2** and **C8**.

Complex	C2	C8
Pd(1)-N(1)	2.028(5)	2.102(3)
Pd(1)-C(6)	1.979(6)	2.011(3)
C(7)-N(1)	1.288(8)	1.285(5)
Pd(1)-Cl(1)	2.447(2)	2.3647(7)
Pd(1)-Cl(A)	2.329(2)	-
Pd(1)-P(1)	-	2.2520(9)
Pd(1)··Pd	3.477	-
N(1)-Pd(1)-C(6)	178.2(2)	80.8(1)
N(1)-Pd(1)-Cl(1)	176.3(2)	91.80(8)
N(1)-Pd(1)-Cl(A)	96.9(2)	-
C(6)-Pd(1)-Cl(1)	94.9(2)	167.43(9)
C(6)-Pd-Cl(A)	178.2(2)	-
Cl(1)-Pd(1)-Cl(a)	86.59(6)	-
N(1)-Pd(1)-P(1)	-	172.65(8)
P(1)-Pd(1)-C(6)	-	96.40(9)
P(1)-Pd(1)-Cl(1)	-	92.13(3)

This difference demonstrates the differing *trans* influence of the two coordinating atoms. The Pd-P bond length of 2.2523(7) Å falls into the range observed for similar complexes and is observed to be slightly shorter than expected value based on the sum of the van der Waals radii.

2.2.4 Reactivity of μ-Cl palladacycles toward bidentate phoshines; dppm and dppe.

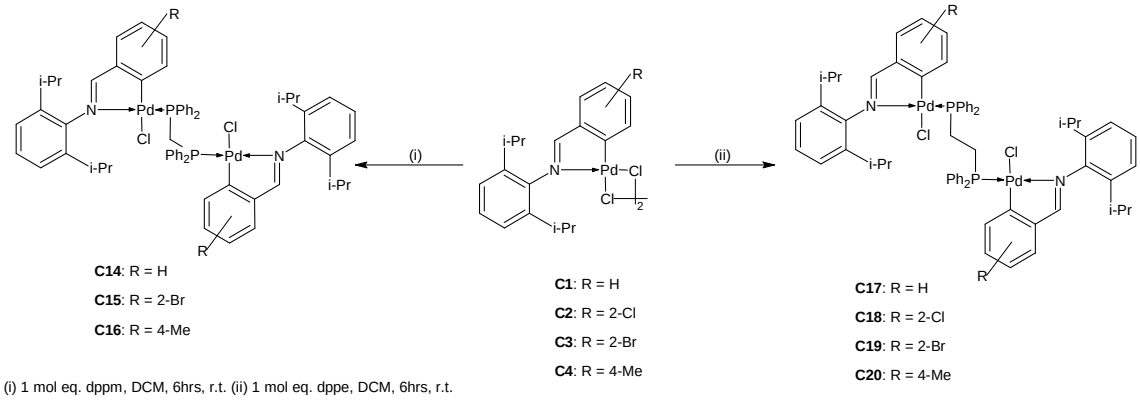

Scheme 2.5 A general reaction scheme for the synthesis of μ-dppm and μ-dppe palladacycles.

Following the successful preparation of mononuclear palladacycles bearing monodentate tertiary phosphines as ligands we directed our attention to the synthesis of dinuclear palladacycles bridged by bidentate phosphines. Our efforts involved the reaction of the dinuclear μ-Cl palladacycles, **C1-C4**, with either bis(diphenylphosphino)methane (dppm) or 1,2-bis(diphenylphosphino)ethane (dppe) (Scheme 2.5). In both cases pale-yellow/off-white solids were isolated with product yields in the range 70-85 %. The dinuclear μ-phosphine palladacycles were observed to be both air- and moisture-stable and displayed solubility in chlorinated organic solvents, partial solubility in toluene and was insoluble in ethers, alkanes and alcohols. To the best of our knowledge both the dinuclear μ-dppm (**C14-C16**) and μ-dppe palladacycles (**C17-C20**) are novel complexes. The dinuclear palladacycles were characterised by a range of analytical techniques.

In the FT-IR spectra of the dinuclear μ-phosphine palladacycles the imine absorption band was observed in the range 1600-1615 cm^{-1} and was analogous to those observed for the monodentate phosphine-cleaved palladacycles (Table 2.10). An increase in e^--density on the

metal centre upon coordination of the phosphine and subsequent back-donation onto the imine moiety resulted in a slight shift to higher wavenumbers of the $\upsilon_{C=N}$ absorption band when compared to that of the μ-Cl palladacycles. Furthermore, C-P and Pd-P bond stretching vibrations were observed in the range 1430-1440 and 680-690 cm^{-1} respectively, which demonstrated coordination of the phosphine to the palladium centre.[6-8]

Table 2.10 Analytical data pertaining to the dinuclear μ-phosphine palladacycles.

Complex	FT-IR ($\upsilon_{C=N}$, cm^{-1})[a]	Decomposition Temp. (°C)[b]
C14	1608	250-253
C15	1608	270-273
C16	1607	246-248
C17	1611	257-260
C18	1608	285-287
C19	1607	290-292
C20	1606	250-254

[a] Recorded as neat spectra employing an ATR accessory. [b] Decomposition temperatures reported are uncorrected. No melting prior to decomposition was observed.

In the ^{1}H NMR spectra of the dinuclear μ-phosphine palladacycles the imine proton resonances were observed in the range δ 7.95-8.55 ppm and were split into doublets which integrated for a total of two protons (Table 2.11). The aromatic protons of the phenyl substituents on the bridging phosphines were observed as broad multiplets integrating for a total of twenty protons. The protons of the *o*-metallated aromatic ring were observed in the range δ 6-7 ppm with the H-atom *ortho* to the Pd-C bond observed as the most deshielded. In most cases $^{4}J_{H\text{-}P}$ coupling of the *ortho* H-atom to the phosphorus atom could be observed.

Table 2.11 ^{1}H NMR spectral data for dinuclear μ-dppm and μ-dppe palladacycles.[a]

Compd.	C***H***=N	Aromatic Region	Aliphatic Region			
			P-(CH$_2$)$_n$-P[b]	**(Me)$_2$C*H***	**Ar-*Me***	**CH(*Me*)$_2$**
C14	7.98 (d, 2H, $^{4}J_{H-P}$ 7.42 Hz)	8.09-8.14 (m, 8H, $^{3}J_{H-H}$ 7.62 Hz); 7.14-7.31 (m, 20H, $^{3}J_{H-H}$ 6.64 Hz); 6.91 (t, 2H, $^{3}J_{H-H}$ 7.42 Hz); 6.56 (t, 2H, $^{3}J_{H-H}$ 7.23 Hz); 6.09 (br. t, 2H, $^{3}J_{H-H}$ 6.83 Hz)	5.12 (t, 2H, $^{2}J_{H-P}$ 12.50 Hz)	3.41-3.52 (m, 4H, $^{3}J_{H-H}$ 7.03 Hz)	-	1.48 (d, 12H, $^{3}J_{H-H}$ 6.84 Hz); 1.22 (d, 12H, $^{3}J_{H-H}$ 7.23 Hz)
C15	8.49 (d, 2H, $^{4}J_{H-P}$ 7.34 Hz)	8.04-8.10 (m, 8H, $^{3}J_{H-H}$ 8.36 Hz); 7.24-7.34 (m, 10H, $^{3}J_{H-H}$ 6.75 Hz); 7.15-7.20 (m, 8H, $^{3}J_{H-H}$ 7.34 Hz); 7.00 (d, 2H, $^{3}J_{H-H}$ 7.03 Hz); 6.38 (t, 2H, $^{3}J_{H-H}$ 7.78 Hz); 6.01 (t, 2H, $^{3}J_{H-H}$ 5.87 Hz)	5.05 (t, 2H, $^{2}J_{H-P}$ 12.62 Hz)	3.37-3.47 (m, 4H, $^{3}J_{H-H}$ 6.90 Hz)	-	1.48 (d, 6H, $^{3}J_{H-H}$ 6.60 Hz); 1.25 (d, 12H, $^{3}J_{H-H}$ 6.90 Hz)
C16	8.02 (d, 2H, $^{4}J_{H-P}$ 7.19 Hz)	8.26-8.32 (m, 8H, $^{3}J_{H-H}$ 7.92 Hz); 7.25-7.38 (m, 18H, $^{3}J_{H-H}$ 7.34 Hz); 6.81 (d, 2H, $^{3}J_{H-H}$ 7.63 Hz); 5.67 (d, 2H, $^{3}J_{H-H}$ 4.70 Hz)	5.24 (t, 2H, $^{2}J_{H-P}$ 12.77 Hz)	3.50-3.58 (m, 4H, $^{3}J_{H-H}$ 6.90 Hz)	1.78 (s, 6H)	1.52 (d, 12H, $^{3}J_{H-H}$ 6.90 Hz); 1.29 (d, 12H, $^{3}J_{H-H}$ 6.75 Hz)

[a] Spectra run in $CDCl_3$ as solvent. Chemical shifts are reported as δ ppm values, referenced relative to residual solvent peak. [b] For **C14-C16** n = 1, **C17-C20**, n = 2.

Table 2.11 ^{1}H NMR spectral data for dinuclear μ-dppm and μ-dppe palladacycles (continued).[a]

Compd.	C*H*=N	Aromatic Region	Aliphatic Region			
			P-$(CH_2)_n$-P[b]	$(Me)_2CH$	Ar-*Me*	$CH(Me)_2$
C17	8.02 (d, 2H, $^4J_{H-P}$ 7.19 Hz)	7.88-7.94 (m, 8H); 7.20-7.34 (m, 20H); 6.93 (t, 2H, $^3J_{H-H}$ 7.34 Hz); 6.61 (t, 2H, $^3J_{H-H}$ 7.63 Hz); 6.32-6.36 (br. t, 2H, $^4J_{H-P}$ 7.18 Hz)	3.00 (br. m, 4H)	3.37-3.46 (dt, 4H, $^3J_{H-H}$ 6.75 Hz)	-	1.33 (d, 12H, $^3J_{H-H}$ 6.75 Hz); 1.19 (d, 12H, $^3J_{H-H}$ 6.90 Hz)
C18	8.52 (d, 2H, $^4J_{H-P}$ 6.46 Hz)	7.86-7.92 (m, 8H); 7.29-7.37 (m, 9H); 7.21-7.28(m, 9H); 6.84 (t, 2H, $^3J_{H-H}$ 7.92 Hz); 6.52 (t, 2H, $^3J_{H-H}$ 7.92 Hz); 6.22 (br. t, 2H, $^4J_{H-P}$ 7.48 Hz)	2.95 (br. m, 4H)	3.35-3.44 (dt, 4H, $^3J_{H-H}$ 6.90 Hz)	-	1.33 (d, 12H, $^3J_{H-H}$ 6.75 Hz); 1.21 (d, 12H, $^3J_{H-H}$ 6.90 Hz)
C19	8.52 (d, 2H, $^4J_{H-P}$ 6.46 Hz)	7.85-7.91 (m, 8H); 7.22-7.37 (m, 18H); 7.02 (d, 2H, $^3J_{H-H}$ 7.92 Hz); 6.42 (t, 2H, $^3J_{H-H}$ 7.78 Hz); 6.27 (br. t, 2H, $^3J_{H-H}$ 7.19 Hz)	2.95 (br. m, 4H)	3.36-3.44 (dt, 4H, $^3J_{H-H}$ 6.90 Hz)	-	1.33(d, 12H, $^3J_{H-H}$ 6.75 Hz); 1.22 (d, 12H, $^3J_{H-H}$ 6.75 Hz)
C20	7.95 (d, 2H, $^4J_{H-P}$ 7.48 Hz)	7.83-7.89 (m, 8H); 7.47-7.59 (m, 4H); 7.23-7.33 (m, 8H); 7.18-7.21 (m, 8H); 6.74 (d, 2H, $^3J_{H-H}$ 7.04 Hz); 6.01 (br. s, 2H)	3.16 (br. m, 4H)	3.37-3.47 (dt, 4H, $^3J_{H-H}$ 6.90 Hz)	1.72 (s, 6H)	1.33 (d, 12H, $^3J_{H-H}$ 6.75 Hz); 1.18 (d, 12H, $^3J_{H-H}$ 6.90 Hz)

[a] Spectra run in $CDCl_3$ as solvent. Chemical shifts are reported as δ ppm values, referenced relative to residual solvent peak. [b] For **C14-C16** n = 1, **C17-C20**, n = 2.

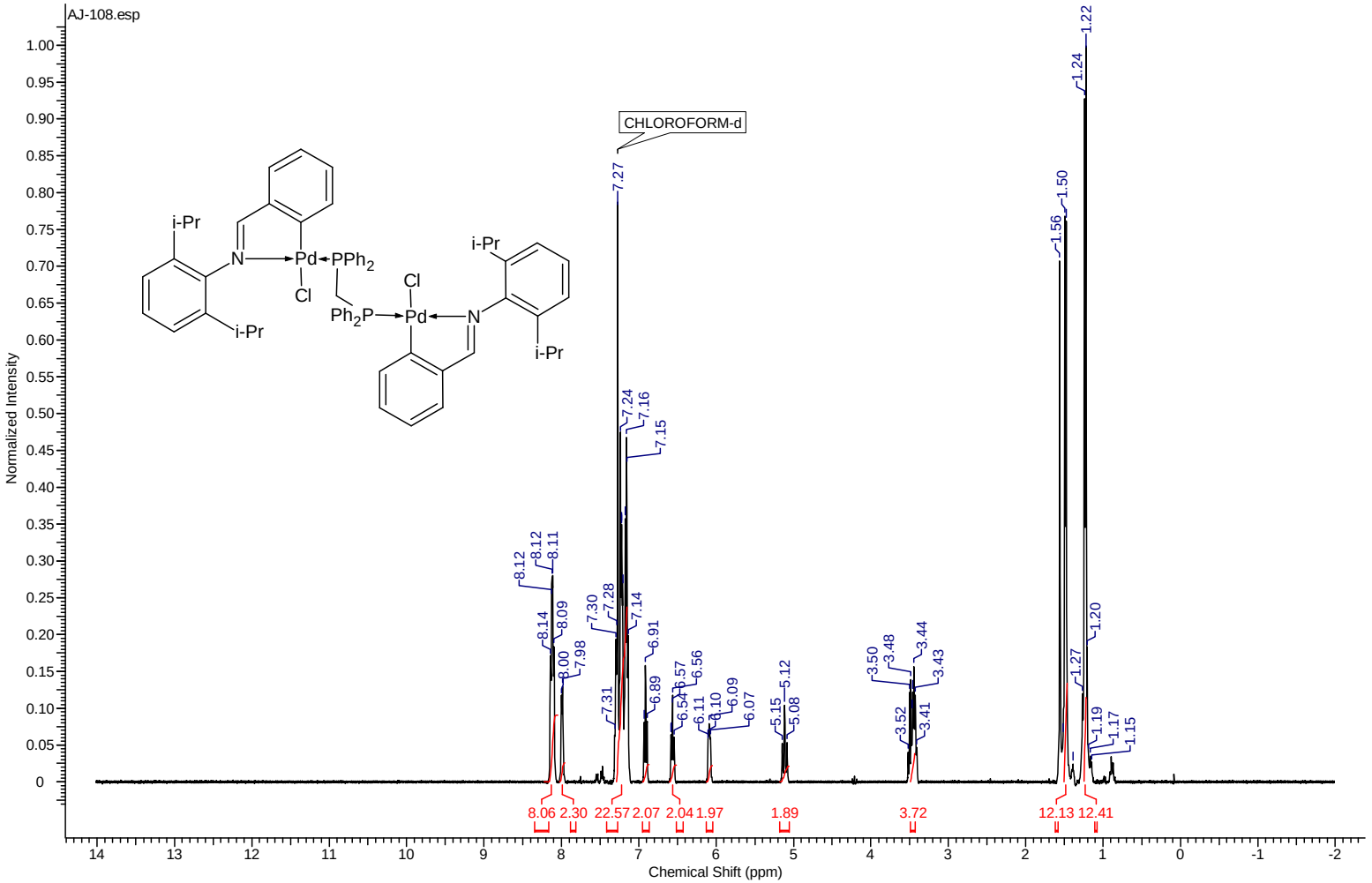

Fig. 2.11 ^{1}H NMR spectrum of complex, **C14**, recorded in $CDCl_3$ at 25 °C.

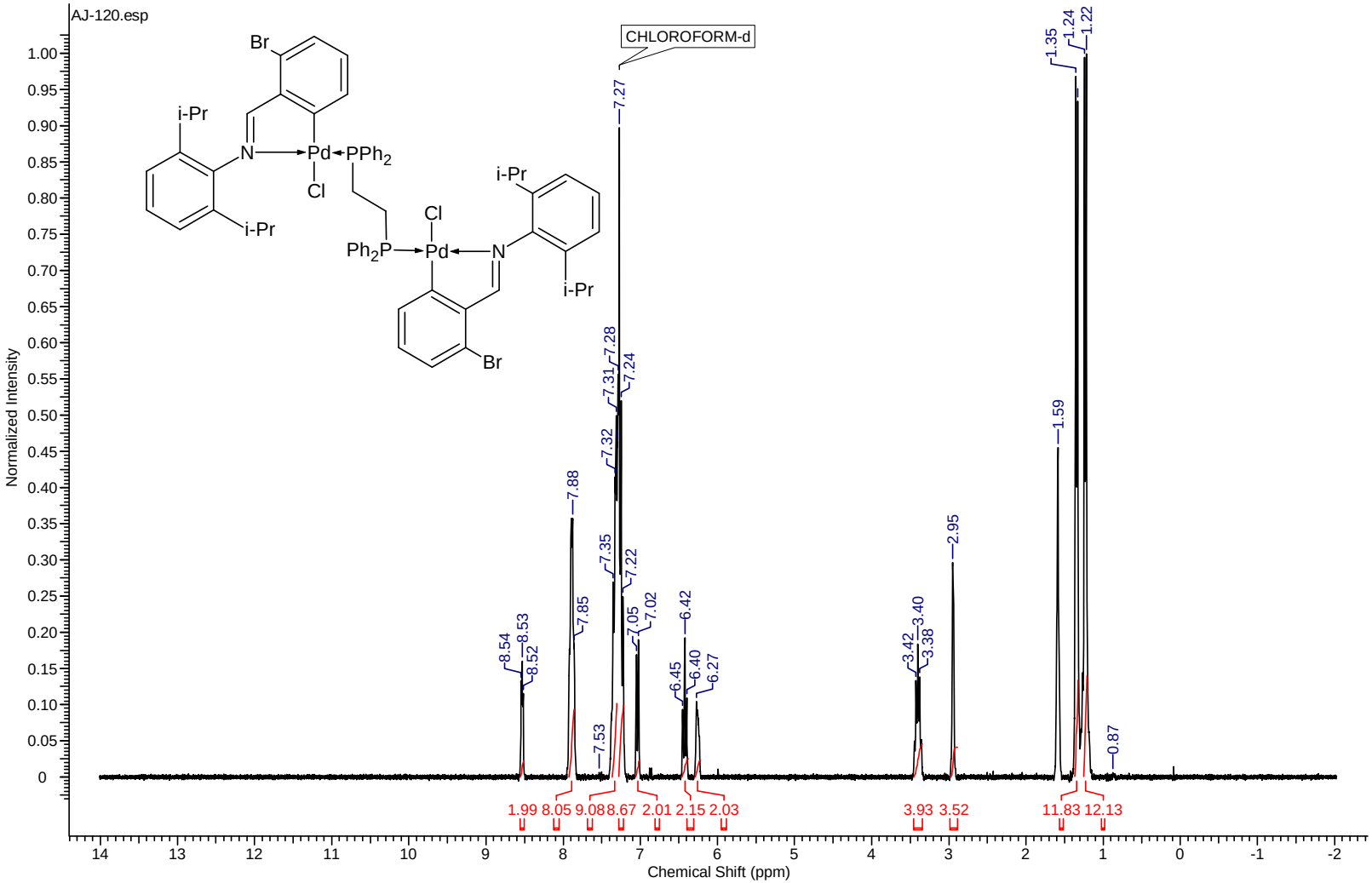

Fig. 2.12 ^{1}H NMR spectrum of complex **C19**, recorded in $CDCl_3$ at 25 °C.

These results demonstrated the *trans* geometry with respect to palladium of N- and P-donor atoms and demonstrated the 'transphobic effect' as coined by Vicente and co-workers.[23] In the case of the μ-dppm palladacycles, **C14**-**C16**, the methylene proton resonance of the P-C*H*$_2$-P unit was observed as a triplet in the range δ 5.00-5.25 ppm, with $^2J_{H\text{-}P}$ coupling constants in the range 12.50-12.80 Hz (Fig 2.11).[16] For the μ-dppe palladacycles the methylene protons of the ethane bridge was observed as a broad multiplet integrating for a total of four protons in the range δ 2.90-3.20 ppm (Fig. 2.12). The remainder of the resonances in the aliphatic region was assigned to the ^{i}Pr substituents on the phenyl ring of the ligand and was observed in the same range as for the mononuclear palladacycles.

^{13}C NMR analysis of the dinuclear palladacycles demonstrated that the metallacycle framework remained intact after reaction with the bidentate phosphines. The imine carbon resonance were observed in the range δ 175-178 ppm while the C1-carbon and the *o*-metallated carbon resonance was observed in the range δ 158-163 and δ 145-148 ppm respectively.[16] For both μ-dppm and μ-dppe palladacycles the P-(*C*H$_2$)$_n$-P (for μ-dppm, n = 1; for μ-dppe, n = 2) was observed in the range δ 22-23 ppm. Single resonances were observed for the μ-dppe palladacycles which demonstrated the symmetric nature of the complexes.

The ^{31}P{^{1}H} NMR spectra of the μ-dppm palladacycles showed a singlet in the range δ 32-34 ppm, while the μ-dppe palladacycles showed a singlet in the range δ 39-41 ppm (Table 2.12).

In both cases the signals were shifted to higher frequency in comparison to that of the free phosphine and demonstrated the equivalence of the two phosphorus nuclei present in the complex.[24]

In the ESI-MS (+) spectra of the dinuclear μ-phosphine palladacycles characteristic clusters of peaks spanning approximately 10 mass units were observed. This was attributed to the presence of several palladium; chlorine and in the case of **C15** and **C19**, bromine isotopes (Fig 2.13).[21-22] The major fragments observed in the spectra of both μ-dppm and μ-dppe palladacycles were assigned to fragments corresponding to $[M\text{-}Cl]^+$, $[LPdPP]^+$ and $[LPdCl]^+$. This type of fragmentation has been observed for analogous complexes.[25] In all cases the base peak was ascribed to the fragment $[LPdPP]^+$. A plausible fragmentation pathway is given in Scheme 2.6.

Table 2.12 ESI-MS (+) and $^{31}P\{^1H\}$ NMR data for dinuclear μ-phosphine palladacycles.

Complex	$^{31}P\{^1H\}^a$	ESI-MS (*m/z*)^b
14	34.07	1161
15	32.95	1319
16	34.39	1189
17	39.54	1175
18	40.51	1244
19	40.29	1333
20	39.62	1203

[a] Recorded in $CDCl_3$ with chemical shifts given in ppm, referenced relative to H_3PO_4. [b] Recorded in positive ion mode. Reported ion corresponds to $[M\text{-}Cl]^+$.

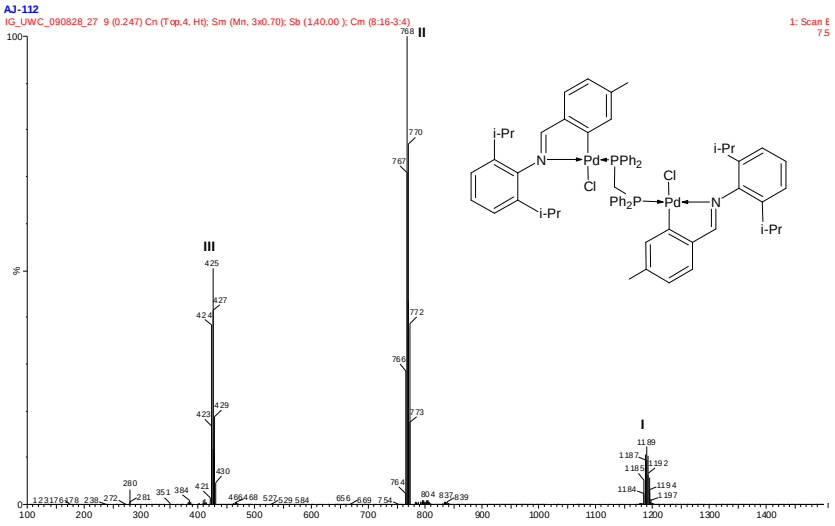

Fig. 2.13 ESI-MS (+) spectrum of complex **C16**, with major fragments annotated.

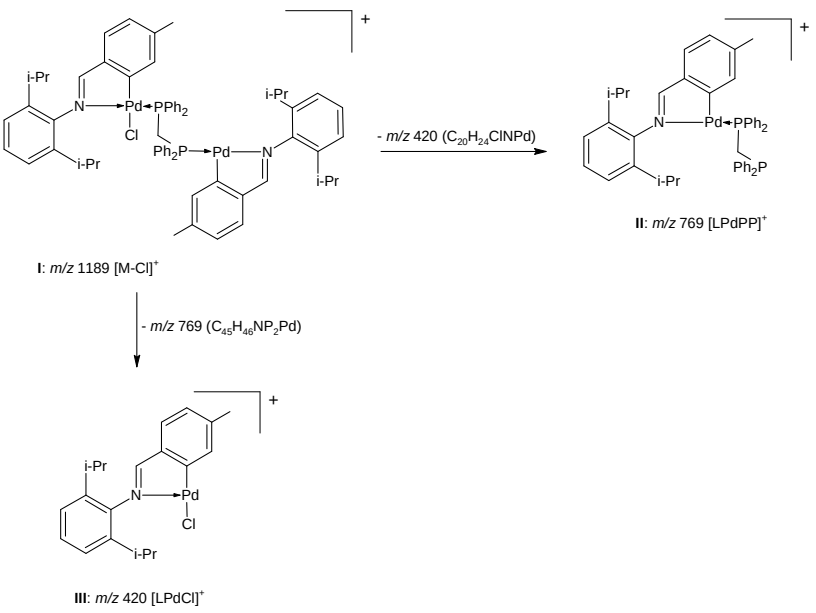

Scheme 2.6 Plausible fragmentation pathway for complex **C12**, with major fragments annotated as in Fig. 2.12.

Simulation[26] of the isotope patterns for each of the assigned fragments in Fig. 2.13 correlated well with the experimentally observed fragments (Fig. 2.14).

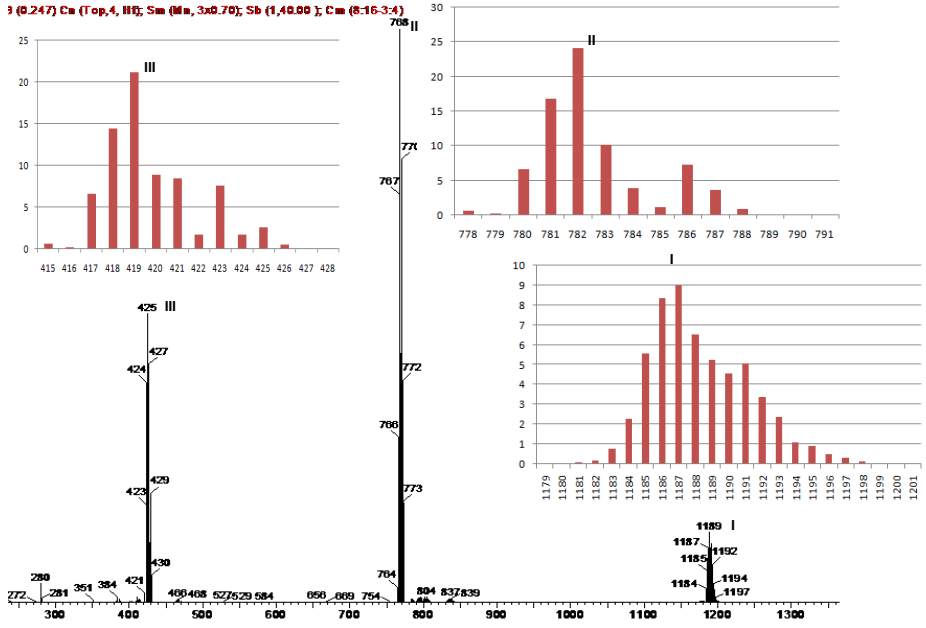

Fig. 2.14 Annotated peaks assigned to fragments **I**, **II** and **III** with simulated fragment shown (insets **I**, **II** and **III** respectively).

2.3 Conclusions.

Bidentate C,N monofunctional ligands were prepared by Schiff base condensation of substituted aniline and various monosubstituted aldehydes and fully characterised. Dinuclear μ-Cl palladacycles were prepared by electrophilic C-H activation and fully characterised. The chloro-bridged palladacycles could be cleaved with both mono- and bidentate tertiary phosphine ligands. Thus mononuclear and dinuclear μ-phosphine palladacycles could be isolated and fully characterised.

2.4 Materials and Methods

All transformations were performed using standard Schlenk techniques under a nitrogen atmosphere. Solvents were dried by distillation prior to use and all other reagents were employed as obtained. NMR (^{1}H: 300 and 400 MHz; ^{13}C: 75 and 100 MHz) spectra were recorded on Varian VNMRS 300 MHz; Varian Unity Inova 400 MHz spectrometers and chemical shifts were reported in ppm, referenced to the residual protons of the deuterated solvents and tetramethyl silane (TMS) as internal standard. ESI-MS (positive mode) analyses were performed on Waters API Quattro Micro and Waters API Q-TOF Ultima instruments by direct injection of sample. FT-IR analysis was performed on a Thermo Nicolet AVATAR 330 instrument, and was recorded as neat spectra (ATR) unless otherwise specified. Melting point determinations were performed on a Stuart Scientific SMP3 melting point apparatus and are reported as uncorrected.

2.4.1 Synthesis of monofunctional imine ligands (L1-L4).

2.4.1.1 benzylidene-2,6-diisopropylphenylamine (L1).

To a stirring solution of 2,6-diisopropylaniline (1.8 ml, 9.423 mmol) in EtOH (10 ml) was added benzaldehyde (0.96 ml, 9.423 mmol). The resulting yellow solution was stirred for 24 hrs at room temperature. After the allotted time the solvent was removed, the oily residue obtained redissolved in dichloromethane (20 ml) and washed with H_2O (10 x 20 ml portions). The organic layer was dried over $MgSO_4$, filtered and the solvent removed. The yellow oily residue was recrystallised from DCM/MeOH at low temperature and was isolated as a yellow crystalline solid. Yield: 2.25 g, 90 %. ^{13}C {^1H} NMR (100 MHz, $CDCl_3$, numbering as per Fig. 2.3): δ 160.2 (*C*H=N, C^7); δ 147.5 (C_{Ar}, C^8); δ 138.3 (C_{Ar}, C^9); δ 133.8 (C_{Ar}, C^1); δ 131.1 (C_{Ar}, C^4); δ 129.2 (C_{Ar}, $C^{2,6}$); δ 128.9 (C_{Ar}, $C^{3,5}$); δ 126.7 (C_{Ar}, C^{11}); δ 124.7 (C_{Ar}, C^{10}); δ 27.96 (C^{12}); δ 23.45 (C^{13}). *Anal*. Found: C, 85. 92; H, 8.70; N, 5.20. Calc. for $C_{19}H_{23}N$: C, 85.99; H, 8.74; N, 5.28.

2.4.1.2 2-chlorobenzylidene-2,6-diisopropylphenylamine (L2).

The same synthetic procedure as outlined above (**L1**) was employed for the synthesis of **L2**, using 2-chlorobenzaldehyde as reagent. Yield: 2.46 g, 87 %. ^{13}C {^1H} NMR (100 MHz, $CDCl_3$, numbering as per Fig. 2.3): δ 159.2 (*C*H=N, C^7); δ 149.1 (C_{Ar}, C^8); δ 137.6 (C_{Ar}, C^9); δ 135.9 (C_{Ar}, C^2); δ 133.2 (C_{Ar}, C^1); d 132.2 (C_{Ar}, C^4); δ 129.9 (C_{Ar}, C^6); δ 128.4 (C_{Ar}, C^3); δ 127.2 (C_{Ar}, C^5); δ 124.4 (C_{Ar}, C^{11}); δ 123.1 (C_{Ar}, C^{10}); δ 27.9 (C^{12}); δ 23.5 (C^{13}). *Anal*. Found: C, 76.05; H, 7.35; N, 4.63. Calc. for $C_{19}H_{22}ClN$: C, 76.11; H, 7.40; N, 4.67.

2.4.1.3 2-bromobenzylidene-2,6-diisopropylphenylamine (L3).

The same synthetic procedure as outlined above (**L1**) was employed for the synthesis of **L3**, using 2-bromobenzaldehyde as reagent. Yield: 2.98 g, 92 %. ^{13}C NMR {^{1}H} (100MHz, $CDCl_3$, numbering as per Fig. 2.3): δ 161.4 (*C*H=N, C^7); δ 148.9 (C_{Ar}, C^8); δ 137.6 (C_{Ar}, C^9); δ 134.6 (C_{Ar}, C^2); δ 133.2 (C_{Ar}, C^1); δ 132.4 (C_{Ar}, C^4); δ 128.8 (C_{Ar}, C^6); δ 127.8 (C_{Ar}, C^3); δ 125.7 (C_{Ar}, C^5); δ 124.4 (C_{Ar}, C^{11}); δ 123.1 (C_{Ar}, C^{10}); δ 27.9 (C^{12}); δ 23.5 (C^{13}). *Anal.* Found: C, 66.23; H, 6.41; N, 4.02. Calc. for $C_{19}H_{22}BrN$: C, 66.28; H, 6.44; N, 4.07.

2.4.1.4 4-methylbenzylidene-2,6-diisopropylphenylamine (L4).

The same synthetic procedure as outlined above (**L1**) was employed for the synthesis of **L4**, using *p*-tolualdehyde as reagent. Yield: 2.11 g, 80 %. ^{13}C {^{1}H} NMR (100 MHz, $CDCl_3$, numbering as per Fig. 2.3): δ 162.2 (*C*H=N, C^7); δ 148.7 (C_{Ar}, C^9); δ 142.3 (C_{Ar}, C^4) δ 137.9 (C_{Ar}, C^{10}); δ 133.0 (C_{Ar}, C^1); δ 129.6 (C_{Ar}, $C^{3,5}$); δ 128.8 (C_{Ar}, $C^{2,6}$); δ 124.3 (C_{Ar}, C^{11}); δ 123.3 (C_{Ar}, C^{10}); δ 27.9 (C^{12}); δ 23.5 (C^{14}); δ 21.6 (C^{13}). *Anal*. Found: C, 85. 90; H, 9.01; N, 4.96. Calc. for $C_{20}H_{25}N$: C, 85.97; H, 9.02; N, 5.01.

2.4.2 Synthesis of μ-Cl palladacycles (C1-C4).

2.4.2.1 Synthesis of $[PdCl(C_6H_4)CH=N\{2,6\text{-}^{i}Pr_2\text{-}C_6H_3\}]_2$ (C1).

To a stirring solution of $(MeCN)_2PdCl_2$ (100 mg, 0.386 mmol) in dichloromethane (10ml) was added benzylidene-2,6-diisopropylphenylamine (**L1**, 102 mg, 0.386 mmol). The

reaction mixture was stirred for 18 hrs at room temperature, after which the solvent was removed. The yellow solid residue obtained was redissolved in dichloromethane (20 ml) and filtered through celite. The solvent was removed, and the pale-yellow solid obtained recrystallised from dichloromethane:hexane. Yield: 120 mg, 79 %. ^{13}C {^{1}H} NMR ($CDCl_3$, 75 MHz): δ 176.21 (*C*H=N); δ 155.43 (C_1); δ 145.67 (*o*-metallated C); δ 141.48 (C_{Ar}); δ 133.90 (C_{Ar}); δ 132.56 (C_{Ar}); δ 130.86 (C_{Ar}); δ 128.29 (C_{Ar}); 127.74 (C_{Ar}); 124.68 (C_{Ar}); 123.23 (C_{Ar}); δ 28.19 (^{i}Pr-*C*H); δ 22.99, 24.45 (^{i}Pr-*Me*).

2.4.2.2 Synthesis of [PdCl(2-Cl-C$_6$H$_3$)CH=N{2,6-iPr$_2$-C$_6$H$_3$}]$_2$ (C2).

The same synthetic procedure as outlined above (**C1**) was employed for the synthesis of **C2**, using **L2** as reagent. Yield: 145 mg, 85 %. ^{13}C ($CDCl_3$, 75 MHz): δ 174.75 (*C*H=N); δ 156.38 (C_1); δ 142.88 (*o*-metallated C); δ 141.40 (C_{Ar}); δ 133.82 (C_{Ar}); δ 132.25 (C_{Ar}); δ 130.52 (C_{Ar}); δ 128.04 (C_{Ar}); δ 127.97 (C_{Ar}) δ 124.89 (C_{Ar}); δ 123.35 (C_{Ar}); δ 28.28 (^{i}Pr-*C*H); δ 24.48 (^{i}Pr-*Me*); δ 22.94 (^{i}Pr-*Me*).

2.4.2.3 Synthesis of [PdCl(2-Br-C$_6$H$_3$)CH=N{2,6-^{i}Pr$_2$-C$_6$H$_3$}]$_2$ (C3).

The same synthetic procedure as outlined above (**C1**) was employed for the synthesis of **C3**, using **L3** as reagent and stirring for 6 hrs. Yield: 149 mg, 80 %. ^{13}C {^{1}H} ($CDCl_3$, 75 MHz): δ 174.15 (*C*H=N); δ 156.89 (C_1); δ 142.56 (*o*-metallated C); δ 141.35 (C_{Ar}); δ 133.85 (C_{Ar}) δ 132.45 (C_{Ar}); δ 130.62 (C_{Ar}); 128.35 (C_{Ar}); δ 127.95 (C_{Ar}); δ 124.73 (C_{Ar}); δ 123.30 (C_{Ar}); δ 28.25 (^{i}Pr-*C*H); δ 24.49 (^{i}Pr-*Me*); δ 22.90 (^{i}Pr-*Me*).

2.4.2.4 Synthesis of [PdCl(4-Me-C_6H_3)CH=N{2,6-^{i}Pr$_2$-C_6H_3}]$_2$ (C4).

The same synthetic procedure as outlined above (**C1**) was employed for the synthesis of **C4**, using **L4** as reagent and stirring for 21 hrs. Yield: 125 mg, 77 %. ^{13}C {^{1}H} ($CDCl_3$, 100 MHz): δ 176.18 (*C*H=N); δ 155.43 (C_{Ar}); δ 145.67 (*o*-metallated C); δ 141.47 (C_{Ar}); δ 133.91 (C_{Ar}); δ 132.69 (C_{Ar}); 130.87 (C_{Ar}); 128.31 (C_{Ar}) δ 127.88 (C_{Ar}); δ 124.68 (C_{Ar}); δ 123.24 (C_{Ar}); δ 28.20 (^{i}Pr-*C*H); δ 24.46 (Ar-*Me*); δ 23.01 (^{i}Pr-*Me*); δ 22.91 (^{i}Pr-*Me*).

2.4.3 Cleavage of μ-Cl palladacycles with monodentate phosphines, PPh_3.

2.4.3.1 Synthesis of [Pd(PPh_3)(C_6H_4)CH=N{2,6-^{i}Pr-C_6H_3}Cl] (C5).

To a stirring solution of [PdCl(C_6H_4)CH=N{2,6-^{i}Pr$_2$-C_6H_3}]$_2$ (**C1**, 128 mg, 0.158 mmol) in dichloromethane (5 ml) was added triphenylphosphine (83 mg, 0.316 mmol). The reaction mixture was stirred under an inert atmosphere and at room temperature for 1 hr, after which the solvent was removed. The yellow solid residue obtained was recrystallised from dichloromethane:Et_2O. Yield: 162 mg, 77 %. ^{13}C {^{1}H} NMR ($CDCl_3$, 75 MHz): δ 177.03 (*C*H=N); δ 159.54 (C_1); δ 145.15 (*o*-metallated C); δ 141.48 (C_{Ar}); δ 140.80 (C_{Ar}); δ 138.20 (C_{Ar}); δ 135.41 (C_{Ar}); δ 135.04 (C_{Ar}); δ 131.68 (C_{Ar}); δ 130.83 (C_{Ar}); δ 130.56 (C_{Ar}); δ 128.84 (C_{Ar}); δ 127.92 (C_{Ar}); δ 126.88 (C_{Ar}); δ 124.09 (C_{Ar}); δ 122.77 (C_{Ar}); δ 28.64 (^{i}Pr-*C*H); δ 24.51 (^{i}Pr-*Me*); δ 23.02 (^{i}Pr-*Me*). *Anal.* Found: C, 66.42; H, 5.54; N, 2.04. Calc for $C_{37}H_{37}ClNPPd$: C, 66.47; H, 5.58; N, 2.10.

2.4.3.2 Synthesis of [Pd(PPh$_3$)(2-Cl-C$_6$H$_3$)CH=N{2,6-^{i}Pr$_2$-C$_6$H$_3$}Cl] (C6):

The same synthetic procedure as outlined above (**C5**) was employed for the synthesis of **C6**, using [PdCl(2-Cl-C_6H_3)CH=N{2,6-^{i}Pr$_2$-C_6H_3}]$_2$ (**C2**) as reagent. Yield: 182 mg, 83 %. ^{13}C {^{1}H} NMR ($CDCl_3$, 75 MHz): δ 175.58 (*C*H=N); δ 160.21 (C_1); δ 145.81 (*o*-metallated C); δ 141.05 (C_{Ar}); δ 140.38 (C_{Ar}); δ 138.14 (C_{Ar}); δ 135.04 (C_{Ar}); 134.96 (C_{Ar}); δ 130.76 (C_{Ar}); δ 130.71 (C_{Ar}); δ 128.22 (C_{Ar}); δ 128.03 (C_{Ar}); δ 127.19 (C_{Ar}); δ 124.12 (C_{Ar}); δ 122.86 (C_{Ar}); δ 28.64 (^{i}Pr-*C*H); δ 24.56 (^{i}Pr-*Me*); δ 22.97 (^{i}Pr-*Me*). *Anal.* Found: C, 63.18; H, 5.11; N, 1.92. Calc for $C_{37}H_{36}Cl_2NPPd$: C, 63.22; H, 5.16; N, 1.99.

2.4.3.3 Synthesis of [Pd(PPh$_3$)(2-Br-C$_6$H$_3$)CH=N{2,6-^{i}Pr-C$_6$H$_3$}Cl] (C7):

The same synthetic procedure as outlined above (**C5**) was employed for the synthesis of **C7**, using [PdCl(2-Br-C_6H_3)CH=N{2,6-^{i}Pr$_2$-C_6H_3}]$_2$ (**C3**) as reagent. Yield = 184 mg, 78 %. ^{13}C {^{1}H} NMR ($CDCl_3$, 75 MHz): δ 177.70 (*C*H=N); δ 160.69 (C_1); δ 145.92 (*o*-metallated C); δ 141.23 (C_{Ar}); δ 140.74 (C_{Ar}); δ 137.27 (C_{Ar}); δ 135.04 (C_{Ar}); 134.96 (C_{Ar}); δ 130.84 (C_{Ar}); δ 130.49 (C_{Ar}); δ 128.29 (C_{Ar}); δ 128.01 (C_{Ar}); δ 127.13 (C_{Ar}); δ 124.38 (C_{Ar}); δ 122.13 (C_{Ar}); δ 28.65 (^{i}Pr-*C*H); δ 24.58 (^{i}Pr-*Me*); δ 22.96 (^{i}Pr-*Me*). *Anal.* Found: C, 59.40; H, 4.82; N, 1.80. Calc for $C_{37}H_{36}BrClNPPd$: C, 59.46; H, 4.85; N, 1.87.

2.4.3.4 Synthesis of [Pd(PPh$_3$)(4-Me-C$_6$H$_3$)CH=N{2,6-^{i}Pr$_2$-C$_6$H$_3$}Cl] (C8):

The same synthetic procedure as outlined above (**C5**) was employed for the synthesis of **C8**, using [PdCl(4-Me-C_6H_3)CH=N{2,6-^{i}Pr$_2$-C_6H_3}]$_2$ (**C4**) as reagent. Yield: 185 mg, 86 %. ^{13}C {^{1}H} NMR ($CDCl_3$, 75 MHz): δ 176.44 (*C*H=N); δ 159.27 (C_1); δ 145.15

(*o*-metallated C); δ 141.61 (C_{Ar}); δ 140.94 (C_{Ar}); δ 138.81 (C_{Ar}); δ 135.28 (C_{Ar}); 135.03 (C_{Ar}); δ 131.57 (C_{Ar}); δ 130.50 (C_{Ar}); δ 128.71 (C_{Ar}); δ 128.06 (C_{Ar}); δ 126.78 (C_{Ar}); δ 124.78 (C_{Ar}); δ 122.73 (C_{Ar}); δ 28.55 (^{i}Pr-*C*H); δ 24.52 (Ar-*Me*); δ 22.98 (^{i}Pr-*Me*); δ 21.94 (^{i}Pr-*Me*). *Anal.* Found: C, 66.85; H, 5.72; N, 2.00. Calc for $C_{38}H_{39}ClNPPd$: C, 66.87; H, 5.76; N, 2.05.

2.4.4 Cleavage of μ-Cl palladacycles with monodentate phosphine, PMe_3.

2.4.4.1 Synthesis of [Pd(PMe_3)(C_6H_4)CH=N{2,6-^{i}Pr-C_6H_3}Cl] (C9):

To a stirring solution of [PdCl(C_6H_4)CH=N-{2,6-$^{i}Pr_2$-C_6H_3}]$_2$ (**C1**, 128 mg, 0.158 mmol) in dichloromethane (5 ml) was added trimethylphosphine (0.316 ml, 0.316 mmol). The reaction mixture was stirred for 1hr at room temperature, after which the solvent was removed. The off-white solid residue that was obtained was recrystallised from dichloromethane:Et_2O and an off-white solid was isolated. Yield: 111 mg, 73 %. ^{13}C {^{1}H} NMR ($CDCl_3$, 75 MHz): δ 176.67 (*C*H=N); δ 159.54 (C_1); δ 145.02 (*o*-metallated C); δ 141.81 (C_{Ar}); δ 140.84 (C_{Ar}); δ 138.76 (C_{Ar}); δ 135.69 (C_{Ar}); δ 129.60 (C_{Ar}); δ 126.95 (C_{Ar}); δ 124.56 (C_{Ar}); δ 122.81 (C_{Ar}); δ 28.34 (^{i}Pr-*C*H); δ 22.97 (P*Me*$_3$); δ 17.11 (^{i}Pr-*Me*); δ 16.45 (^{i}Pr-*Me*). *Anal.* Found: C, 54.74; H, 6.40; N, 2.82. Calc for $C_{22}H_{31}ClNPPd$: C, 54.78; H, 6.48; N, 2.90.

2.4.4.2 Synthesis of [Pd(PMe_3)(2-Cl-C_6H_3)CH=N{2,6-$^{i}Pr_2$-C_6H_3}Cl] (C10):

The same synthetic procedure as outlined above (**C9**) was employed for the synthesis of **C10**, using [PdCl(2-Cl-C_6H_3)CH=N{2,6-$^{i}Pr_2$-C_6H_3}]$_2$ (**C2**) as reagent. Yield: 131 mg, 80 %. ^{13}C NMR ($CDCl_3$, 100 MHz): δ 174.92 (*C*H=N); δ 160.54 (C_1); δ 145.32

(*o*-metallated C); δ 141.71 (C_{Ar}); δ 140.79 (C_{Ar}); δ 138.65 (C_{Ar}); δ 135.21 (C_{Ar}); δ 129.79 (C_{Ar}); δ 125.47 (C_{Ar}); δ 123.36 (C_{Ar}); δ 122.89 (C_{Ar}); δ 28.40 (^{i}Pr-*C*H); δ 22.90 (P*Me*$_3$); δ 16.99 (^{i}Pr-*Me*); δ 16.33 (^{i}Pr-*Me*). *Anal.* Found: C, 51.05; H, 5.76; N, 2.68. Calc for $C_{22}H_{30}Cl_2NPPd$: C, 51.13; H, 5.85; N, 2.71.

2.4.4.3 Synthesis of [Pd(PMe$_3$)(4-Me-C$_6$H$_3$)CH=N{2,6-^{i}Pr$_2$-C$_6$H$_3$}Cl] (C11):

The same synthetic procedure as outlined above (**C9**) was employed for the synthesis of **C11**, using [PdCl(4-Me-C_6H_3)CH=N{2,6-^{i}Pr$_2$-C_6H_3}]$_2$ (**C4**) as reagent. Yield: 117 mg, 75 %. ^{13}C NMR {^{1}H} ($CDCl_3$, 100 MHz): δ 176.12 (*C*H=N); δ 159.16 (C_1); δ 145.37 (*o*-metallated C); δ 144.97 (C_{Ar}) δ 142.14 (C_{Ar}); δ 140.92 (C_{Ar}); δ 136.70 (C_{Ar}); δ 129.45 (C_{Ar}); δ 126.45 (C_{Ar}); δ 125.23 (C_{Ar}); δ 122.89 (C_{Ar}); δ 28.31 (^{i}Pr-*C*H); δ 24.52 (Ar-*Me*); δ 22.97 (P*Me*$_3$); δ 16.96 (^{i}Pr-*Me*); δ 16.52 (^{i}Pr-*Me*). *Anal.* Found: C, 55.59; H, 6.62; N, 2.78. Calc for $C_{23}H_{33}ClNPPd$: C, 55.65; H, 6.70; N, 2.82.

2.4.4.4 Synthesis of [Pd(PMe$_3$)$_2$(2-Br-C$_6$H$_3$)CH=N{2,6-^{i}Pr-C$_6$H$_3$}Cl] (C12):

The same synthetic procedure as outlined above (**C9**) was employed for the synthesis of **C12**, using [PdCl(2-Br-C_6H_3)CH=N{2,6-^{i}Pr$_2$-C_6H_3}]$_2$ (**C3**) and excess trimethylphosphine (4mol eq.) as reagents. Yield: 149 mg, 74 %. ^{13}C NMR {^{1}H} (100MHz, $CDCl_3$): δ 161.47 (*C*H=N); δ 148.87 (C_{Ar}); δ 140.71 (C_{Ar}); δ 137.57 (C_{Ar}); δ 133.19 (C_{Ar},); δ 132.43 (C_{Ar}); δ 128.80 (C_{Ar}); δ 127.78 (C_{Ar}); δ 125.74 (C_{Ar}); δ 124.37 (C_{Ar}); δ 123.05 (C_{Ar}); δ 27.92 (^{i}Pr-*C*H); δ 24.76 (^{i}Pr-*Me*); δ 13.46 (P*Me*$_3$). *Anal*. Found: C, 47.02; H, 5.99; N, 2.05. Calc. for $C_{25}H_{39}BrClNP_2Pd$: C, 47.11; H, 6.17; N, 2.20.

2.4.4.5 Synthesis of [Pd{(PMe$_3$)$_2$(4-Me-C$_6$H$_3$)CH=N{2,6-^{i}Pr$_2$-C$_6$H$_3$}Cl] (C13):

The same synthetic procedure as outlined above (**C9**) was employed for the synthesis of **C13**, using [PdCl(4-Me-C_6H_3)CH=N{2,6-^{i}Pr$_2$-C_6H_3}]$_2$ (**C4**) and excess trimethylphosphine (4mol eq.) as reagents. Yield: 149 mg, 74 %. ^{13}C NMR {^{1}H} (100MHz, $CDCl_3$): δ 162.32 (*C*H=N); δ 148.64 (C_{Ar}); δ 142.46 (C_{Ar}) δ 138.1 (C_{Ar}); δ 133.14 (C_{Ar}); δ 129.62 (C_{Ar}); δ 128.73 (C_{Ar}); δ 124.28 (C_{Ar}); δ 123.42 (C_{Ar}); δ 27.83 (^{i}Pr-*C*H); δ 23.59 (^{i}Pr-*Me*); δ 21.64 (Ar-*Me*); δ 13.42 (P*Me*$_3$). *Anal*. Found: C, 54.33; H, 7.29; N, 2.29. Calc. for $C_{26}H_{42}ClNP_2Pd$: C, 54.55; H, 7.40; N, 2.45.

2.4.5 Cleavage of μ-Cl palladacycles with bidentate phosphines; dppm.

2.4.5.1 Synthesis of [{PdCl(C$_6$H$_4$)CH=N(2,6-^{i}Pr$_2$-C$_6$H$_3$)}$_2$(μ-Ph$_2$PCH$_2$PPh$_2$)] (C14):

To a stirring solution of [PdCl(C_6H_4)CH=N-{2,6-^{i}Pr$_2$-C_6H_3}]$_2$ (**C1**) (81 mg, 0.100 mmol) in dichloromethane (5 ml) was added bis(diphenylphosphino)methane (dppm, 38 mg, 0.100 mmol). The reaction mixture was stirred for 6 hrs at room temperature and under an inert atmosphere, after which the solvent was removed. An off-white solid residue was obtained which was recrystallized from dichloromethane: hexane. An off-white solid was isolated. Yield: 88 mg, 74 %. ^{13}C {^{1}H} NMR ($CDCl_3$, 75 MHz): δ 177.26 (*C*H=N); δ 159.18 (C_1); δ 147.39 (*o*-metallated C); δ 145.46 (C_{Ar}) δ 140.87 (C_{Ar}); δ 137.70 (C_{Ar}); δ 135.40 (C_{Ar}); δ 133.24 (C_{Ar}); δ 132.62 (C_{Ar}); δ 130.32 (C_{Ar}); δ 129.49 (C_{Ar}); δ 128.55 (C_{Ar}); δ 127.08 (C_{Ar}); δ 124.00 (C_{Ar}); δ 122.88 (C_{Ar}); δ 28.54 (^{i}Pr-*C*H); δ 24.64 (CH-*Me*$_2$); δ 23.06 (P-*C*H$_2$-P). *Anal*. Found: C, 63.18; H, 5.49; N, 2.30. Calc for $C_{63}H_{66}Cl_2N_2P_2Pd_2$: C, 63.22; H, 5.56; N, 2.34.

2.4.5.2 Synthesis of [{PdCl(2-Br-C_6H_3)CH=N(2,6-^{i}Pr$_2$-C_6H_3)}$_2$(μ-$Ph_2PCH_2PPh_2$)] (C15):

The same synthetic procedure as outlined above (**C14**) was employed for the synthesis of **C15**, using [PdCl(2-Br-C_6H_3)CH=N{2,6-^{i}Pr$_2$-C_6H_3}]$_2$ (**C2**) as reagent. Yield: 110 mg, 81 %. ^{13}C {^{1}H} NMR ($CDCl_3$, 75 MHz): δ 177.84 (*C*H=N); δ 161.39 (C_1); δ 146.50 (*o*-metallated C); δ 145.33 (C_{Ar}) δ 140.80 (C_{Ar}); δ 136.69 (C_{Ar}); δ 135.29 (C_{Ar}); δ 133.24 (C_{Ar}); δ 132.62 (C_{Ar}); δ 130.54 (C_{Ar}); δ 129.50 (C_{Ar}); δ 128.06 (C_{Ar}); δ 127.35 (C_{Ar}); δ 122.97 (C_{Ar}); δ 121.77 (C_{Ar}); δ 28.63 (^{i}Pr-*C*H); δ 24.72 (CH-*Me*$_2$); δ 22.97 (P-*C*H$_2$-P). *Anal*. Found: C, 55.79; H, 4.67; N, 1.98. Calc for $C_{63}H_{64}Br_2Cl_2N_2P_2Pd_2$: C, 55.86; H, 4.76; N, 2.07.

2.4.5.3 Synthesis of [{PdCl(4-Me-C_6H_3)CH=N(2,6-iPr-C_6H_3)}$_2$(μ-$Ph_2PCH_2PPh_2$)] (C16):

The same synthetic procedure as outlined above (**C14**) was employed for the synthesis of **C16**, using [PdCl(4-Me-C_6H_3)CH=N{2,6-iPr$_2$-C_6H_3}]$_2$ (**C2**) as reagent. Yield: 96 mg, 79 %. ^{13}C NMR ($CDCl_3$, 100 MHz): δ 176.52 (*C*H=N); δ 158.67 (C_1); δ 145.39 (*o*-metallated C); δ 144.61 (C_{Ar}) δ 141.04 (C_{Ar}); δ 138.56 (C_{Ar}); δ 135.62 (C_{Ar}); δ 133.23 (C_{Ar}); δ 130.23 (C_{Ar}); δ 129.40 (C_{Ar}); δ 128.47 (C_{Ar}); δ 127.86 (C_{Ar}); δ 126.97 (C_{Ar}); δ 124.61 (C_{Ar}); δ 122.84 (C_{Ar}); δ 28.51 (^{i}Pr-*C*H); δ 24.77 (Ar-*Me*); δ 23.09 (CH-*Me*$_2$); δ 22.09 (P-*C*H$_2$-P). *Anal*. Found: C, 63.69; H, 5.66; N, 2.12. Calc for $C_{65}H_{70}Cl_2N_2P_2Pd_2$: C, 63.73; H, 5.76; N, 2.29.

2.4.6 Cleavage of μ-Cl palladacycles with bidentate phosphines, dppe:

2.4.6.1 Synthesis of [{PdCl(C$_6$H$_4$)CH=N(2,6-iPr-C$_6$H$_3$)}$_2$(μ-Ph$_2$P(CH$_2$)$_2$PPh$_2$)] (C17):

To a stirring solution of [PdCl(C$_6$H$_4$)CH=N-{2,6-iPr$_2$-C$_6$H$_3$}]$_2$ (**C1**) (81 mg, 0.100 mmol) in dichloromethane (5ml) was added 1,2-bis(diphenylphosphino)ethane (dppe, 40 mg, 0.100 mmol). The reaction mixture was stirred for 6 hrs at room temperature. and under an inert atmosphere after which the solvent was removed. An off-white solid residue was obtained which was crystallized from dichloromethane: hexane. An off-white solid was isolated. Yield: 106 mg, 88 %. ^{13}C NMR (CDCl$_3$, 75 MHz): δ 176.14 (*C*H=N); δ 159.06 (C$_1$); δ 145.14 (*o*-metallated C); δ 144.68 (C$_{Ar}$) δ 141.32 (C$_{Ar}$); δ 137.61 (C$_{Ar}$); δ 134.23 (C$_{Ar}$); δ 133.48 (C$_{Ar}$); δ 132.19 (C$_{Ar}$); δ 130.48 (C$_{Ar}$); δ 129.05 (C$_{Ar}$); δ 128.11 (C$_{Ar}$); δ 127.54 (C$_{Ar}$); δ 125.30 (C$_{Ar}$); δ 122.57 (C$_{Ar}$); δ 28.06 (^{i}Pr-*C*H); δ 22.65 (CH-*Me*$_2$); δ 21.87 (P-(*C*H$_2$)$_2$-P). *Anal*. Found: C, 63.39; H, 5.58; N, 2.27. Calc for C$_{66}$H$_{72}$Cl$_2$N$_2$P$_2$Pd$_2$: C, 63.48; H, 5.66; N, 2.31.

2.4.6.2 Synthesis of [{PdCl(2-Cl-C$_6$H$_3$)CH=N(2,6-iPr$_2$-C$_6$H$_3$)}$_2$(μ-Ph$_2$P(CH$_2$)$_2$PPh$_2$)] (C18):

The same synthetic procedure as outlined above (**C17**) was employed for the synthesis of **C18**, using [PdCl(2-Cl-C$_6$H$_3$)CH=N{2,6-iPr$_2$-C$_6$H$_3$}]$_2$ (**C2**) as reagent. Yield: 89 mg, 70 %. ^{13}C NMR (CDCl$_3$, 75 MHz): δ 175.29 (*C*H=N); δ 161.69 (C$_1$); δ 145.10 (*o*-metallated C); δ 144.14 (C$_{Ar}$) δ 140.93 (C$_{Ar}$); δ 136.31 (C$_{Ar}$); δ 134.54 (C$_{Ar}$); δ 133.60 (C$_{Ar}$); δ 132.21 (C$_{Ar}$); δ 130.86 (C$_{Ar}$); δ 129.14 (C$_{Ar}$); δ 128.43 (C$_{Ar}$); δ 127.20 (C$_{Ar}$); δ 124.87

(C_{Ar}); δ 122.93 (C_{Ar}); δ 28.58 (^{i}Pr-*C*H); δ 24.48 (CH-*Me*$_2$); δ 23.08 (P-(*C*H$_2$)$_2$-P). *Anal.* Found: C, 59.91; H, 5.03; N, 2.01. Calc for $C_{64}H_{66}Cl_4N_2P_2Pd_2$: C, 60.06; H, 5.20; N, 2.19.

2.4.6.3 Synthesis of [{PdCl(2-Br-C$_6$H$_3$)CH=N(2,6-iPr$_2$-C$_6$H$_3$)}$_2$(μ-Ph$_2$P(CH$_2$)$_2$PPh$_2$)] (C19):

The same synthetic procedure as outlined above (**C17**) was employed for the synthesis of **C19**, using [PdCl(2-Br-C_6H_3)CH=N{2,6-iPr_2-C_6H_3}]$_2$ (**C3**) as reagent. Yield: 104 mg, 76 %. ^{13}C NMR ($CDCl_3$, 100 MHz): δ 177.88 (*C*H=N); δ 162.13 (C_1); δ 145.71 (*o*-metallated C); δ 145.37 (C_{Ar}) δ 141.25 (C_{Ar}); δ 137.25 (C_{Ar}); δ 134.84 (C_{Ar}); δ 133.92 (C_{Ar}); δ 132.53 (C_{Ar}); δ 131.19 (C_{Ar}); δ 129.46 (C_{Ar}); δ 128.76 (C_{Ar}); δ 127.52 (C_{Ar}); δ 123.26 (C_{Ar}); δ 122.32 (C_{Ar}); δ 28.92 (^{i}Pr-*C*H); δ 24.83 (CH-*Me*$_2$); δ 23.36 (P-(*C*H$_2$)$_2$-P). *Anal.* Found: C, 56.07; H, 4.80; N, 1.96. Calc for $C_{64}H_{66}Br_2Cl_2N_2P_2Pd_2$: C, 56.16; H, 4.86; N, 2.05.

2.4.6.4 Synthesis of [{PdCl(4-Me-C$_6$H$_3$)CH=N(2,6-iPr$_2$-C$_6$H$_3$)}$_2$(μ-Ph$_2$P(CH$_2$)$_2$PPh$_2$)] (C20):

The same synthetic procedure as outlined above (**C17**) was employed for the synthesis of **C20**, using [PdCl(4-Me-C_6H_3)CH=N{2,6-iPr_2-C_6H_3}]$_2$ (**C4**) as reagent. Yield: 88 mg, 71 %. ^{13}C NMR ($CDCl_3$, 100 MHz): δ 176.32 (*C*H=N); δ 159.11 (C_1); δ 145.03 (*o*-metallated C); δ 144.78 (C_{Ar}) δ 141.61 (C_{Ar}); δ 137.70 (C_{Ar}); δ 134.36 (C_{Ar}); δ 133.60 (C_{Ar}); δ 132.20 (C_{Ar}); δ 130.43 (C_{Ar}); δ 129.14 (C_{Ar}); δ 128.21 (C_{Ar}); δ 127.68 (C_{Ar}); δ 125.50 (C_{Ar}); δ 122.96 (C_{Ar}); δ 28.15 (^{i}Pr-*C*H); δ 24.47 (Ar-*Me*); δ 22.85 (CH-*Me*$_2$); δ 21.91

(P-(*C*H_2)$_2$-P). *Anal.* Found: C, 63.88; H, 5.73; N, 2.15. Calc for $C_{66}H_{72}Cl_2N_2P_2Pd_2$: C, 63.98; H, 5.86; N, 2.26.

2.4.7 X-Ray Crystal structure determination:

Single crystals of complexes **C2** and **C8** were mounted on glass fibers or nylon loops and centred in a stream of cold nitrogen at 100(2) K. Crystal evaluation and data collection was performed on a Bruker-Nonius SMART Apex-CCD diffractometer with Mo K_α radiation (λ = 0.71073 Å). Data collection, reduction and refinement were performed using SMART and SAINT software. Reflections were corrected for Lorentz and polarisation effects and absorption using SADABS software. The structures were solved by direct methods and refined by full-matrix least-squares on F^2 using SHELX-97.[27] All non-hydrogen atoms were refined anisotropically and all hydrogen atoms were placed using calculated positions and riding models.

References

1. H. Schiff, *Ann. Suppl.*, 1864, **3**, 343.
2. T. P. Noon and E. N. Jacobsen, *Science*, 2003, **299**, 1691.
3. P.-P. Yang, X.-Y. Song, R.-N. Liu, L.-C. Li and D.-Z. Liao, *Dalton. Trans.*, 2010, **39**, 6285-6294.
4. J.-C. Jiang, Z.-L. Chu, W. Huang, G. Wang and X.-Z. You, *Inorg. Chem.*, 2010, **49**, 5897-5911.
5. P. K. Sasmal, R. Majumdar, R. R. Dighe and A. R. Chakravarty, *Dalton. Trans.*, 2010, **39**, 7104-7113.

6. J. Albert, J. Granell, J. Sales, X. Solans and M. Font-Altaba, *Organometallics*, 1986, **5**, 2567-2568.

7. J. Albert, M. Gomez, J. Granell, X. Solans and J. Sales, *Organometallics*, 1990, **9**, 1405-1413.

8. J. Albert, R. M. Ceder, M. Gomez, J. Granell and J. Sales, *Organometallics*, 1992, **11**, 1536-1541.

9. D. Vázquez-García, A. Fernández, M. López-Torres, A. Rodríguez, N. Gómez-Blanco, C. Viader, J. M. Vila and J. s. J. Fernández, *Organometallics*, 2010, **29**, 3303-3307.

10. C.-L. Chen, Y.-H. Liu, S.-M. Peng and S.-T. Liu, *J. Organomet. Chem.*, 2004, **689**, 1806-1815.

11. N. Mungwe, *M.Sc. Thesis* University of the Western Cape, **2007**.

12. J. Albert, J. Granell and J. Sales, *J. Organomet. Chem.*, 1984, **273**, 393-399.

13. D. L. Davies, S. M. A. Donald and S. A. Macgregor, *J. Am. Chem. Soc.*, 2005, **127**, 13754-13755.

14. H. Onoue and I. Moritani, *J. Organomet. Chem.*, 1972, **43**, 431-436.

15. Y. A. Ustynyuk, V. A. Chertkov and I. V. Barinov, *J. Organomet. Chem.*, 1971, **29**, C53-C54.

16. R. Ares, M. López-Torres, A. Fernández, S. Castro-Juiz, A. Suarez, G. Alberdi, J. J. Fernández and J. M. Vila, *Polyhedron*, 2002, **21**, 2309-2315.

17. A. G. Orpen, L. Brammer, F. H. Allen, O. Kennard, D. G. Watson and R. Taylor, *J. Chem. Soc., Dalton Trans.*, 1989, S1-S83.

18. J. M. Vila, M. Gayoso, M. T. Pereira, J. M. Ortigueira, A. Fernandez, N. A. Bailey and H. Adams, *Polyhedron*, 1993, **12**, 171-180.

19. J. M. Vila, M. Gayoso, T. Pereira, C. Rodriguez, J. M. Ortigueira, J. J. Fernandez and M. Lopez Torres, *J. Organomet. Chem.*, 1994, **479**, 37-46.

20. R. Ares, D. Vazquez-Garcia, M. Lopez Torres, A. Fernandez, N. Gomez-Blanco, J. M. Vila and J. J. Fernandez, *J. Organomet. Chem.*, 2008, **693**, 3655-3667.

21. L. Tusek-Bozic, M. Curic and P. Traldi, *Inorg. Chim. Acta*, 1997, **254**, 49-55.

22. L. Tusek-Bozic, M. Komac, M. Curic, A. Lycka, M. D. Alpaos, V. Scarcia and A. Furlani, *Polyhedron*, 2000, **19**, 937.

23. J. Vicente, J.-A. Abad, A. D. Frankland and M. C. R. d. Arellano, *Chem, Eur. J.*, 1999, **5**, 3066-3075.

24. P. S. Pregosin and R. W. Kuntz, in *NMR Basic Principles and Progress*, eds. P. Diehl, E. Fluck and R. Kosfeld, Springer, Berlin, 1979.

25. R. Ares, M. López-Torres, A. Fernández, D. Vázquez-García, M. T. Pereira, J. M. Vila, L. Naya and J. J. Fernández, *J. Organomet. Chem.*, 2007, **692**, 4197-4208.

26. A. K. Brisdon, http://fluorine.ch.man.ac.uk/research/mstool.php, Accessed 2010/11/18.

27. G. M. Sheldrick, SHELX-97, University of Gottingen, Germany, 1997

Chapter 3: Synthetic Studies Directed Toward the Preparation of Dendrimer-Supported Palladacycles

3. Introduction.

3.1. Dendrimers as Ligands.

Initial synthetic aspects relating to the class of macromolecules known as dendrimers date back to the 1970's and demonstrated the synthesis of low molecular weight highly branched amines.[1] The seminal work of the Tomalia[2-4] and Fréchet[5-7] groups described the synthesis of "true dendrimers". Dendrimers are monodisperse, hyper-branched macromolecules with a globular shape and nanometre size. The branches extend radially outward from a core with repeat units, each of which constitutes a branch point, to the periphery. Generally the periphery bears functional groups, the number of which is dependent on the dendrimer generation (Fig 3.1).[8]

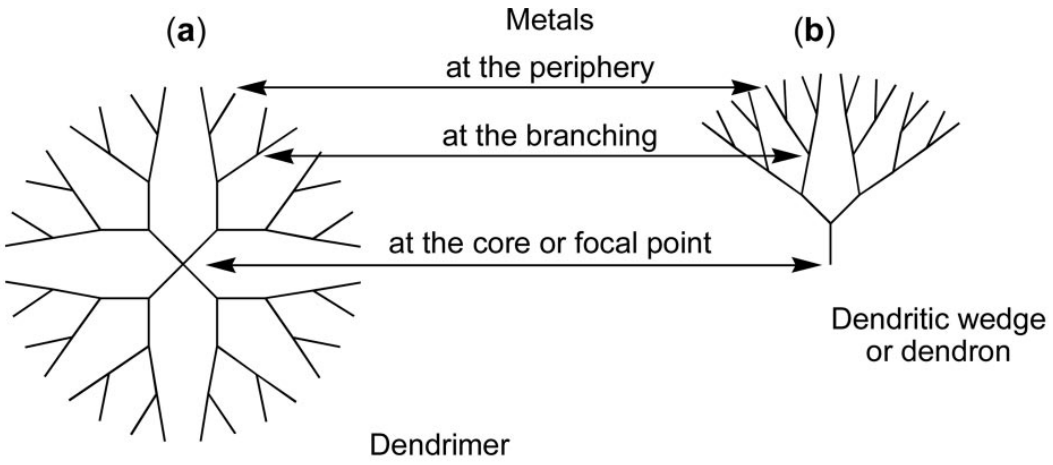

Fig. 3.1 The possible location of functionalities (metals) in the (a) dendrimer and (b) dendron.[9]

The divergent approach to dendrimer synthesis (Tomalia group) is a synthetic method in which the macromolecular architecture is constructed from the core, with branch points added sequentially extending to the periphery (Fig 2.4). The convergent approach

(Fréchet group) proceeds conversely with assembly of the macromolecule proceeding from the periphery inward toward the core.

The initial dendrimers prepared by these two synthetic methodologies have become commercially available and are known as polyamido amine (PAMAM, Tomalia group) and polybenzyl ether (PBE, Fréchet group) dendrimers. Other commercially available dendrimers include those derived from polypropylene imine (PPI),[10] carbosilane (CS),[11-13] and phosphorous (NNPS)[14-16] moieties.

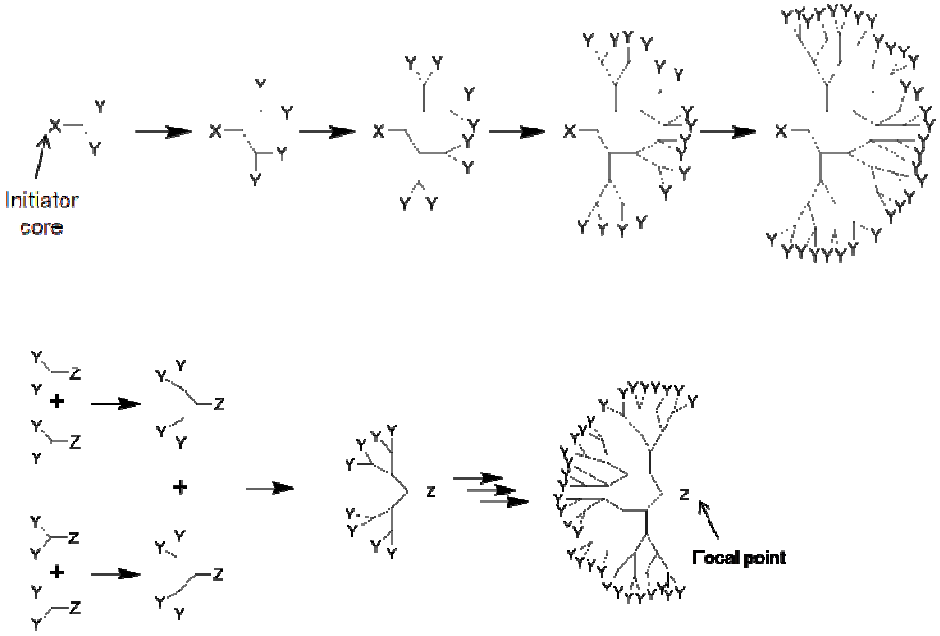

Fig. 3.2 A schematic representation of the divergent (top) and convergent (bottom) approach to dendrimer synthesis.

The selective functionalisation of dendrimer molecules has allowed for the development of metal complexes of this class of molecules, which have been termed metallodendrimers.[17] In recent years the metallodendrimer chemistry of palladium has seen

extensive growth as evidenced by a number of reviews dedicated to their synthesis and applications.[9, 17-20]

A few examples of the synthesis and application of dendrimer-supported Pd(II) complexes will be discussed.

Kaneda and co-workers prepared and characterised PPI dendrimers in which the periphery was modified with diphenylphosphinomethane moieties (Fig. 3.3).[21]

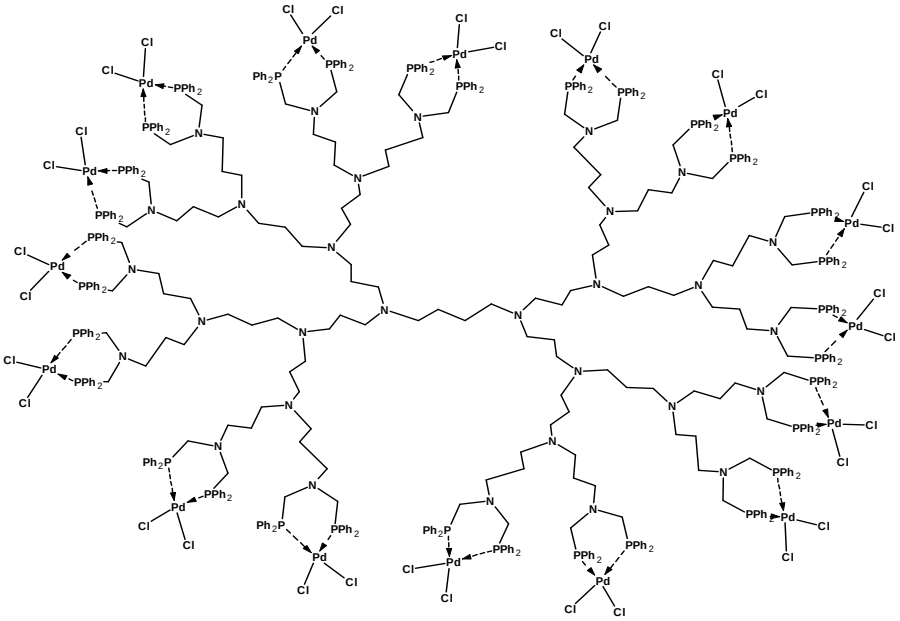

Fig. 3.3 G3 diphenylphosphinomethane-modified PPI metallodendrimer employed in the hydrogenation of dienes.[21]

Metallodendrimers were obtained by reaction of the dendrimer with $(PhCN)_2PdCl_2$. The dendritic Pd(II) complex was found to selectively hydrogenate conjugated dienes to monoenes with catalytic activity exceeding that of the mononuclear analogue, $[PhN(CH_2PPh_2)_2PdCl_2]$. Furthermore, the dendrtitic catalyst displayed recyclability without the loss of activity.

Mapolie and co-workers prepared palladium metallodendrimers by the reaction of (COD)$PdCl_2$ with iminopyridyl moieties on a PPI dendrimer periphery (Fig. 3.4).[22] These dendritic complexes were found to be highly active catalysts in the Heck reaction of iodobenzene with both activated and deactivated olefins. No attempts at catalyst recovery and recycling were reported.

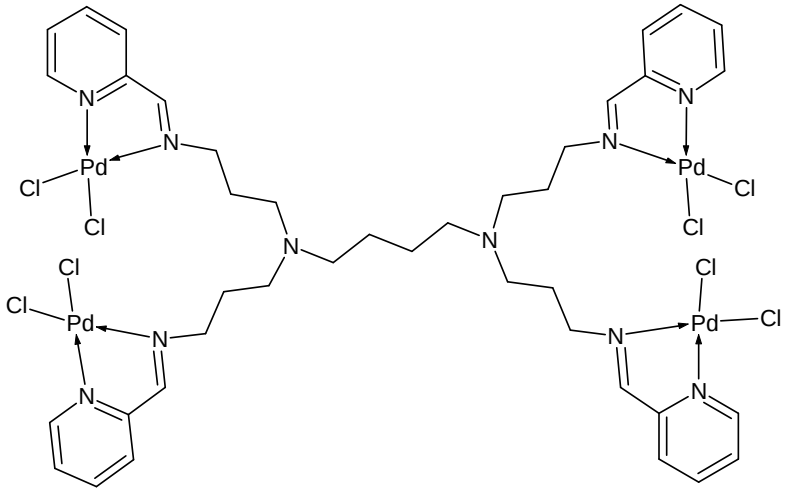

Fig. 3.4 G1 iminopyridyl Pd(II) metallodendrimer employed in the Heck reaction of iodobenzene and activated alkenes.[22]

van Koten and co-workers developed a general strategy for the incorporation of palladium metal centres onto the periphery of dimethylbenzylamine functionalised carbosilane dendrimers via C-H bond activation (Fig. 3.5).[23] These cyclopalladated dendritic complexes were applied in the aldol condensation of benzaldehyde with methyl isocyanoacetate to yield either *cis*- or *trans*-substituted oxazolines. It was found that the reaction was affected negatively by an increase in dendrimer generation, which coincided with a selectivity change in the *cis*/*trans* ratio of the oxazoline product.

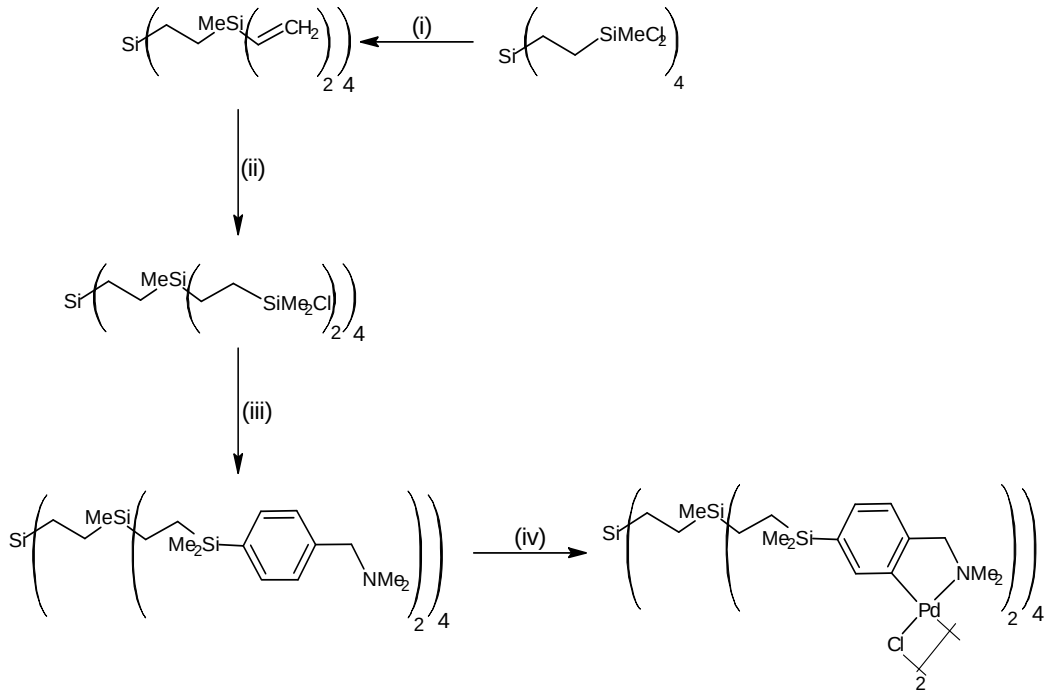

(i) excess VinylMgBr, THF, RT; (ii) neat $HSiMe_2Cl$, RT, $(NBu_4)_2PtCl_6$ as catalyst; (iii) $Li^+(C_6H_4CH_2NMe_2)^-$, Et_2O, - 78 ^oC to rt.; (iv) $Pd(OAc)_2$, MeOH; then LiCl, MeOH

Fig. 3.5 Cyclopalladated carbosilane dendimers developed by van Koten and co-workers.[23]

Here we report our studies directed toward the attempted synthesis of cyclopalladated dendrimer complexes derived from imine peripherally modified dendrimers.

3.2 Results and Discussion.

3.2.1 Synthesis of peripherally modified PPI dendrimers.

In recent years, the research interest of the Mapolie group has been directed toward the peripheral modification of commercially available PPI dendrimers in an attempt to produce dendritic ligands for transition metal complex synthesis.[22, 24-26] Their strategy centred

on functionalising the amino-terminated periphery via Schiff base condensation with various aldehyde derivatives.

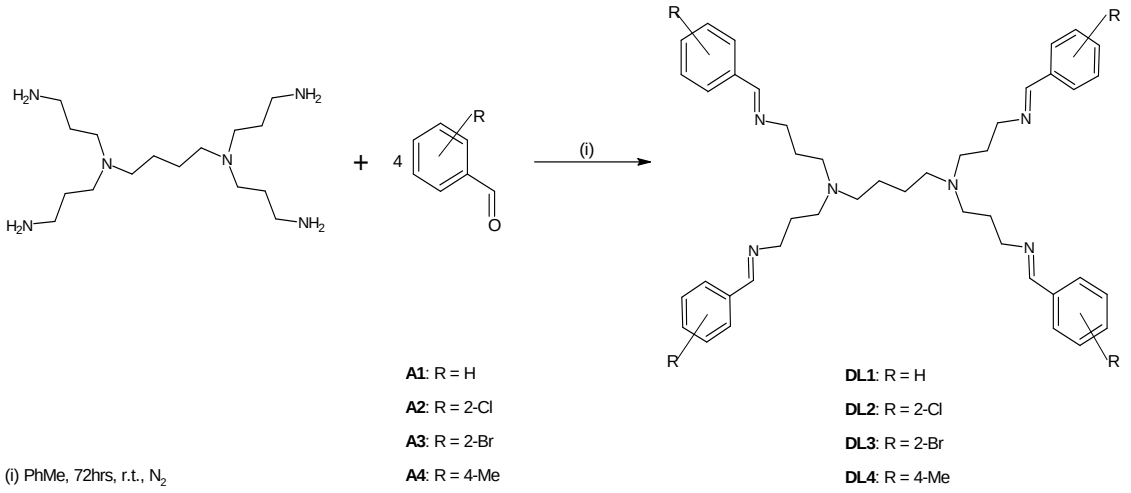

Scheme 3.1 A general scheme for the synthesis of peripherally modified PPI dendrimer ligands, **DL1-DL4**.

These peripherally modified dendrimers could then function as ligand scaffolds for the synthesis of multinuclear metal complexes. It was envisaged that this strategy would allow for the preparation of suitably functionalised dendritic ligand scaffolds for the synthesis of multinuclear dendrimer-supported palladacycles.

Thus the commercially available generation 1 PPI dendrimer, DAB-$(NH_2)_4$, was reacted with various mono-substituted aromatic aldehydes (Scheme 3.1). Even though every effort was made to ensure the correct molar ratio, FT-IR analysis of the product after work-up still showed the presence of unreacted aldehyde starting material as evidenced by the characteristic $\upsilon_{C=O}$ absorption band in the range 1680-1700 cm^{-1}. The product was refluxed in hexane in an attempt to remove the aldehyde but to no avail.

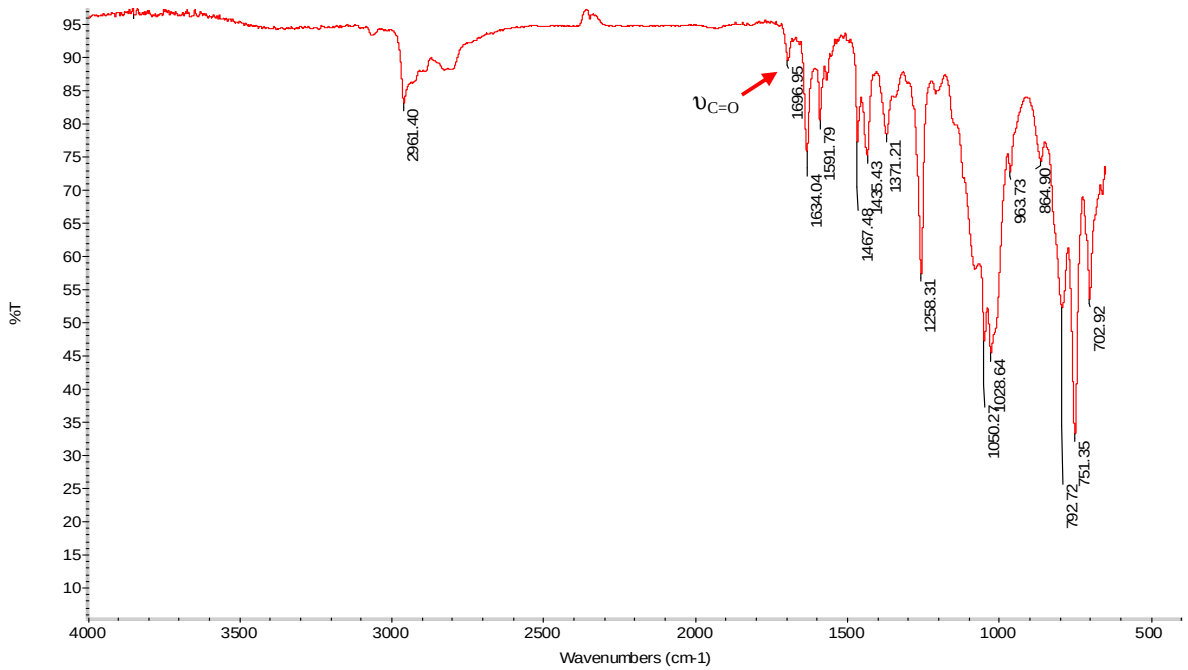

Fig. 3.6 FT-IR spectrum of ligand **DL2**, after reflux of the product in hexane.

The products were thus purified by vacuum distillation at reduced pressure employing a Kugelrühr apparatus which facilitated the removal of residual aldehyde in the product. This allowed for the isolation of the peripherally modified dendrimer ligands, **DL1-DL4**, as pure yellow oils with product yields ranging between 75-90 %. These novel dendritic ligands displayed solubility in chlorinated and aromatic solvents but were found to be insoluble in alkanes, alcohols and ethers.

The dendritic ligands were characterised by a range of analytical techniques. In the FT-IR spectra of the ligands the appearance of an absorption band corresponding to $\upsilon_{C=N}$ of the imine moiety was observed in the range 1630-1650 cm^{-1} (Table 3.1). This coincided with the disappearance, after purification, of the $\upsilon_{C=O}$ absorption band of the aldehyde starting material.

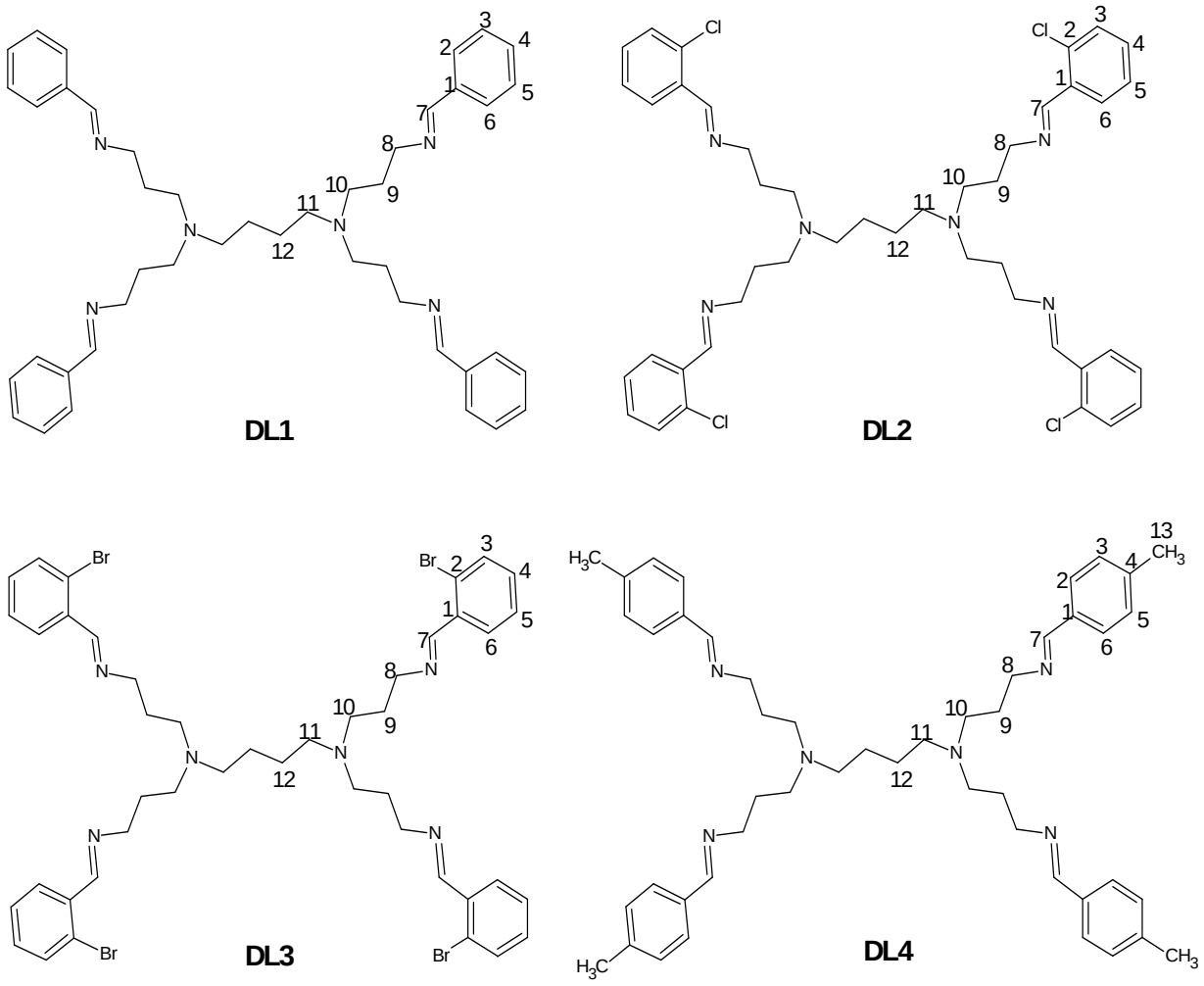

Fig. 3.7 The synthesised dendritic ligands, **DL1**-**DL4**, displaying the numbering scheme employed for NMR analysis.

^{1}H NMR analysis provided further confirmation that the ligands were synthesised successfully (Table 3.2). The resonances observed in the ^{1}H NMR spectra of the ligands also demonstrated the high degree of symmetry present in the ligand. The imine proton resonance was observed in the range δ 8.23-8.64 ppm integrating for a total of four protons. As was observed for the monofunctional ligands **L2** and **L3,** (Chapter 2, Section 2.2.1), the imine

proton resonances of **DL2** and **DL3** are shifted more downfield in comparison to **DL1** and **DL4**, which is as a result of the inductive effect of the halogen substituents.[27]

Table 3.1 Analytical data pertaining to dendritic ligand synthesis.

Ligand No.	FT-IR ($\upsilon_{C=N}$, cm^{-1})[a]	ESI-MS (m/z)[b]
DL1	1645	670
DL2	1636	807
DL3	1634	985
DL4	1645	726

[a] Recorded as neat spectra on a ZnSe crystal, employing an ATR accessory. [b] Reported ion corresponds to the proton adduct of the molecular ion, $[M + H]^+$.

The aromatic region of the dendritic ligands showed resonance patterns typical of monosubstitution (**DL1**), 1,2- (**DL2** and **DL3**) and 1,4-disubstitution (**DC4**) as well as long-range coupling between adjacent protons although in some cases resonance overlap was observed (Fig. 3.8). In the aliphatic region the methylene protons adjacent to the imine moiety was observed to shift downfield by approximately 1 ppm unit in comparison to G1 PPI dendrimer starting material, resonating as a triplet integrating for eight protons in the range δ 3.60-3.68 ppm. The remainder of the dendrimer backbone was observed in the range δ 1.42-2.56 ppm. The most deshielded resonance in the ^{13}C NMR spectra of the ligands corresponds to that of the imine C-atom and was observed in the range δ 158-160 ppm.

Table 3.2 ^{1}H NMR spectral data of dendritic ligands **DL1-DL4**.[a]

Ligand	CH=N	Aromatic Region	Aliphatic region
DL1	8.27 (s, 4H, H^{7})	7.69-7.72 (m, 8H, $H^{2,6}$); 7.37-7.41 (m, 12H, $H^{3,4,5}$)	3.63 (t, 8H, H^{8}, $^{3}J_{H\text{-}H}$ 6.16 Hz); 2.52 (br. t, 8H, H^{10}, $^{3}J_{H\text{-}H}$ 6.60 Hz); 2.42 (br. t, 4H, H^{11}, $^{3}J_{H\text{-}H}$ 6.16 Hz) 1.79-1.89 (m, 8H, H^{9}); 1.43 (br. t, 4H, H^{12})
DL2	8.64 (s, 4H, H^{7})	7.99 (dd, 4H, H^{6}, $^{3}J_{H\text{-}H}$ 7.19 Hz, $^{4}J_{H\text{-}H}$ 2.20 Hz); 7.33-7.37 (m, 4H, H^{3}); 7.23-7.31 (m, 8H, $H^{4,5}$)	3.68 (t, 8H, H^{8}, $^{3}J_{H\text{-}H}$ 6.90 Hz); 2.56 (t, 8H, H^{10}, $^{3}J_{H\text{-}H}$ 7.34 Hz); 2.47 (br. t, 4H, H^{11}, $^{3}J_{H\text{-}H}$ 6.75 Hz); 1.82-1.91 (m, 8H, H^{9}); 1.47 (br. t, 4H, H^{12})
DL3	8.63 (s, 4H, H^{7})	7.98 (dd, 4H, H^{6}, $^{3}J_{H\text{-}H}$ 7.80 Hz, $^{4}J_{H\text{-}H}$ 1.95 Hz); 7.54 (dd, 4H, H^{3}, $^{3}J_{H\text{-}H}$ 7.99 Hz, $^{4}J_{H\text{-}H}$ 1.17 Hz); 7.31 (t, 4H, H^{5}, $^{3}J_{H\text{-}H}$ 7.21 Hz); 7.21-7.25 (dt, 4H, H^{4}, $^{3}J_{H\text{-}H}$ 7.80 Hz, $^{4}J_{H\text{-}H}$ 1.75 Hz)	3.68 (t, 8H, H^{8}, $^{3}J_{H\text{-}H}$ 7.02 Hz); 2.54 (t, 8H, H^{10}, $^{3}J_{H\text{-}H}$ 6.82 Hz); 2.44 (br. t, 4H, H^{11}, $^{3}J_{H\text{-}H}$ 5.85 Hz); 1.82-1.89 (m, 8H, H^{9}); 1.45 (br. t, 4H, H^{12})
DL4	8.23 (s, 4H, H^{7})	7.58 (d, 8H, $H^{3,5}$, $^{3}J_{H\text{-}H}$ 8.22 Hz); 7.17 (d, 8H, $H^{2,6}$, $^{3}J_{H\text{-}H}$ 7.78 Hz)	3.60 (t, 8H, H^{9}, $^{3}J_{H\text{-}H}$ 6.02 Hz); 2.56 (t, 8H, H^{10}, $^{3}J_{H\text{-}H}$ 6.60 Hz); 2.45 (bs, 4H, H^{11}); 2.37 (s, 12H, H^{13}); 1.81-1.90 (m, 8H, H^{9}); 1.42 (br. t, 4H, H^{12})

[a] Spectra run in $CDCl_3$ at 25 °C. Chemical shifts reported as δ ppm values, referenced relative to residual solvent peak. Superscripts denote protons as per numbering scheme (Fig. 3.7).

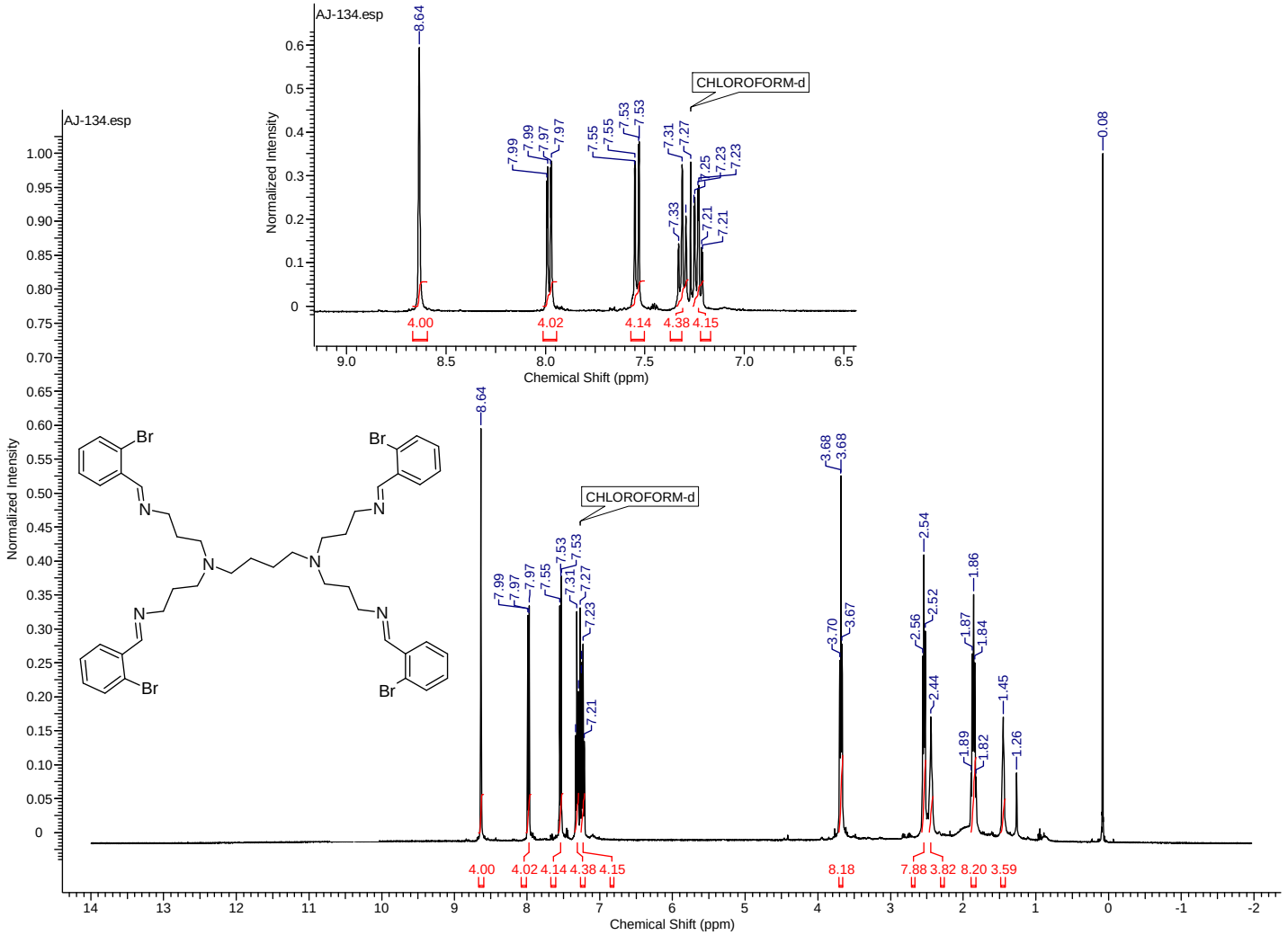

Fig. 3.8 ^{1}H NMR spectrum of ligand **DL3**, displaying the aromatic region (inset).

Interestingly, the carbon resonance in the aliphatic region can be divided into two distinct regions. In the range δ 50-60 ppm three carbon resonances were observed which were assigned to the propyl chains which form the dendrimer branches. In the range δ 20-30 ppm two carbon resonances were observed and were assigned to the diaminobutane chain which comprises the core of the dendrimer. The same features have been observed for peripherally modified dendrimer ligands which have been previously prepared in our group.[24, 26]

The prominent fragments observed in the positive ion ESI-MS spectra correspond to the proton adduct of the molecular ion, $[M + H]^+$ (Table 3.1). As was the case for previously reported dendritic ligands the formation of multiply-charged ions is a unique feature of these ligand systems.[28] Thus for **DL1** an ion peak corresponding to the doubly-charged parent ion, $[M + 2H]^{2+}$, was observed at *m/z* 335 (Fig. 3.9).

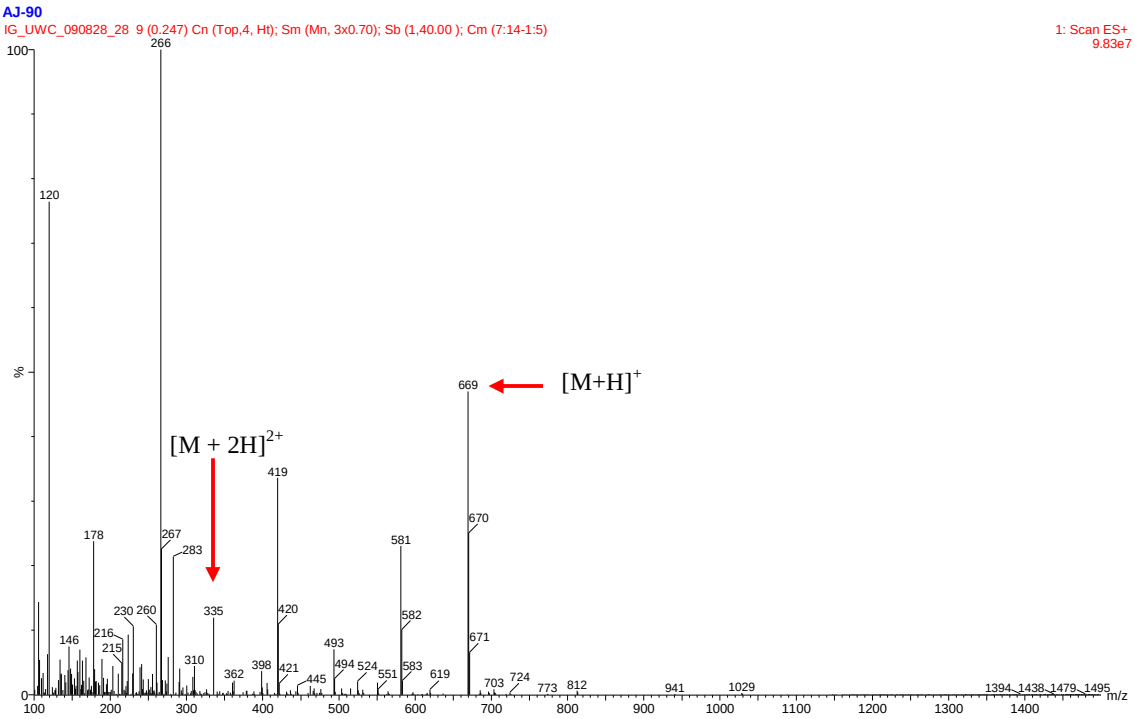

Fig. 3.9 positive ion ESI-MS spectrum of dendritic ligand **DL1**, indicating the doubly-charged ion.

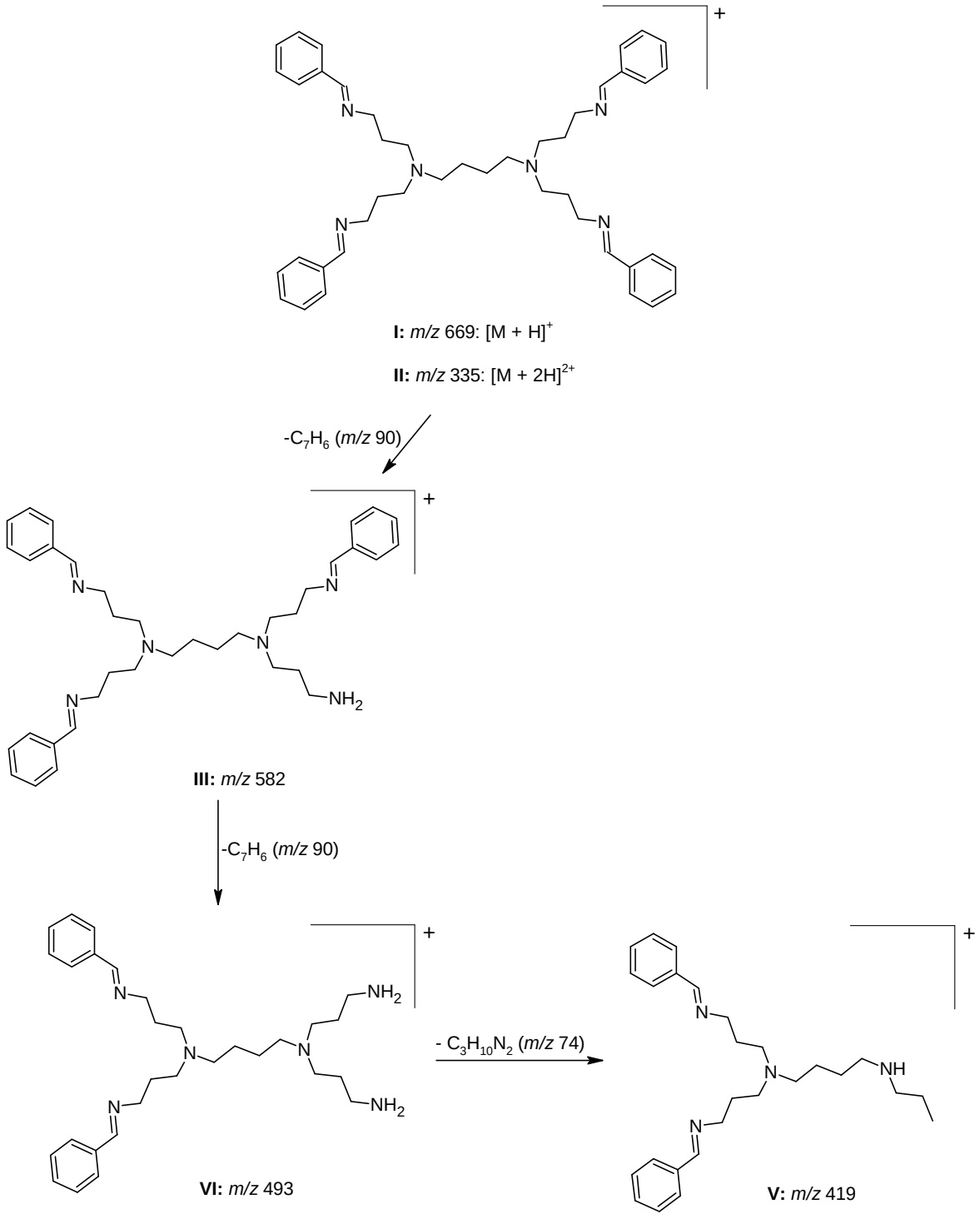

Scheme 3.2 A plausible fragmentation pathway of ligand **DL1** when subjected to positive ion ESI-MS analysis.

A plausible fragmentation pathway is given in Scheme 3.2. The parent ion (**I**) undergoes a two-step fragmentation via the sequential loss of a benzylidene unit producing the corresponding cationic fragments, *m/z* 582 (**III**) and 493 (**VI**). This was followed by the cleavage of a single propyl branch unit coinciding with cleavage of a C-N single bond to form the ion at *m/z* 419 (**V**).

3.2.2. Attempted synthesis of dendrimer-supported palladacycles.

Following the successful syntheses of mono- and dinuclear palladacycles described in Chapter 2 efforts were directed toward the preparation of dendritic palladacycles. It was envisaged that the same synthetic methodology employed in the preparation of monofunctional palladacycles would facilitate the isolation of the desired dendritic palladacycles.

Thus the dendritic ligands, **DL1-DL4**, were reacted with 4 mole equivalents of the palladium precursor, $(MeCN)_2PdCl_2$, in the presence of an excess of NaOAc to form the dendrimer-supported "palladacycles" (Scheme 3.3).

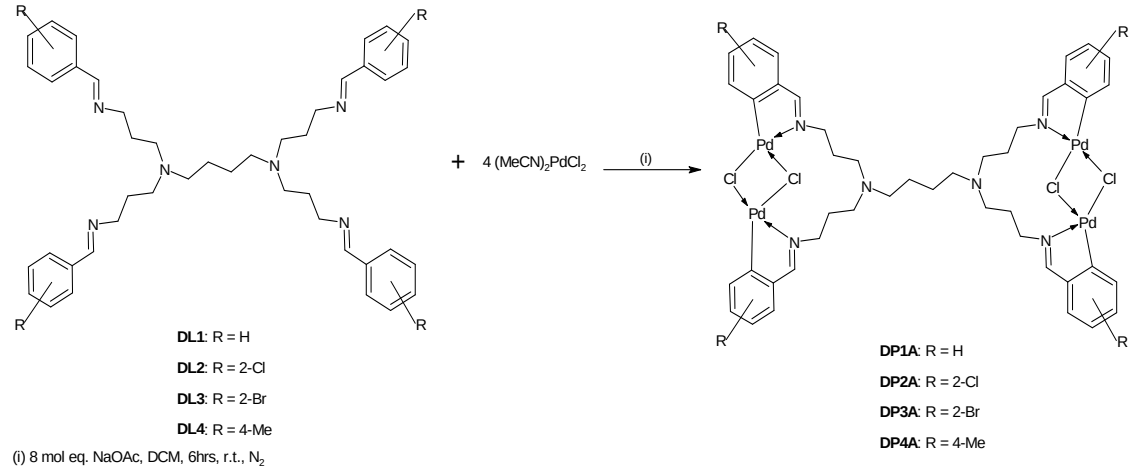

Scheme 3.3 Synthetic method employed for the preparation of dendrimer-supported palladacycles.

During the course of the reaction the onset of an orange-brown precipitate was observed which persisted throughout the reaction time period. The orange-brown solid was isolated by filtration and was air-dried. The crude material displayed solubility only in dimethyl sulphoxide (DMSO) which posed a problem in terms of the requisite purification to remove unreacted NaOAc.

The solubility of NaOAc in aqueous media prompted us to employ a water/solvent wash as purification method. Thus the solid was triturated with water (3 x 2 ml portions), the water layer syringed off and residual water removed by the addition of EtOH. It is well-known that Pd(II) species are reduced to Pd(0) species in the presence of MeOH. The same observation was made when employing EtOH, since the supernatant underwent a colour-change from clear to black. A colour-change from orange-brown to brown-black was observed for the solid product which was indicative of decomposition of the product material.

An alternative purification method was devised which involved substituting the alcohol with acetone. Thus employing a water/acetone wash as a purification method the purified product was successfully isolated, without any visible decomposition of the material.

The purified metallodendrimers, **DP1A-DP4A**, were characterised by FT-IR spectroscopy (Table 3.3). A slight shift to lower wavenumbers of the imine absorption band was observed for the dendritic complexes in comparison to the free ligand. This was attributed to coordination of the imine N-atom to the palladium centre.[29]

The appearance of a broad absorption band at approximately 3400 cm^{-1} was ascribed to the υ_{O-H} stretching vibration of residual water present in the sample due to the water/acetone wash (Fig. 3.10). It was expected that the imine absorption band of the dendritic palladacycles would undergo analogous shifts in wavenumbers to that observed for the dinuclear μ-Cl palladacycles. No significant difference between the imine absorption

band of the complexes and that of the ligands were observed. This observation suggested that there may be distinct differences in the metal coordination sphere of the dendritic complexes and the expected dendritic μ-Cl palladacycles.

Table 3.3 Absorption bands of dendritic palladacycles observed by FT-IR spectroscopy.

Complex	FT-IR ($\upsilon_{C=N}$, cm^{-1})[a]
DP1A	1632
DP2A	1633
DP3A	1633
DP4A	1631

[a] Recorded as neat spectra on a ZnSe crystal, employing an ATR accessory.

Also, the ^{1}H NMR spectra of the crude products did not show analogous bands to those observed for the μ-Cl palladacycles.

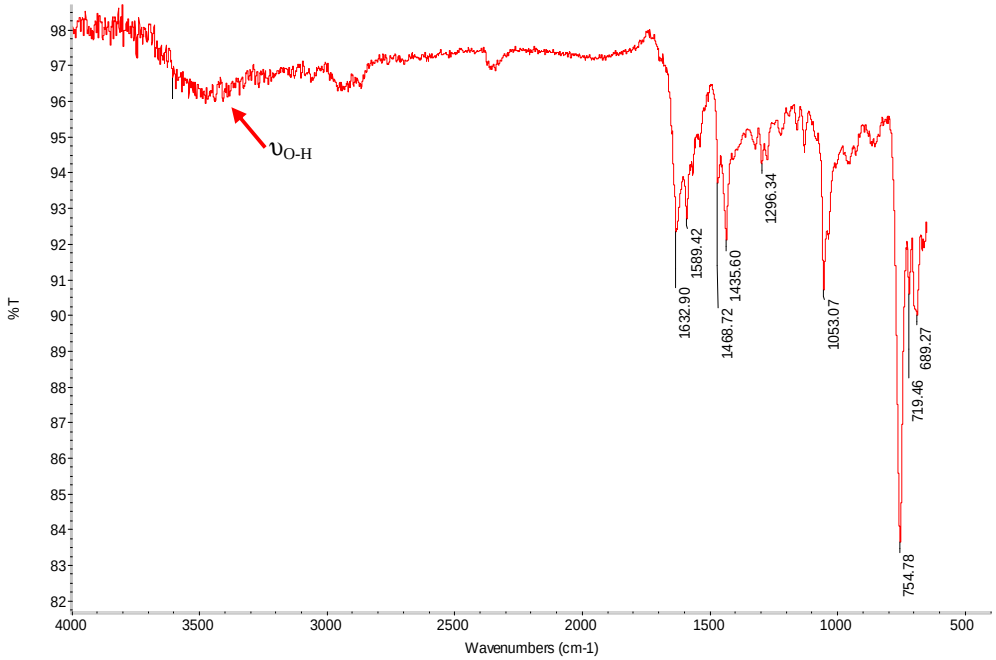

Fig. 3.10 FT-IR spectrum of the dendritic palladacycle, **DP2A**.

Thus it was decided to investigate the effect of base on the reaction by synthesising the dendritic complexes and employing the same reaction conditions in the absence of base. After 5-10 minutes of reaction the onset of an orange-brown precipitate was observed as was the case for the synthesis of the "dendritic palladacycles", **DP1A-DP4A**. The dendritic complexes, **DP1B-DP4B**, were isolated in 70-80 % yield. As was observed for **DP1A-DP4A** the complexes displayed solubility in DMSO only. The complexes were characterised by FT-IR spectroscopy and no difference in the imine absorption band was observed when compared to that of **DP1A-DP4A**, which was obtained in the presence of base.

The unsubstituted dendritic complex, **DP1B**, was characterised by ^{1}H NMR spectroscopy (Fig. 3.11). The ^{1}H NMR spectrum showed broad resonances which are characteristic of metallodendrimers.[22] The imine proton resonance was observed at δ 8.60 ppm as a broad singlet integrating for a total of four protons. A downfield shift from δ 8.27 ppm in the free ligand was indicative of coordination of the imine moiety to the palladium centre.[24] The aromatic protons also displayed a downfield shift from δ 7.40 (multiplet) and δ 7.70 ppm (multiplet) in the free ligand to δ 7.63 (multiplet) and δ 8.51 ppm (multiplet) in the dendritic complex. Interestingly, the aromatic protons integrated for a total of twenty protons which suggested that the palladium centre was not coordinated by the phenyl ring via a Pd-C bond. Thus, from ^{1}H NMR spectroscopy no evidence for C-H activation of the aromatic ring was found. The proton resonances of the dendrimer backbone were observed in the range δ 1-5 ppm. The most significant resonance in this region was that of the methylene protons adjacent to the imine moiety, -C*H*$_2$-CH=N-. This proton resonance was observed as a broad signal integrating for a total of eight protons and was shifted downfield to that observed for the free ligand to δ 3.89 ppm. It should also be noted that some

hydrolysis of the ligand backbone occurred as evidenced by the proton resonance observed at δ 10.01 ppm assigned to the aldehyde proton.

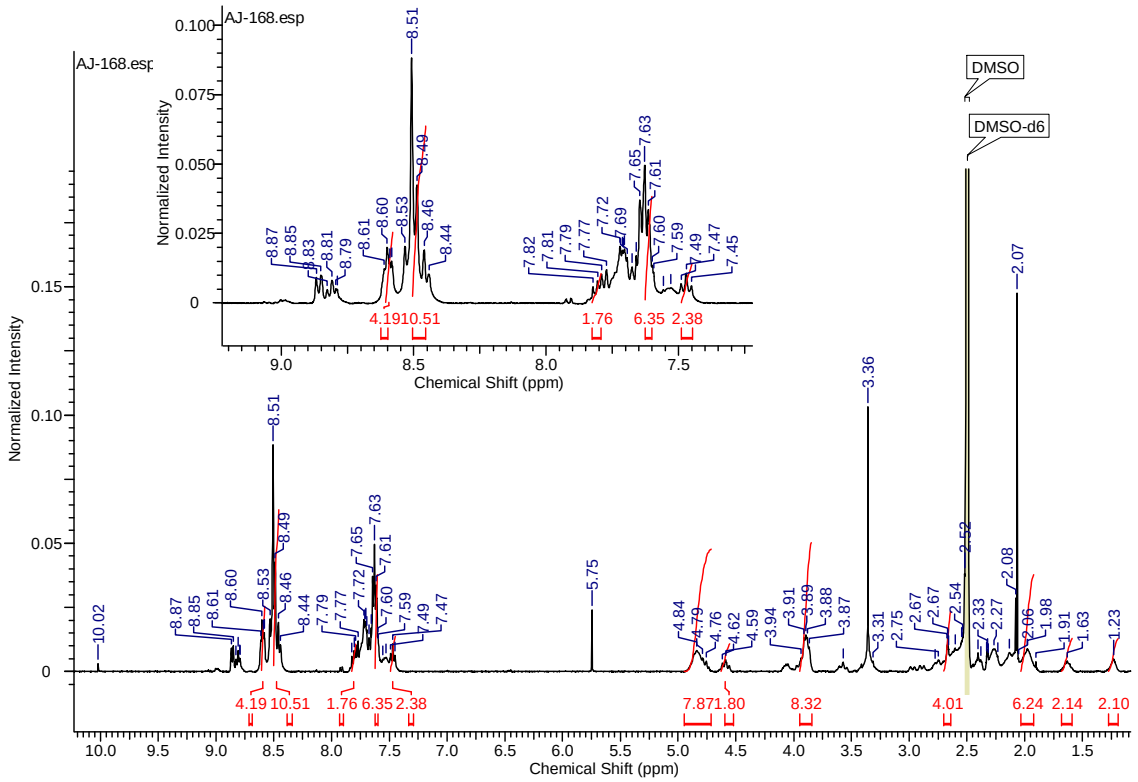

Fig. 3.11 ^{1}H NMR spectrum of dendritic complex, **DP1B**, with inset displaying the aromatic region.

To gain insight into the coordination mode of the Cl-ligands the 2-chlorobenzylaldiminato Pd(II) complex, **DP2B**, was analysed by Far-IR spectroscopy. This technique allowed for IR-analysis in the range 60-500 cm^{-1} in which Pd-Cl stretching vibrations would be visible. Furthermore, it also allowed for the discrimination between terminal and bridging Pd-Cl bonds.[30-31] The Far-IR spectrum of complex **DP2B** is shown in Fig 3.12. A single absorption band was observed at 331 cm^{-1} which was assigned to terminal Pd-Cl stretching vibrations. This value correlated well with those obtained for complexes of the type *cis*-PdX_2L_2, where X = halogen.[32]

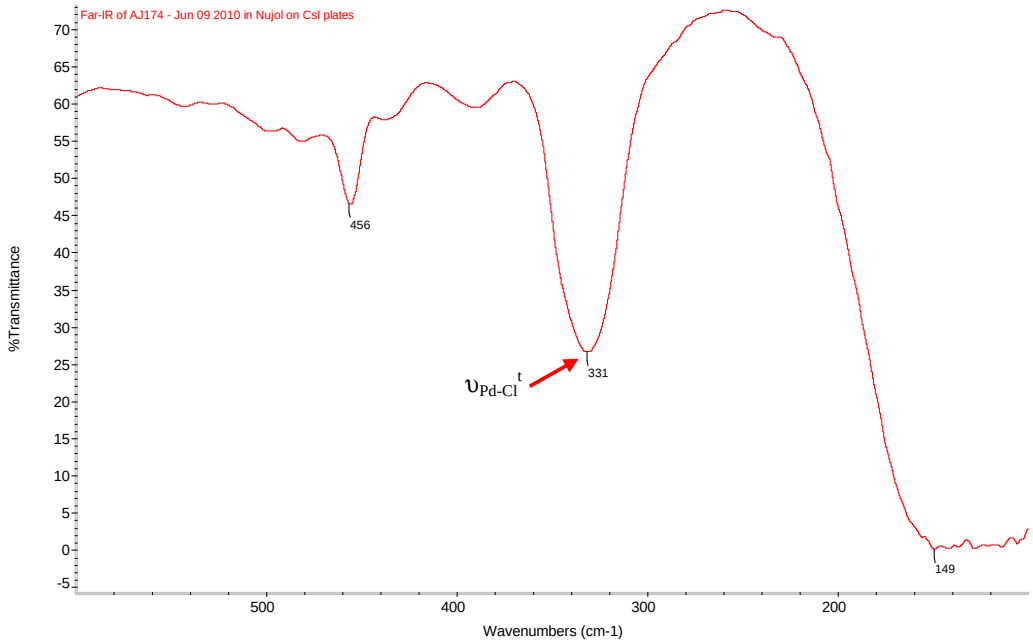

Fig. 3.12 Far-IR spectrum of 2-chlorobenzylaldiminato Pd(II) complex, **DP2B**.

The abovementioned results led to the conclusion that dendritic complexes of the type *cis*-$[PdX_2L_2]_2$ (where L constitutes one arm of the dendrimer) were in fact isolated, in which a palladium centre was coordinated by two adjacent imine moieties (Fig. 3.13).

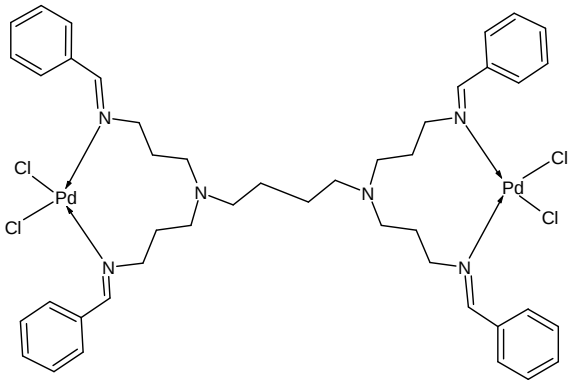

Fig. 3.13 A general structure of the isolated dendritic complexes.

Two possible reasons exist for the selective formation of dendritic Pd(II) coordination complexes. Firstly, the dendritic ligand may be interacting in a terdentate fashion, by

coordinating the metal centre in a N,N',N (where N= imine and N' = amine) fashion. Canovese and co-workers developed potentially terdentate N,N',N ligands and evaluated their coordination behaviour to Pd(II) metal precursors.[33] Although a terdentate binding mode was possible, in all cases the ligands were observed to coordinate in a bidentate fashion. From this result the possibility of a Pd-amine interaction may be excluded.

Secondly, an inappropriate choice of palladium(II) precursor and base may be responsible for the fact that cyclopalladation had not occurred. van Koten and co-workers demonstrated that the cyclopalladation of carbosilane dendrimers, with benzylamine units at the periphery of the dendrimer, could be effected by employing $Pd(OAc)_2$ as a precursor. The enhanced electrophilicity of the palladium centre in this precursor in comparison to bis(acetonitrile)palladium dichloride, would facilitate electrophilic C-H activation. This combined with the presence of the acetate group as an intramolecular base, rather than an intermolecular base (as is the case for NaOAc), would position the base perfectly for the requisite deprotonation step to form the cyclopalladated ring.

The synthetic method thus employed was directed toward the isolation of dendritic Pd(II) coordination complexes (Scheme 3.4).

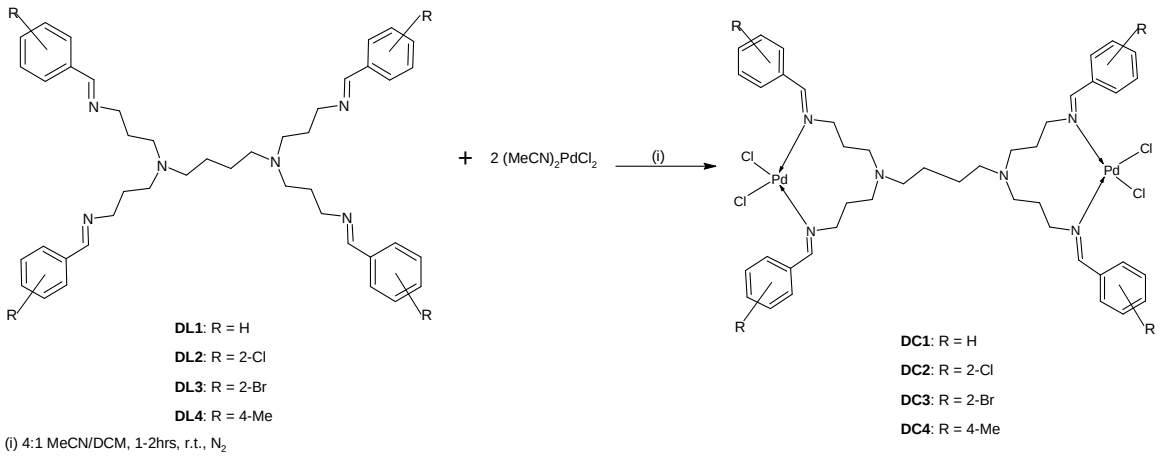

Scheme 3.4 A general reaction scheme for the preparation of dendritic Pd(II) coordination complexes.

The reaction of the dendritic ligands, **DL1-DL4**, with 2 mole equivalents of $(MeCN)_2PdCl_2$ in a 4:1 mixture of acetonitrile and dichloromethane allowed for the isolation of dendritic Pd(II) coordination complexes, **DC1-DC4** (Scheme 3.4). The complexes were isolated as orange-brown amorphous solids in 60-75 % yield. The complexes displayed solubility in DMSO only and were found to be air- and moisture-sensitive. The hygroscopic nature of the complexes was observed when a vacuum-dried sample was exposed to air overnight which resulted in the material adhering to the walls of the sample vial. The complexes were thus stored under an inert atmosphere. The dendritic complexes were analysed by a range of analytical techniques.

In the FT-IR spectra of the complexes, analogous imine absorption bands to that observed for **DP1A-DP4A** were observed in the range δ 1630-1633 cm^{-1}.

^1H NMR analysis of the dendritic coordination complexes, **DC1-DC4,** showed characteristically broad resonances as discussed previously (Table 3.4). The imine proton resonances were downfield shifted in comparison to the free ligands and were observed in the range δ 8.60-9.00 ppm. Broad multiplets were observed for the aromatic protons in the range δ 8.30-8.80 and δ 7.40-7.80 ppm integrating for a total of twenty (**DC1**) and sixteen (**DC2-DC4**) protons. The influence of the metal centre on the dendrimer backbone was observed in the shift of the methylene protons adjacent to the imine moiety. This proton resonance shifted to higher field by approximately 1.0 ppm and was observed as a broad multiplet integrating for a total of eight protons in the region δ 4.70 ppm (Fig. 3.14). This provided evidence that the palladium centre was coordinated to the dendritic ligand via the imine moieties on the periphery of each dendrimer arm. The dendrimer backbone was observed as broad signals spanning δ 1-5 ppm.

The solution stability of the complexes was tested by preparing an NMR sample and analysing the sample at time = 0hrs (immediately, Fig. 3.15, **a**) and time = 24hrs (Fig. 3.15, **b**). The result demonstrated that the complexes underwent significant hydrolysis after extended time periods. This type of hydrolysis process had been observed previously for the preparation of pyridylimine-functionalised Pd(II) metallodendrimers.[34]

It should be noted that the hydrolysis process commenced as soon as the NMR sample was prepared, since the formation of an aldehyde peak was observed even when analysis was performed immediately after sample preparation (Fig. 3.15, **a**).

The ^{13}C NMR spectra of the dendritic complexes, **DC1-DC4,** showed the imine carbon resonance in the range δ 173-175 ppm (Fig. 3.16). The resonance was shifted to higher field as a result of coordination to the palladium centre. Also, the aromatic carbon resonances were observed in the range δ 126-137 ppm. No carbon resonances were observed in the range δ 145-146 ppm, which is where the *o*-metallated carbon atom would resonate in the ^{13}C NMR spectra of palladacycles (see Chapter 2). The aliphatic region of the dendritic complexes showed peaks in the range δ 54-60 and δ 24-27 ppm which were assigned to the arms and the core of the dendrimer scaffold respectively.[24, 26] For **DC4** an additional carbon resonance, assigned to the *Me*-substituent on the aromatic ring, was observed at δ 21.40 ppm.

The ESI-MS spectra of the dendritic complexes showed characteristic clusters of peaks spanning approximately 10 *m/z* units. This observation was attributed to the presence of numerous isotopes of palladium and in the case of **DC2** and **DC3**, to isotopes of chlorine and bromine (Fig. 3.17).[35-36]

Table 3.4 ^{1}H NMR spectral data of the dendritic Pd(II) coordination complexes.[a]

Complex	CH=N	Aromatic Region	Aliphatic region
DC1	8.60 (br. s, 4H)	8.47-8.54 (br. m, 8H); 7.59-7.65 (br. m, 12H)	4.78-4.87 (br. m, -C*H*$_2$-CH=N-, 8H); 1.19-3.91 (broad peaks, 24H);
DC2	8.97 (br. s, 4H)	8.57-8.74 (br. m, 6H); 7.64-7.76 (br. m, 10H)	4.78-4.87 (br. m, -C*H*$_2$-CH=N-, 8H); 1.42-4.38 (broad peaks, 24H)
DC3	8.92 (br. s, 4H)	8.50-8.64 (br. m, 6H); 7.66-7.79 (br. m, 10H)	4.78-4.87 (br. m, -C*H*$_2$-CH=N-, 8H); 1.48-4.37 (broad peaks, 24H)
DC4	8.71 (br. s, 4H)	8.35-8.48 (br. m, 6H); 7.40-7.51 (br. m, 10H)	4.73-4.89 (br. m, -C*H*$_2$-CH=N-, 8H); 2.34 (br. s, C*H*$_3$ on aromatic ring); 1.26-4.56 (broad peaks, 24H)

[a] Spectra run in DMSO-d_6 at 25 °C. Chemical shifts given in ppm, referenced relative to residual solvent peak.

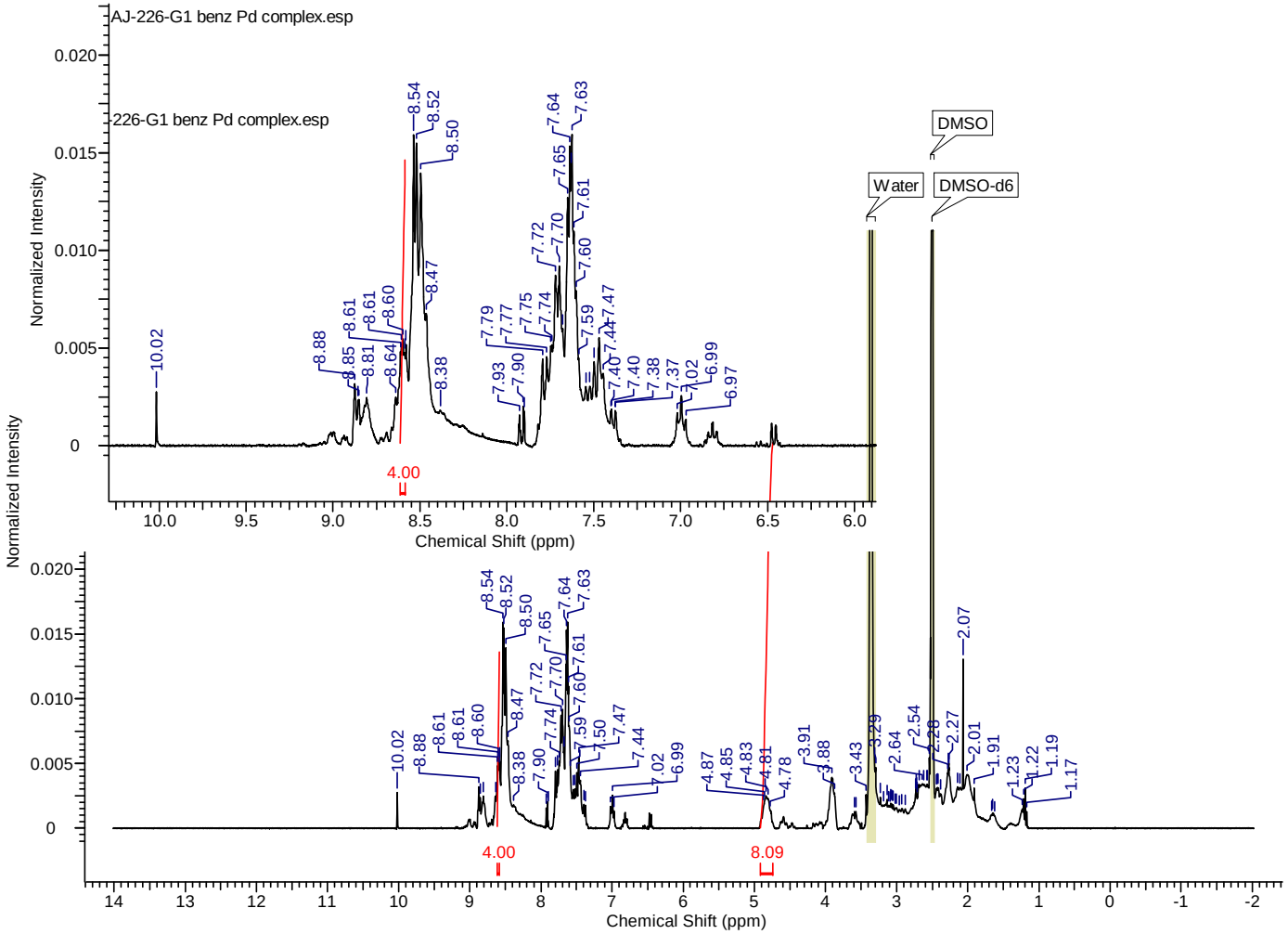

Fig. 3.14 ^{1}H NMR spectrum of the G1 unsubstituted benzylaldiminato Pd(II) complex, **DC1** showing the aromatic region (inset).

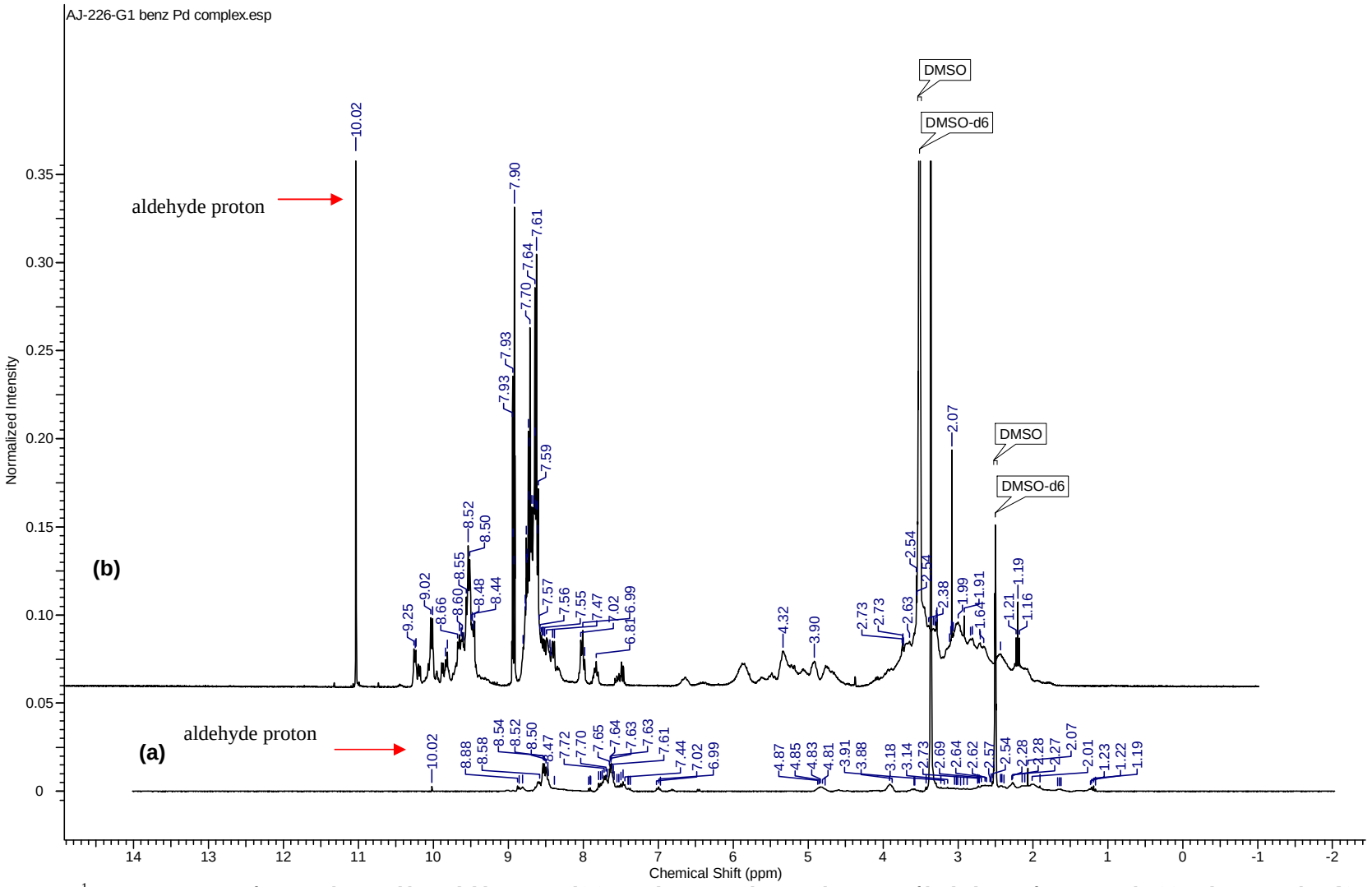

Fig. 3.15 ^{1}H NMR spectrum of G1 unsubstituted benzylaldiminato Pd(II) complex, **DC1**, showing the extent of hydrolysis, after time = 0hr (**a**) and time = 24hrs (**b**).

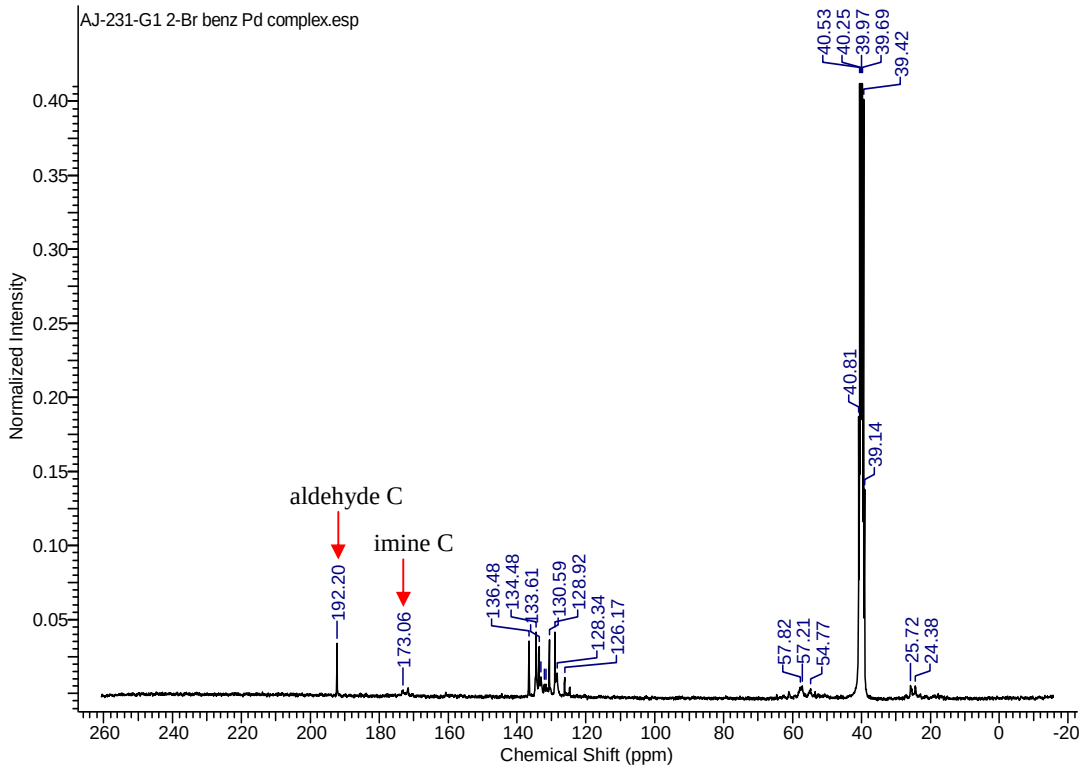

Fig. 3.16 ^{13}C NMR spectrum of 2-bromobenzylaldiminato Pd(II) complex, **DC3**.

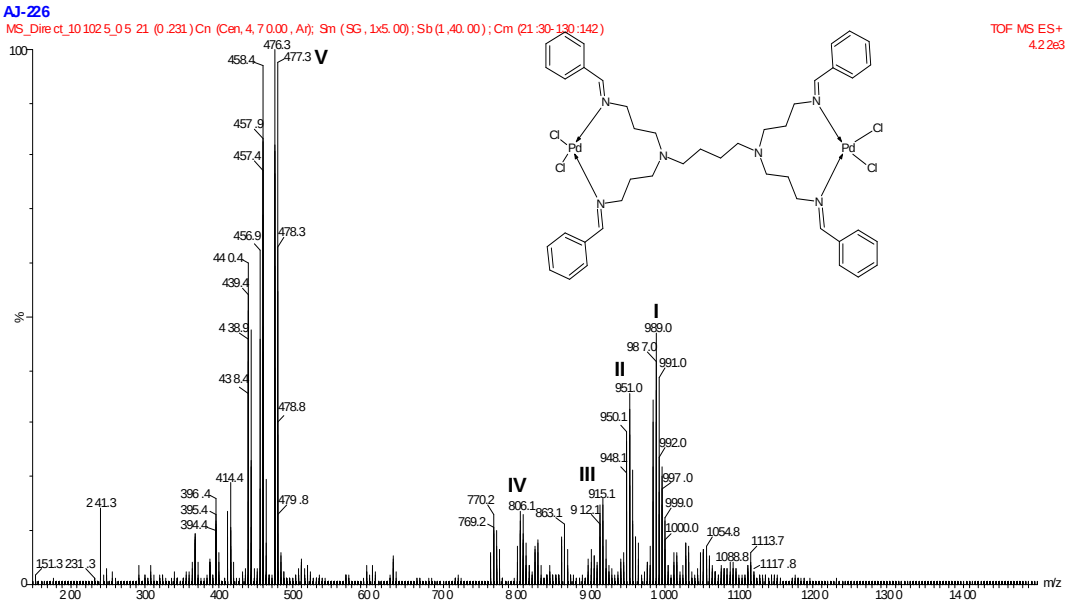

Fig. 3.17 ESI-MS (+) spectrum of **DC1** with major fragments annotated.

The major fragments observed in the ESI-MS spectra of these benzylaldiminato Pd(II) complexes correspond to $[M\text{-}Cl]^+$, $[M\text{-}2Cl]^+$ and the fragment consisting of $[PdC_{22}H_{29}ClN_3]^+$.

Table 3.5 ESI-MS results for dendritic Pd(II) complexes.

Complex	ESI-MS (*m/z*)[a]
DC1	988
DC2	1126
DC3	1303
DC4	1044

[a] ESI-MS spectra recorded in positive ion mode. Reported value corresponds to $[M\text{-}Cl]^+$.

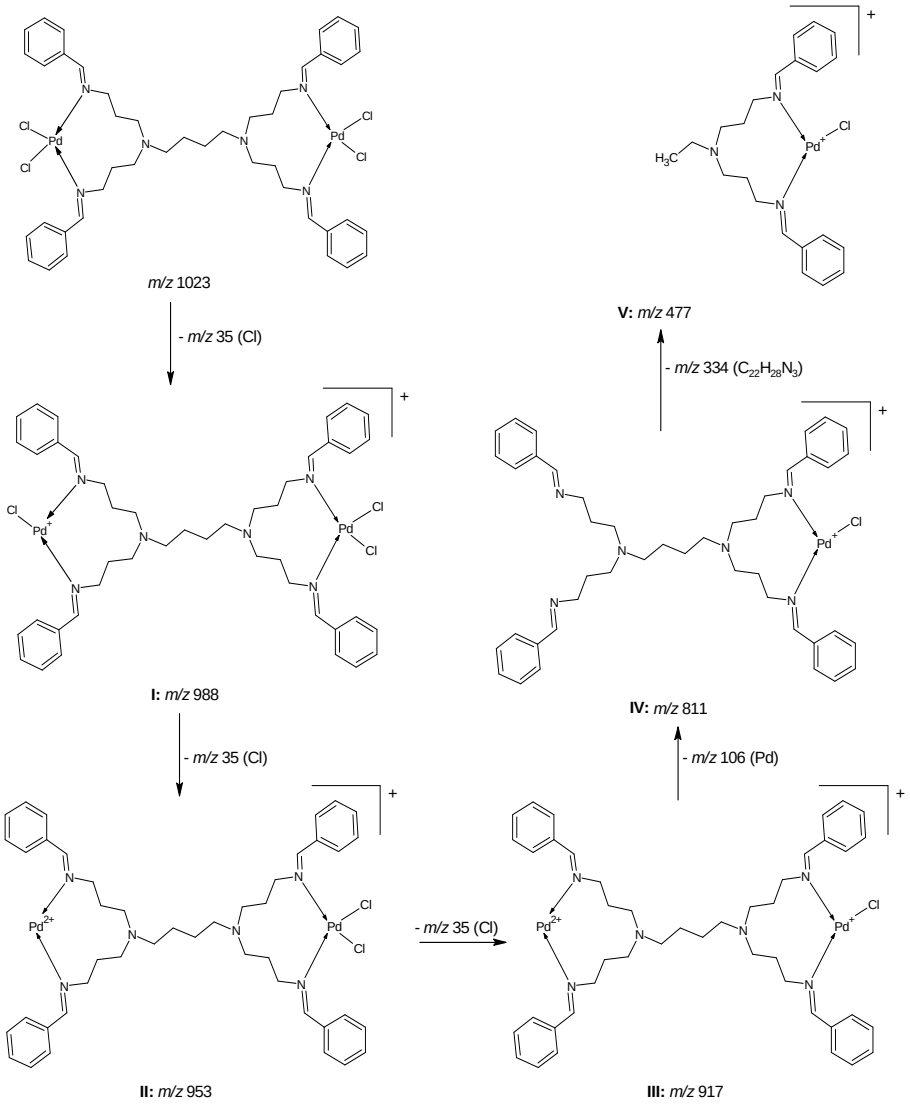

Scheme 3.5 A plausible fragmentation pathway for complex **DC1**.

A plausible fragmentation pathway for G1 unsubstituted benzylaldiminato Pd(II) complex, **DC1**, is given in Scheme 3.5. The parent ion undergoes step-wise loss of Cl^- to yield fragments **I**, **II**, and **III** respectively. This was followed by the de-metallation of a single Pd unit to yield fragment **IV**. The fragment with *m/z* 447 (fragment **V**) formed via cleavage of the butyl core and loss of a fragment corresponding to $C_{22}H_{28}N_3$ (left hand side of fragment **IV**). Fragment **I** had been previously observed as a characteristic fragment ion of cyclopalladated carbosilane dendrimers.[23] Simulation[37] of the isotope patterns of each fragment assigned in the experimental ESI-MS spectra of the complexes correlated well with the experimentally observed fragments (Fig. 3.18).

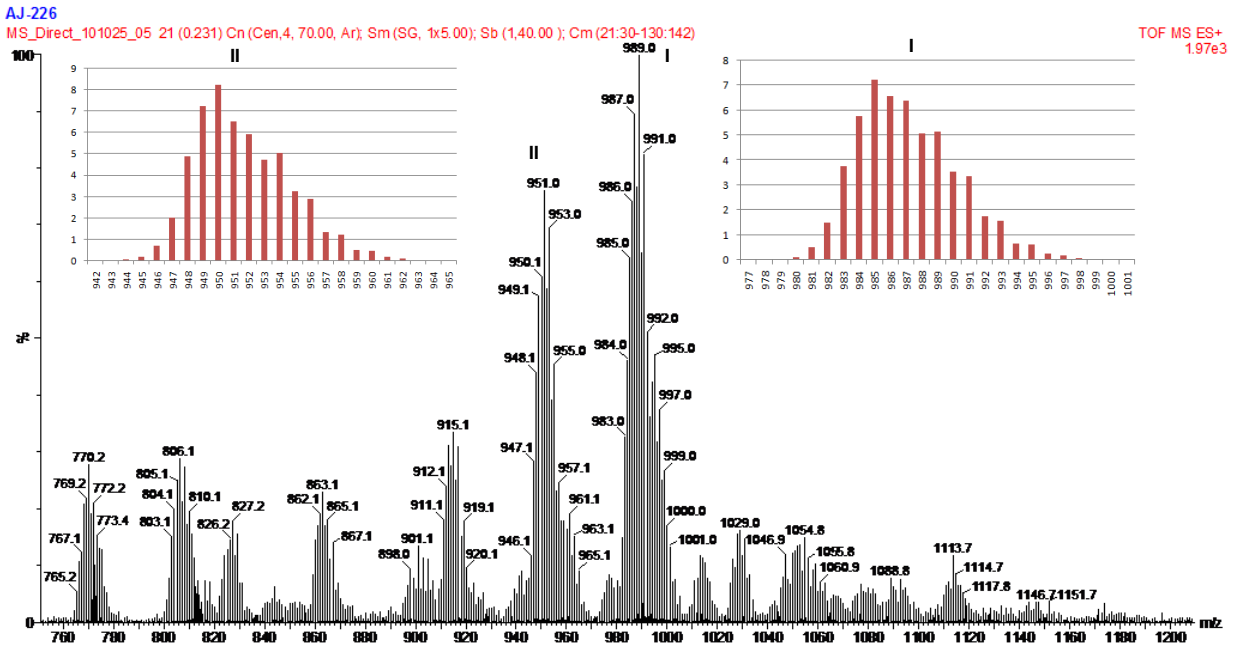

Fig. 3.18 Annotated peaks assigned to fragment **I** and **II**, with the simulated fragments shown (inset **I** and **II** respectively).

Elemental analysis results demonstrated that these metallodendrimers, **DC1-DC4**, often include solvent molecules, as well as absorbed moisture from the atmosphere

(Table 3.6). The same observation had been made previously for other metallodendrimers prepared in our group and was as a result of entrapment of solvent molecules within the voids of the dendrimer, particularly at higher generation.[26, 34, 38]

Table 3.6 Elemental analysis results for the metallodendrimers, **DC1-DC4**.

Complex	Elemental Analysis: Found (Calculated)		
	% C	**% H**	**% N**
DC1[a]	50.70 (51.63)	5.57 (5.51)	8.11 (8.21)
DC2[b]	39.85 (45.50)	4.67 (4.51)	5.87 (7.24)
DC3[c]	39.15 (39.46)	4.87 (3.91)	5.91 (6.28)
DC4[d]	48.00 (53.40)	5.41 (5.97)	6.72 (7.78)

[a] Inclusion of one molecule of water [b] Inclusion of three molecules of dichloromethane. [c] Inclusion of two molecules of water. [d] Inclusion of two molecules of dichloromethane.

3.3 Conclusions

Multifunctional dendritic ligands were prepared by Schiff base condensation of various mono-substituted aldehydes with 1st generation PPI dendrimer, DAB-$(NH_2)_4$. The peripherally modified dendrimer ligands were isolated in high yields and characterised by a range of analytical techniques. Attempts to incorporate cyclopalladated moieties onto the periphery of these multifunctional ligands via electrophilic C-H activation were unsuccessful. Instead, dendritic Pd(II) coordination complexes of the type $[PdX_2L_2]$ where L constitutes one arm of the dendrimer ligand were isolated. These metallodendrimers were characterised by various analytical techniques which confirmed the molecular formulation.

3.4 Materials and Methods

All transformations were performed using standard Schlenk techniques under a nitrogen atmosphere. Solvents were dried by distillation prior to use, and all reagents were employed as obtained. ^{1}H NMR (300 and 400 MHz) and ^{13}C {^{1}H} (75.38 and 100 MHz) spectra were recorded on Varian VNMRS (300 MHz); Varian Unity Inova (400 MHz) spectrometers and chemical shifts was reported in ppm, referenced to the residual protons of the deuterated solvents and tetramethyl silane (TMS) as internal standard. ESI-MS (ESI+) analyses were performed on Waters API Quattro Micro and Waters API Q-TOF Ultima instruments by direct injection of sample. FT-IR analysis was performed on a Thermo Nicolet AVATAR 330 instrument, and was recorded as neat spectra (ATR) unless specified. Melting point determinations was performed on a Stuart Scientific SMP3 melting point apparatus and is reported as uncorrected.

3.4.1 Synthesis of dendritic imine ligands (DL1-DL4):

3.4.1.1. G1 DAB-[N=CH-(C_6H_5)$_4$] (DL1):

To a stirring solution of DAB-(NH_2)$_4$ (1.04 g, 3.285 mmol) in toluene (20 ml) was added benzaldehyde (1.55 ml, 13.14 mmol). The reaction mixture was stirred for 72 hrs, the solvent removed and the yellow oil residue obtained redissolved in dichloromethane (20 ml). The organic layer was washed with water (5x20 ml portions), separated and dried over $MgSO_4$. The solvent was removed and the yellow oil obtained purified by vacuum distillation, using the Kugelruhr apparatus, at 90 °C and 15 mmHg for 60 min. Yield: 1.89 g, 86 %. ^{13}C NMR {^{1}H} (75.38 MHz, $CDCl_3$, numbering as per Fig. 3.7): δ 160.9 (*C*H=N, C^7);

δ 136.2 (C_{Ar}, C^1); δ 130.4 (C_{Ar}, C^4); δ 128.5 (C_{Ar}, $C^{2,6}$); δ 127.9 (C_{Ar}, $C^{3,5}$); δ 59.6 (-N*C*H_2-, C^8); δ 53.9 (-N*C*H_2-, C^{10}); δ 51.6 (-*C*H_2-, C^9); δ 28.1 (-*C*H_2-, C^{11}); δ 24.9 (-*C*H_2-, C^{12}). *Anal.* Found: C, 71.63; H, 7.59; N, 11.05. Calc. for $C_{44}H_{56}N_6.CH_2Cl_2$: C, 71.69; H, 7.75; N, 11.15.

3.4.1.2 G1 DAB-[N=CH-(2-Cl-C_6H_4)$_4$] (DL2).

The same synthetic procedure as outlined above (**DL1**) was employed for the synthesis of **DL2**, using 2-chlorobenzaldehyde as reagent. Yield = 2.07 g, 78 %. ^{13}C NMR {^{1}H} (75.38 MHz, $CDCl_3$, numbering scheme as per Fig. 3.7): δ 158.2 (*C*H=N, C^7); δ 135.3 (C_{Ar}, C^1); δ 133.7 (C_{Ar}, C^4); δ 131.7 (C_{Ar}, C^3); δ 130.1 (C_{Ar}, C^6); δ 128.6 (C_{Ar}, C^5); δ 127.3 (C_{Ar}, C^2); δ 60.2 (-N*C*H_2-, C^8); δ 54.4 (-N*C*H_2-, C^{10}); δ 51.9 (-*C*H_2-, C^9); δ 28.6 (-*C*H_2-, C^{11}); δ 25.4 (-*C*H_2-, C^{12}). *Anal.* Found: C, 65.58; H, 6.42; N, 10.36. Calc. for $C_{44}H_{52}Cl_4N_6$: C, 65.51; H, 6.50; N, 10.42.

3.4.1.3 G1 DAB-[N=CH-(2-Br-C_6H_4)$_4$] (DL3).

The same synthetic procedure as outlined above (**DL1**) was employed for the synthesis of **DL3**, using 2-bromobenzaldehyde as reagent. Yield = 2.43 g, 75 %. ^{13}C NMR {^{1}H} (75.38 MHz, $CDCl_3$, numbering scheme as per Fig. 3.7): δ 160.5 (*C*H=N, C^7); δ 135.1 (C_{Ar}, C^1); δ 133.4 (C_{Ar}, C^4); δ 131.9 (C_{Ar}, C^3); δ 129.1 (C_{Ar}, C^6); δ 127.9 (C_{Ar}, C^5); δ 125.3 (C_{Ar}, C^2); δ 60.0 (-N*C*H_2-, C^8); δ 54.4 (-N*C*H_2-, C^{10}); δ 51.9 (-*C*H_2-, C^9); δ 28.5 (-*C*H_2-, C^{11});

δ 25.4 (-*C*H_2-, C^{12}). *Anal.* Found: C, 53.59; H, 5.24; N, 8.51. Calc. for $C_{44}H_{52}Br_4N_6$: C, 53.68; H, 5.32; N, 8.54.

3.4.1.4 G1 DAB-[N=CH-(4-Me-C_6H_4)$_4$] (DL4):

The same synthetic procedure as outlined above (**DL1**) was employed for the synthesis of **DL4**, using *p*-tolualdehyde as reagent. Yield = 1.83 g, 77 %. ^{13}C NMR {^{1}H} (75.38 MHz, $CDCl_3$, numbering scheme as per Fig. 3.7): δ 160.9 (*C*H=N, C^7); δ 140.6 (C_{Ar}, C^4); δ 133.6 (C_{Ar}, C^1); δ 129.4 (C_{Ar}, $C^{3,5}$); δ 127.9 (C_{Ar}, $C^{2,6}$); δ 59.5 (-N*C*H_2-, C^8); δ 53.8 (-N*C*H_2-, C^{10}); δ 51.5 (-*C*H_2-, C^9); δ 27.9 (-*C*H_2-, C^{11}); δ 24.8 (-*C*H_2-, C^{12}); δ 21.4 (*C*H_3, C^{13}). *Anal*. Found: C, 79.43; H, 8.84; N, 11.44. Calc. for $C_{48}H_{64}N_6$: C, 79.51; H, 8.90; N, 11.59.

3.4.2 Synthesis of generation 1 benzylaldiminato Pd(II) complexes (DC1-DC4).

3.4.2.1 G1 DAB benzylaldiminato Pd(II) complex (DC1).

To a stirring solution of G1 benzylaldimine ligand (DL1, 189 mg, 0.193 mmol) in dichloromethane (2 ml) was added a solution of $(MeCN)_2PdCl_2$ (100 mg, 0.386 mmol) in acetonitrile (10 ml). The reaction mixture was stirred at room temperature for 1hr. After the allotted time the product was filtered and washed with copious amounts of dichloromethane and acetronitrile (approximately 300 ml total solvent volume). The orange-brown solid obtained was dried under vacuum while heating at 90 °C and stored under an inert atmosphere in a glovebox. Yield = 138 mg, 70 %. ^{13}C {^{1}H} NMR (75.38 MHz, $CDCl_3$, numbering scheme as per Fig. 3.7): δ 174.86 (*C*H=N, C^7); δ 135.77

(C_{Ar}, C^{1}); δ 134.73 ($C_{Ar,}$ C^{4}); δ 131.64 (C_{Ar}, $C^{2,6}$); δ 129.94 (C_{Ar}, $C^{3,5}$); δ 59.13 (-N*C*H_2-, C^{8}); δ 58.28 (-N*C*H_2-,C^{10}); δ 56.15 (-*C*H_2-, C^{9}); δ 26.99 (-*C*H_2-, C^{11}); δ 25.17 (-*C*H_2-, C^{12}).

3.4.2.2 G1 DAB 2-Br-benzylaldiminato Pd(II) complex (DC2).

The same synthetic procedure as outlined above (**DC1**) was employed for the synthesis of **DC2**, using DAB-[N=CH-(2-Cl-C_6H_4)$_4$] (**DL2**) as reagent. Yield = 152 mg, 68 %. ^{13}C NMR {^{1}H} (75.38 MHz, $CDCl_3$, numbering scheme as per Fig. 3.7): δ 173.1 (*C*H=N, C^{7}); δ 135.8 (C_{Ar}, C^{1}); δ 134.1 (C_{Ar}, C^{4}); δ 132.1 (C_{Ar}, C^{3}); δ 130.8 (C_{Ar}, C^{6}); δ 129.8 (C_{Ar}, C^{5}); δ 127.9 (C_{Ar}, C^{2}); δ 57.4 (-N*C*H_2-, C^{8}); δ 54.6 (-N*C*H_2-, C^{10}); δ 51.2 (-*C*H_2-, C^{9}); δ 26.9 (-*C*H_2-, C^{11}); δ 23.9 (-*C*H_2-, C^{12}).

3.4.2.3 G1 DAB 2-Br-benzylaldiminato Pd(II) complex (DC3).

The same synthetic procedure as outlined above (**DC1**) was employed for the synthesis of **DC3**, using DAB-[N=CH-(2-Br-C_6H_4)$_4$] (**DL3**) as reagent. Yield = 187 mg, 73 %. ^{13}C {^{1}H} NMR (75.38 MHz, $CDCl_3$, numbering scheme as per Fig. 3.7): δ 173.06 (*C*H=N, C^{7}); δ 136.48 (C_{Ar}, C^{1}); δ 133.61 (C_{Ar}, C^{4}); δ 133.61 (C_{Ar}, C^{3}); δ 130.59 (C_{Ar}, C^{6}); δ 128.92 (C_{Ar}, C^{5}); δ 126.17 (C_{Ar}, C^{2}); δ 61.06 (-N*C*H_2-, C^{8}); δ 57.82 (-N*C*H_2-, C^{10}); δ 54.77 (-*C*H_2-, C^{9}); δ 25.72 (-*C*H_2-, C^{11}); δ 24.38 (-*C*H_2-, C^{12}).

3.4.2.4 G1 DAB 2-Br-benzylaldiminato Pd(II) complex (DC4).

The same synthetic procedure as outlined above (**DC1**) was employed for the synthesis of **DC4**, using DAB-[N=CH-(4-Me-C_6H_4)$_4$] (**DL4**) as reagent. Yield = 144 mg, 69 %. ^{13}C {^{1}H} NMR (100 MHz, $CDCl_3$, numbering scheme as per Fig. 3.7): δ 173.3

(*C*H=N, C^{7}); δ 133.9 (C_{Ar}, C^{4}); δ 131.2 (C_{Ar}, C^{1}); δ 130.6 (C_{Ar}, $C^{3,5}$); δ 129.4 (C_{Ar}, $C^{2,6}$); δ 57.9 (-N*C*H_2-, C^{8}); δ 57.0 (-N*C*H_2-, C^{10}); δ 54.8 (-*C*H_2-, C^{9}); δ 25.8 (-*C*H_2-, C^{11}); δ 23.8 (-*C*H_2-, C^{12}); δ 21.4 (*C*H_3, C^{13}).

References

1. E. Buhleier and W. Wehner, *Synthesis*, 1978, 155.
2. D. A. Tomalia, H. Baker, J. Dewald, M. Hall, G. Kallos, S. Martin, J. Roeck, J. Ryder and P. Smith, *Polym. J.*, 1985, **17**, 117-132.
3. D. A. Tomalia, H. Baker, J. Dewald, M. Hall, G. Kallos, S. Martin, J. Roeck, J. Ryder and P. Smith, *Macromolecules*, 1986, **19**, 2466-2468.
4. D. A. Tomalia, A. M. Naylor and W. A. Goddard, *Angew. Chem. Int. Ed. Engl.*, 1990, **29**, 138-175.
5. C. Hawker and J. M. J. Frechet, *J. Chem. Soc., Chem. Commun.*, 1990, 1010-1013.
6. C. J. Hawker and J. M. J. Frechet, *J. Am. Chem. Soc.*, 1990, **112**, 7638-7647.
7. C. J. Hawker and J. M. J. Frechet, *Macromolecules*, 1990, **23**, 4726-4729.
8. J. M. J. Frechet, *J. Polym. Sci., Part A: Polym. Chem.*, 2003, **41**, 3713-3725.
9. E. de Jesús and J. C. Flores, *Ind. Eng. Chem. Res.*, 2008, **47**, 7968-7981.
10. E. M. M. de Brabander-van den Berg and E. W. Meijer, *Angew. Chem. Int. Ed. Engl.*, 1993, **32**, 1308-1311.
11. A. W. van der Made and P. W. N. M. van Leeuwen, *J. Chem. Soc., Chem. Commun.*, 1992, 1400-1401.
12. A. W. van der Made, P. W. N. M. van Leeuwen, J. C. de Wilde and R. A. C. Brandes, *Adv. Mater.*, 1993, **5**, 466-468.

13. L. L. Zhou and J. Roovers, *Macromolecules*, 1993, **26**, 963-968.

14. A.-M. Caminade and J.-P. Majoral, *Acc. Chem. Res.*, 2004, **37**, 341-348.

15. A.-M. Caminade and J.-P. Majoral, *Coord. Chem. Rev.*, 2005, **249**, 1917-1926.

16. A. M. Caminade, A. Maraval and J. P. Majoral, *Eur. J. Inorg. Chem.*, 2006, **2006**, 887-901.

17. D. Astruc, E. Boisselier and C. t. Ornelas, *Chem. Rev.*, 2010, **110**, 1857-1959.

18. S.-H. Hwang, C. D. Shreiner, C. N. Moorefield and G. R. Newkome, *New J. Chem.*, 2007, **31**, 1192-1217.

19. R. Andres, E. de Jesus and J. C. Flores, *New J. Chem.*, 2007, **31**, 1161-1191.

20. D. Mery and D. Astruc, *Coord. Chem. Rev.*, 2006, **250**, 1965-1979.

21. T. Mizugaki, M. Ooe, K. Ebitani and K. Kaneda, *J. Mol. Catal. A: Chem.*, 1999, **145**, 329-333.

22. G. S. Smith and S. F. Mapolie, *J. Mol. Catal. A: Chem.*, 2004, **213**, 187-192.

23. A. W. Kleij, R. J. M. Klein Gebbink, P. A. J. van den Nieuwenhuijzen, H. Kooijman, M. Lutz, A. L. Spek and G. van Koten, *Organometallics*, 2001, **20**, 634-647.

24. G. Smith, R. Chen and S. Mapolie, *J. Organomet. Chem.*, 2003, **673**, 111-115.

25. R. Malgas-Enus, S. F. Mapolie and G. S. Smith, *J. Organomet. Chem.*, 2008, **693**, 2279-2286.

26. J. N. Mugo, S. F. Mapolie and J. L. van Wyk, *Inorg. Chim. Acta*, 2010, **363**, 2643-2651.

27. J. Albert, J. Granell and J. Sales, *J. Organomet. Chem.*, 1984, **273**, 393-399.

28. J. L. van Wyk, *Mononuclear and Multinuclear Salicylaldimine Metal Complexes as Catalysts Precursors in the Oxidation of Phenol and Cyclohexene*, Ph.D, University of the Western Cape, **2008**.

29. H. Onoue and I. Moritani, *J. Organomet. Chem.*, 1972, **43**, 431-436.

30. D. M. Adams, *Metal-Ligand and Related Vibrations: A critical Survey of the Infrared and Raman spectra of metallic and organometallic compounds*, Edward Arnold Ltd London, 1966.

31. D. M. Adams and P. J. Chandler, *Chem. Commun. (London)*, 1966, 69-69.

32. G. E. Coates and C. Parkin, *J. Chem. Soc.*, 1963, 421-429.

33. L. Canovese, F. Visentin, G. Chessa, P. Uguagliati, C. Levi, A. Dolmella and G. Bandoli, *Organometallics*, 2006, **25**, 5355-5365.

34. N. Mketo, *Palladium and Copper Complexes based on Dendrimeric and Monofunctional N, N' Chelating Ligands as Potential Catalysts in the Oxidative Carbonylation of Alcohols* MSc Thesis, Stellenbosch University, **2010**.

35. L. Tusek-Bozic, M. Curic and P. Traldi, *Inorg. Chim. Acta*, 1997, **254**, 49-55.

36. L. Tusek-Bozic, M. Komac, M. Curic, A. Lycka, M. D. Alpaos, V. Scarcia and A. Furlani, *Polyhedron*, 2000, **19**, 937.

37. A. K. Brisdon, Mass spectrum isotope pattern calculator, http://fluorine.ch.man.ac.uk/research/mstool.php, Accessed 2010/11/18.

38. R. Malgas, S. F. Mapolie, S. O. Ojwach, G. S. Smith and J. Darkwa, *Catal. Commun.*, 2008, **9**, 1612-1617.

Chapter 4: Catalytic Applications of Mononuclear Palladacycles and Pd(II) Metallodendrimers

4.1 Introduction.

The catalytic functionalisation of C-C double bonds has developed into an active area of research both in industry and academia. This is evidenced by the considerable number of named C-C coupling reactions that have been developed and patented. In recent years this has been augmented by the development of late transition-metal complexes with superior applicability in terms of activity and selectivity in catalytic functionalisation processes.

Palladium and its complexes occupy an enviable position in catalytic C-C bond formation and their scope has been extended to encompass both traditional and more complex substrates.[1-3]

4.2 The Heck coupling of aryl halides and α-olefins.

The Heck coupling of aryl halides and olefins have recently been propelled onto the centre stage with the award of the 2010 Nobel Prize in Chemistry to Richard F. Heck, Ei-ichi Negishi and Akira Suzuki for "palladium-catalyzed cross-couplings in organic synthesis".[4]

Traditionally the Heck reaction had been catalysed by a palladium salt in the presence of excess phosphine and base.[5] Following this initial protocol much research effort has been directed toward improvement of the catalyst, by changing the nature of the phosphine, replacement of the phosphine completely, or by facilitating catalyst separation, recovery and recyclability.[1, 6-10]

The application of palladacycles in, amongst others, the Heck coupling reaction has been discussed previously (Chapter 1, Section 1.6.1). Thus, mechanistic aspects of the Heck

reaction and the application of palladium metallodendrimers in the Heck coupling will be discussed here.

4.2.1 Mechanistic aspects of the Heck reaction.

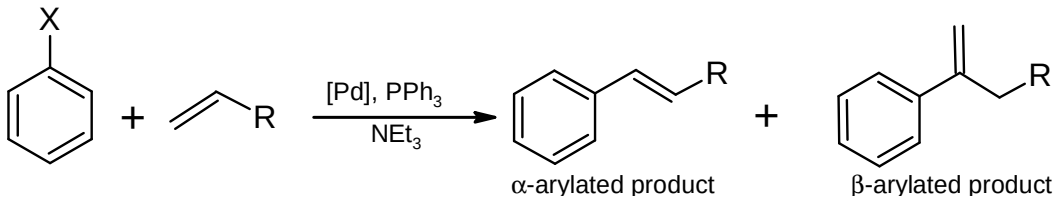

Scheme 4.1 A general scheme for the Heck coupling of aryl halides and olefins.

Traditionally the Heck coupling of aryl halides and olefins has been mediated by a palladium salt, typically $Pd(OAc)_2$, a phosphine ligand and a base (Scheme 4.1). Typical reaction conditions involve heating the substrates in the presence of the palladium precursor, phosphine ligand and base to effect the transformation. A general mechanism is given in Scheme 4.2. The preactivation step generates the catalytically active Pd(0) species. In phosphine-assisted catalysis this is accomplished by the phosphine ligand [11-12] and may be assisted by the presence of hard nucleophiles such as hydroxide ions and water and acetate ions.[13-14] In phosphine-free systems the primary reduction is mediated by the base, which traditionally may be an amine such as triethylamine.

Following the reduction to catalytically active Pd(0) species, oxidative addition of the aryl halide, R-X, via addition of the C-X bond to the low-valent transition metal species occurs. This process is concerted with the rupture of the C-X bonds coinciding with simultaneous M-C and M-X bond formation. The key feature in this step is the C-X bond strength and is the underlying cause for the inherent difficulty associated with the Heck

coupling of aryl chlorides.[15] The ultimate product of oxidative addition possesses *trans* geometry, which is preceded by the formation of the *cis* addition product. Moreover it has been demonstrated that the *cis* complex is the species which enters the next step of the catalytic cycle.[16]

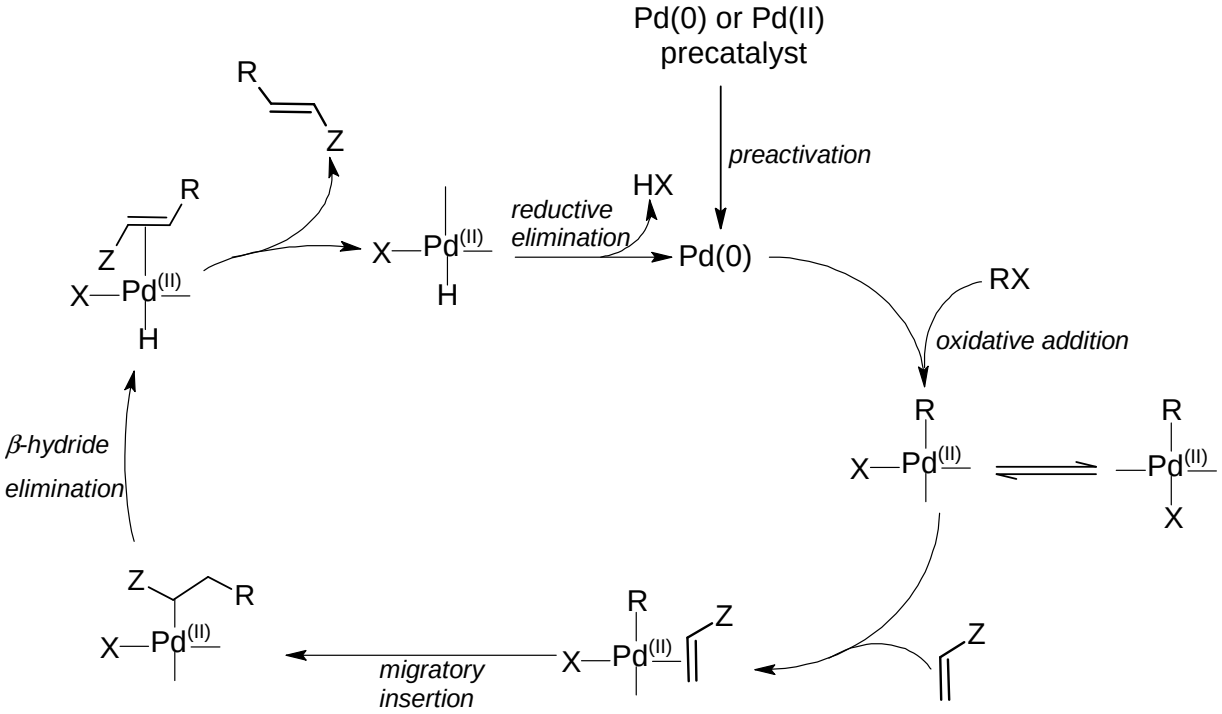

Scheme 4.2 A general catalytic cycle for the Heck coupling of aryl halides and olefins.[6]

The migratory insertion step requires the formation of a vacant coordination site for the incoming olefin. This may be accomplished by two routes. The first route involves the loss of a neutral ligand, typically a phosphine. The second route involves the loss of an ionic ligand.[17-18] For complexes bearing monodentate phosphine ligands the possibility exists for the migratory insertion step to proceed via both routes. This step results in the formation of a new C-C bond and the observed regioselectivity stems from this step. It has been found that

the C-C bond formation may proceed via electrophilic addition in which RPdX and RPd^+ intermediates attack the double bond or via an SN_2-type mechanism, where RPdX and RPd^+ intermediates are added to the olefin double bond in a concerted process. The regioselectivity of the Heck reaction has been shown to be strongly influenced by the nature of the phosphine ligand (mono- or bidentate) and by subsequent chelate ring formation upon coordination of the bidentate phosphine ligand.[19-24]

The β-hydride elimination step yields the coupling product and a Pd-hydride species. Theoretical calculations have revealed that β-hydride elimination occurs via *syn*-elimination and proceeds via an agostic interaction.[25-26] The *syn*-elimination process further directs the observed stereoselectivity of the Heck reaction, with predominant formation of the *E*-isomer as the coupling product. The presence of base serves as a scavenger fulfilling the dual role of generating the catalytically active species and preventing the readdition of the double bond of the coupling product to the Pd-hydride species. The reductive elimination step regenerates the catalytically active Pd(0) species with release of HX.

4.2.2 Application of palladium metallodendrimers in Heck coupling.

Krishna *et. al.* immobilised $Pd(COD)_2Cl_2$ (COD = 1,5-cyclooctadiene) on the periphery of phosphine-functionalised poly(ether imine) dendrimers (Fig 4.1).[27]

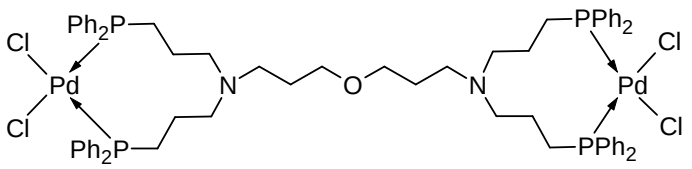

Fig. 4.1 1st generation palladium metallodendrimers derived from phosphine-functionalised poly(ether imine) dendrimers.[27]

Dendritic complexes, up to the third generation, were prepared and evaluated in the Heck coupling of iodobenzene and a variety of olefinic substrates. A negative dendritic effect on conversion was observed when going to successively higher generations. However, the dendritic catalysts displayed slightly higher activity in comparison to the mononuclear analogue.

The group of Caminade and Majoral reported the preparation of G1 and G3 triphosphazene-cored dendrimers bearing tyramine and L-tyrosine methyl ester diphosphine end groups (Fig 4.2).[28] The peripherally modified dendrimers were evaluated *in situ* as ligands in the Heck coupling of iodobenzene and styrene, forming *E*-stilbene. A negative dendritic effect on conversion was observed. Furthermore, the tyramine derivatives displayed greater efficiency in catalysis than their L-tyrosine methyl ester analogues. Both these observations were attributed to local and general steric hindrance of the catalytic sites by the peripheral units of the dendrimer.

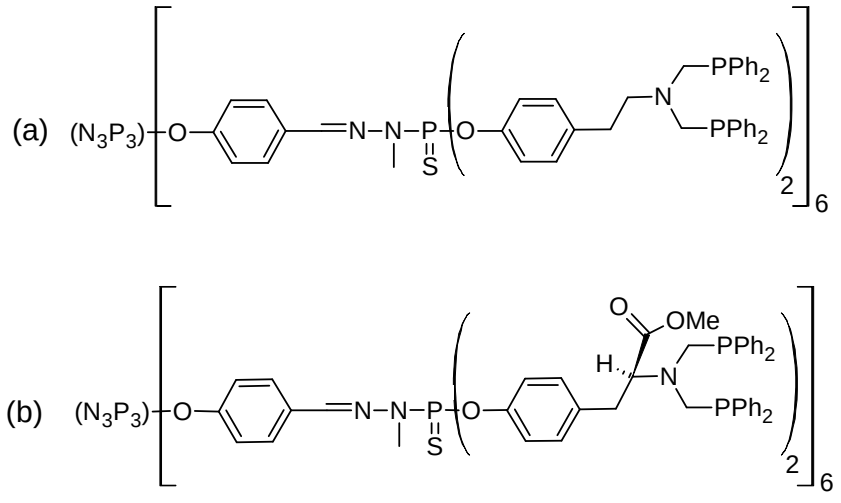

Fig. 4.2 Trisphosphazene dendrimers bearing peripheral (a) tyramine and (b) L-tyrosine methyl ester phosphine endgroups.[28]

Jayamurugan *et. al.* reported the preparation of poly(ether imine) dendrimers which were peripherally modified with bis(diphenylphosphinomethyl)amine moieties.[29] Complexation of $Pd(COD)Cl_2$ to the dendrimer periphery allowed for the isolation of palladium metallodendrimers, up to the second dendrimer generation (Fig. 4.3). The palladium metallodendrimers were evaluated as catalyst precursors in the Heck coupling of iodobenzene and *tert*-butyl acrylate in the presence of Cs_2CO_3 and 1,4-dioxane as solvent. High conversions were obtained for all the evaluated catalysts. In addition, a positive dendritic effect was noted with increasing dendrimer generation. The observed dendritic effect was attributed to an increase in the number of localised catalytic sites upon increasing dendrimer generation. Furthermore, the dendritic catalysts could be recovered almost quantitatively although no attempts were made to reuse the recovered catalysts.

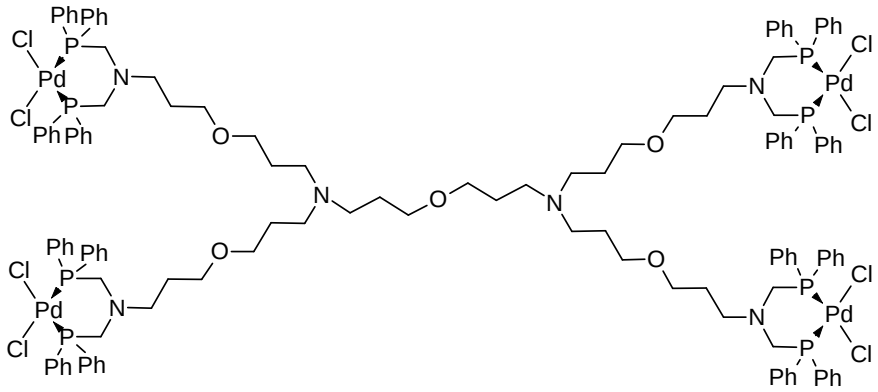

Fig. 4.3 1st generation poly(ether imine) dendrimer bearing bis(diphenylphosphinomethyl)aminato Pd(II) complexes at the periphery.[29]

In this section we report the application of mononuclear palladacycles and 1st generation palladium metallodendrimers in the Heck coupling of iodobenzene and 1-octene.

4.2.3 Results and discussion: Heck coupling of iodobenzene and 1-octene.

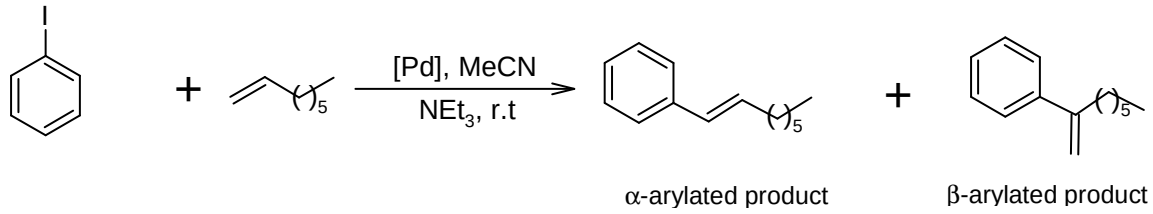

Scheme 4.3 A general scheme for the Heck coupling of iodobenzene and 1-octene.

The mononuclear palladacycles, **C5**-**C8**, and the 1st generation Pd(II) metallodendrimers, **DC1**-**DC4**, were evaluated as catalyst precursors in the Heck coupling of iodobenzene and 1-octene (Scheme 4.3). The reaction conditions employed were based on a previously reported protocol.[30] The conversion was determined by GC-FID analysis with *o*-xylene as internal standard by monitoring the consumption of iodobenzene as a function of time.

4.2.4 Heck coupling catalysed by mononuclear palladacycles, C5-C8

The mononuclear palladacycles, **C5**-**C8** (Fig. 4.4), were found to be active catalysts in the Heck coupling of iodobenzene and 1-octene forming *E*-1-(oct-1-enyl)benzene (α-arylated product) and 1-(oct-1-en-2yl)benzene (β-arylated product).

The activity of the catalysts was observed to increase as a function of time with the highest conversion of 88 % observed for the 2-bromo substituted palladacycle, **C8** (Fig. 4.5). The catalytic activity of the palladacycles was compared to that of the palladium precursor in the absence of imine ligand, $(MeCN)_2PdCl_2$, and for all cases the activity of the mononuclear palladacycles exceeded that of the palladium salt. A number of conclusions can be drawn from the closer inspection of Fig. 4.5.

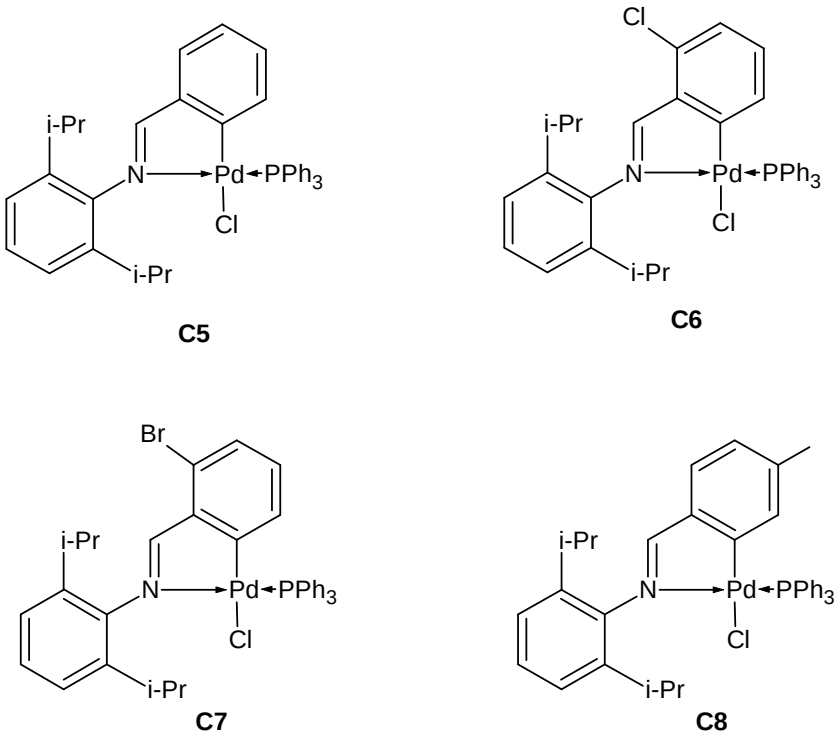

Fig. 4.4 A schematic representation of the mononuclear palladacycles, **C5-C8**.

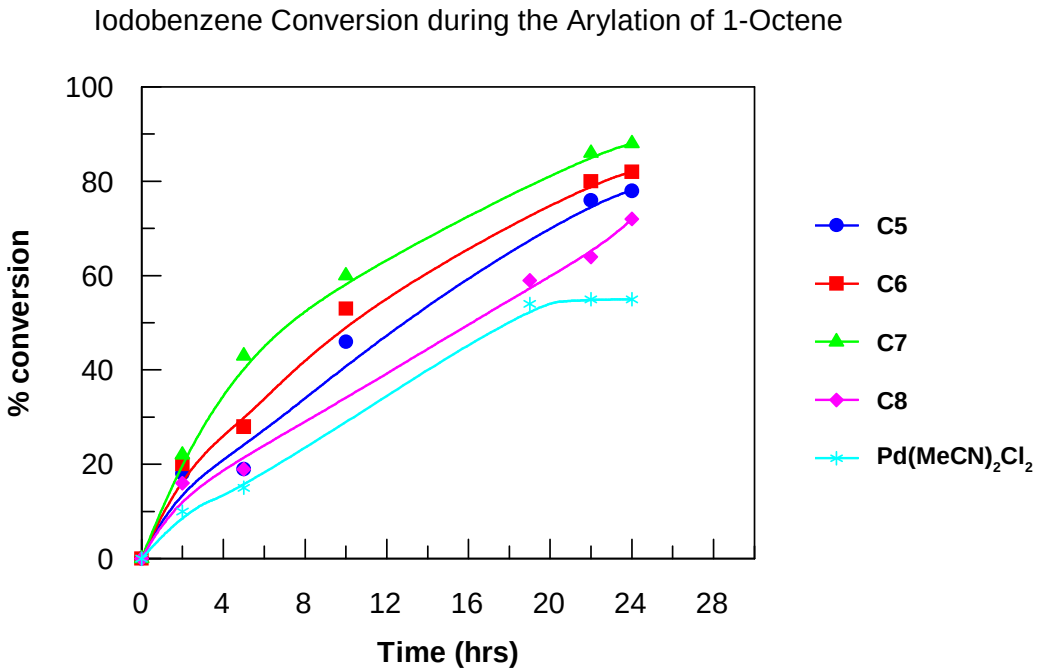

Fig. 4.5 Plot of conversion as a function of time for the arylation of 1-octene.

Firstly, for the mononuclear palladacycles an induction period of approximately 1 hour was observed in which the reaction mixture underwent a colour change from pale-yellow to deep-red. Amatore and co-workers studied the kinetics of palladium reduction in phosphine-assisted systems i.e. a palladium salt and triphenylphosphine.[31-32] They found that Pd(II) was readily reduced to Pd(0) by the phosphine ligand and that the rate-determining step in the process was the intramolecular reduction of Pd(II) by triphenylphosphine via an inner sphere atom transfer. Furthermore, they evaluated the effect of triethylamine as base on the reduction process and observed a significant reduction in the rate of formation of Pd(0) species when triethylamine was present in large excess. The catalyst system evaluated in this study contained no additional free phosphine thus the induction period may be attributed to the formation of catalytically active Pd(0) species via base reduction which is significantly slower than that observe for phosphine-assisted systems.

The conversion of iodobenzene also showed a sigmoidal S-shape curve for **C5-C8** and $(MeCN)_2PdCl_2$ which had been previously observed for PCP-palladacycles in which preactivation was observed.[33] Chen and co-workers evaluated analogous palladacycles in the Suzuki coupling of phenylboronic acid and a variety of aryl halides.[34] During the course of their reactions they observed the formation of palladium nanoparticles which were characterised by transmission electron microscopy (TEM). It is most probable that the catalytically active species present in our study are palladium nanoparticles. Also, it is well-known that palladacycles serve as a reservoir for catalytically active palladium nanoparticles.[15]

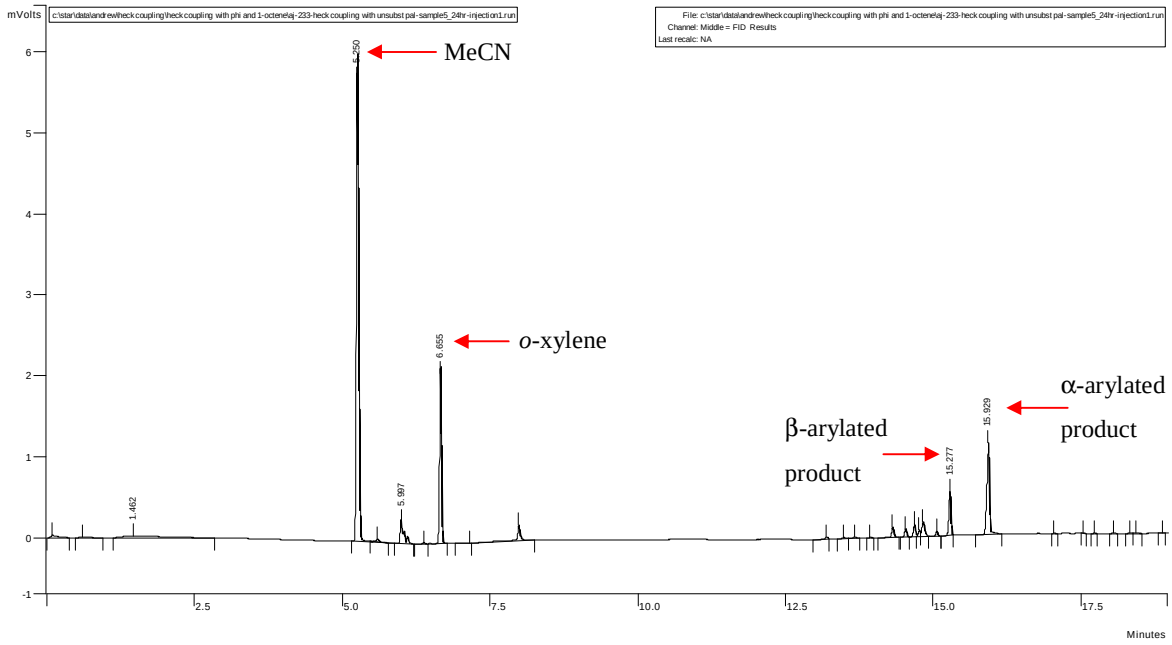

Fig. 4.6 GC-chromatogram of the arylation of 1-octene, after 24 hrs, catalysed by complex **C5**.

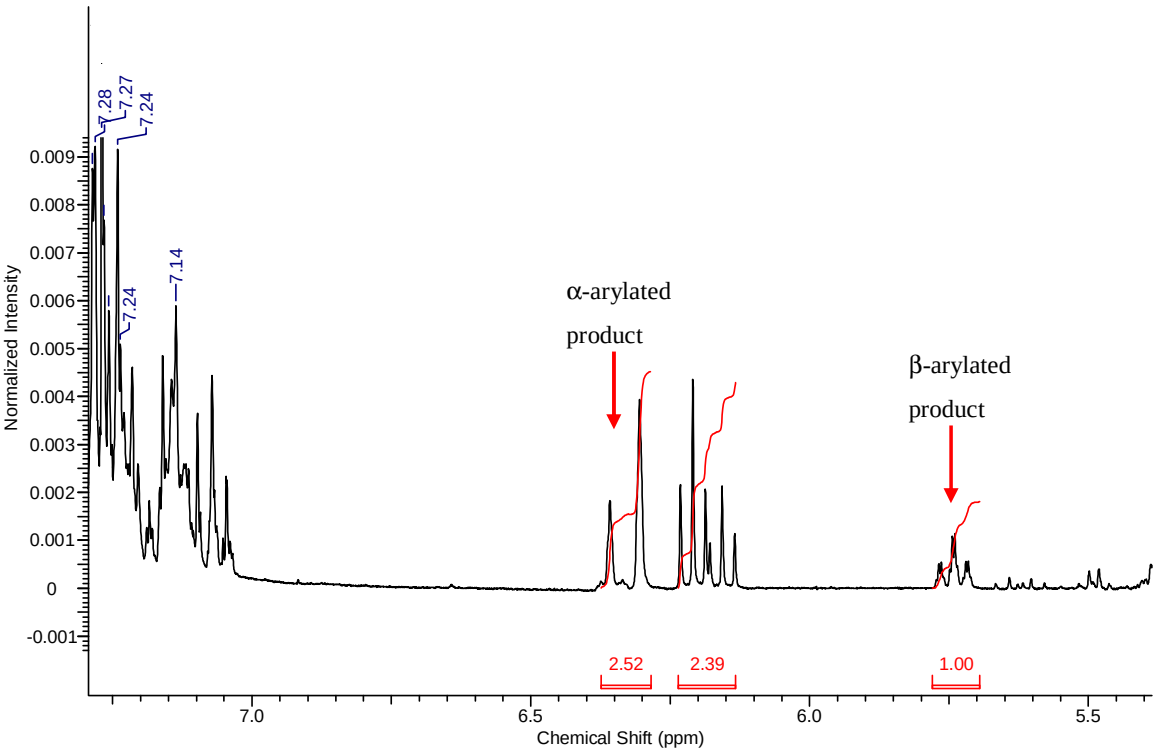

Fig. 4.7 ^{1}H NMR spectrum of the crude product of arylation of 1-octene, after 24hrs, catalysed by complex **C5**.

The catalytic activity for the series of mononuclear palladacycles may be arranged in decreasing order:

C7 > **C6** > **C5** > **C8**

The increased catalytic activity for complexes **C7** and **C6** was attributed to their increased thermal stability in comparison to complex **C5** and **C8** (see Chapter 2). The thermal stability may be arranged in decreasing order:

C7 > **C6** > **C5** > **C8**

Thus under the employed reaction conditions the agglomeration and deactivation of Pd(0) particles occurs at a slower rate for complexes **C7** and **C6**, and allows for the observed increase in catalytic efficiency.

The mononuclear palladacycles catalysed the arylation of 1-octene with significant selectivity for the α-arylated product (Fig. 4.6). The regioselectivity of the reaction was determined by ^{1}H NMR spectroscopy.

Regardless of the catalyst precursor i.e. **C5**-**C8**, the same regioselectivity of approximately 67 % for the α-arylated product was observed (Fig. 4.7) suggesting the same catalytically active species. For mono-phosphine systems the selective formation of the α-arylated product had been observed previously.[6] Of significance was the fact that the observed regioselectivity was greater than that reported for pyridyliminato Pd(II) complexes.[30]

4.2.5 Heck coupling catalysed by Pd(II) metallodendrimers, DC1-DC4.

The 1st generation benzylaldiminato Pd(II) metallodendrimers, **DC1**-**DC4** (Fig. 4.8), were found to be highly active catalysts for the Heck coupling of iodobenzene and 1-octene forming *E*-1-(oct-1-enyl)benzene (α-arylated product) and 1-(oct-1-eny-2yl)benzene (β-arylated product).

Quantitative conversion of iodobenzene was observed after 20 hrs of reaction for all the dendritic catalysts evaluated and demonstrated the increased catalytic efficiency of the palladium metallodendrimers in comparison to the mononuclear palladacycles (Fig. 4.9).

No significant induction period for catalysis was observed (Fig. 4.9) as evidenced by a colour change from pale-yellow to deep-red within ten minutes after commencing the reaction. The steric effect was found to be much less pronounced for the palladium metallodendrimers, in comparison to the mononuclear palladacycles. The lack of an induction period was further evidenced by the iodobenzene conversion exceeding 70 % within 2 hours of reaction. The effect of catalyst support i.e. monofunctional ligands versus dendrimer ligand became apparent in that the dendrimer provided increased stability toward the catalytically active Pd(0) species. For the dendritic complexes, **DC1**-**DC4**, the formation of metallic palladium was observed which, combined with the high catalytic activity of these complexes allowed for the inference that the catalytically active species may be dendrimer encapsulated nanoparticles. However, no attempts at catalyst recovery and recycling were made. Thus the dendrimer ligand stabilises the ensuing palladium nanoparticles and prevents particle agglomeration and subsequent deactivation to a greater extent than that observed for the mononuclear palladacycles. This may be a reason for the significant difference in catalytic activity.

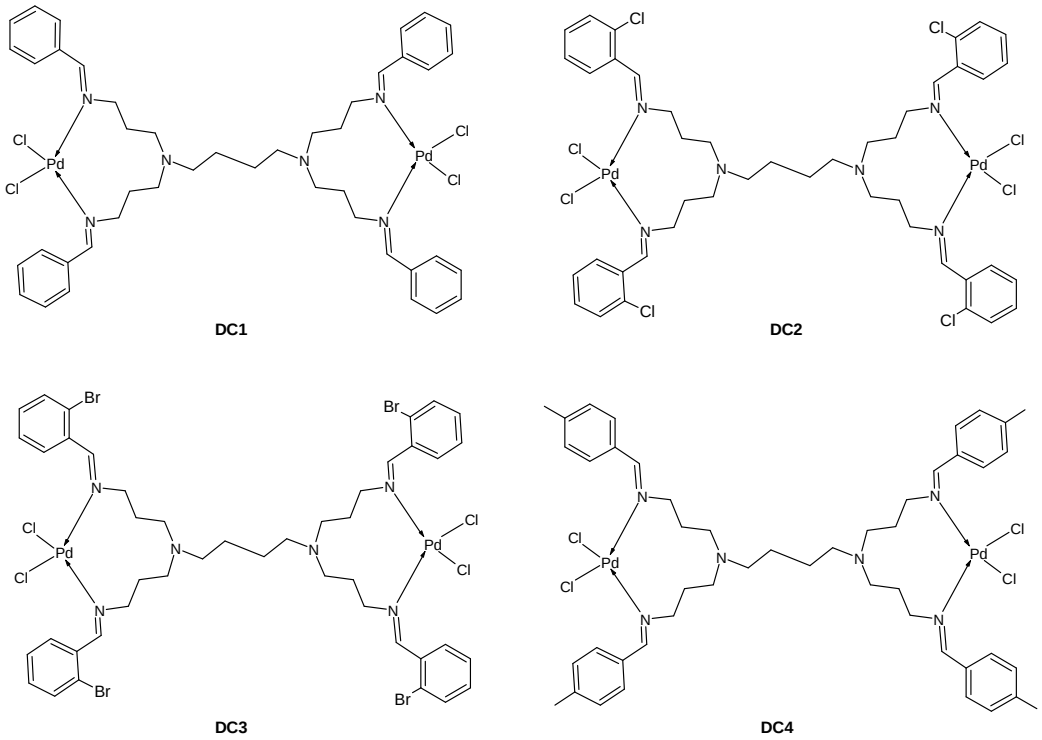

Fig. 4.8 A schematic representation of the benzylaldiminato Pd(II) metallodendrimers evaluated in the arylation of 1-octene.

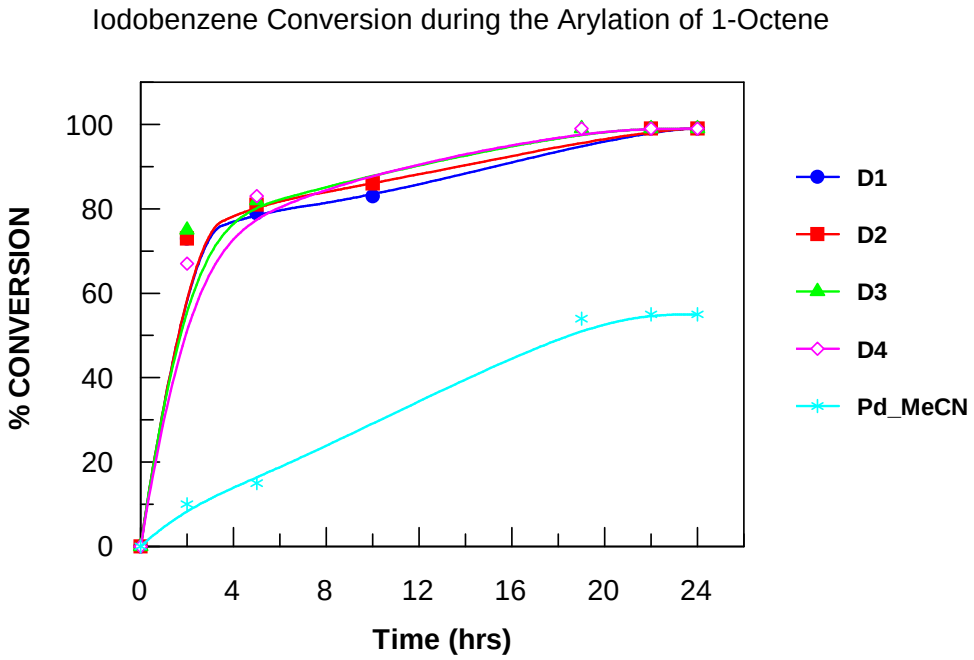

Fig. 4.9 Plot of conversion as a function of time for the arylation of 1-octene.

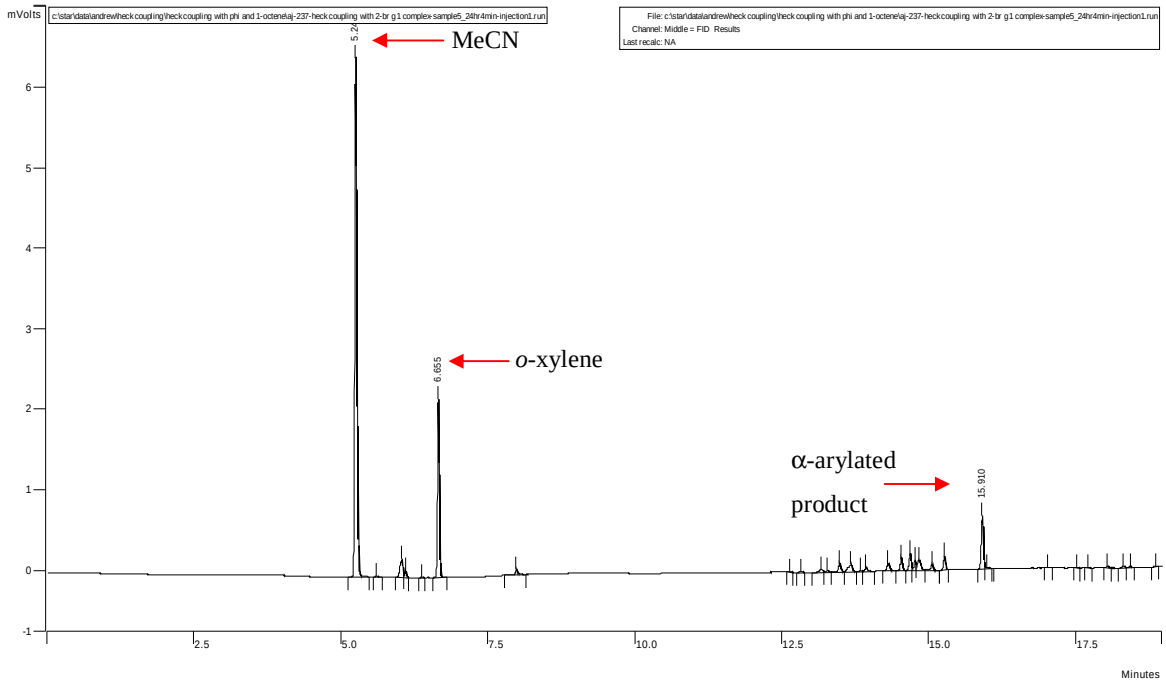

Fig. 4.10 GC-chromatogram of the arylation of 1-octene, after 24 hrs, catalysed by complex **C7**.

The selective formation of the α-arylated product was observed in all cases and displayed higher selectivity for this regioisomer than was observed for the mononuclear palladacycles (Fig. 4.10). The regioselectivity of the arylation of 1-octene catalysed by the Pd(II) metallodendrimers, **DC1-DC4**, was determined by ^{1}H NMR spectroscopy (Fig. 4.11). The observed regioselectivity was the same for all dendritic complexes evaluated.

The enhanced regioselectivity may be attributed to the absence of tertiary phosphine when employing the palladium metallodendrimers as catalysts. Seminal work by Cabri and co-workers demonstrated that employing bis-chelating tertiary phosphine ligands in the Heck reaction of aryl triflates and α-olefins, particularly 1,3-bis(diphenylphosphino)propane, resulted in the regioselective isolation of β-arylated products. This observation was attributed to the size of the chelate ring formed when employing this phosphine as ligand.[18-23] Furthermore, they observed that the regiodiscrimination is much less pronounced when

employing monodentate phosphine ligands, and that the preferential formation of the α-arylated product prevails.

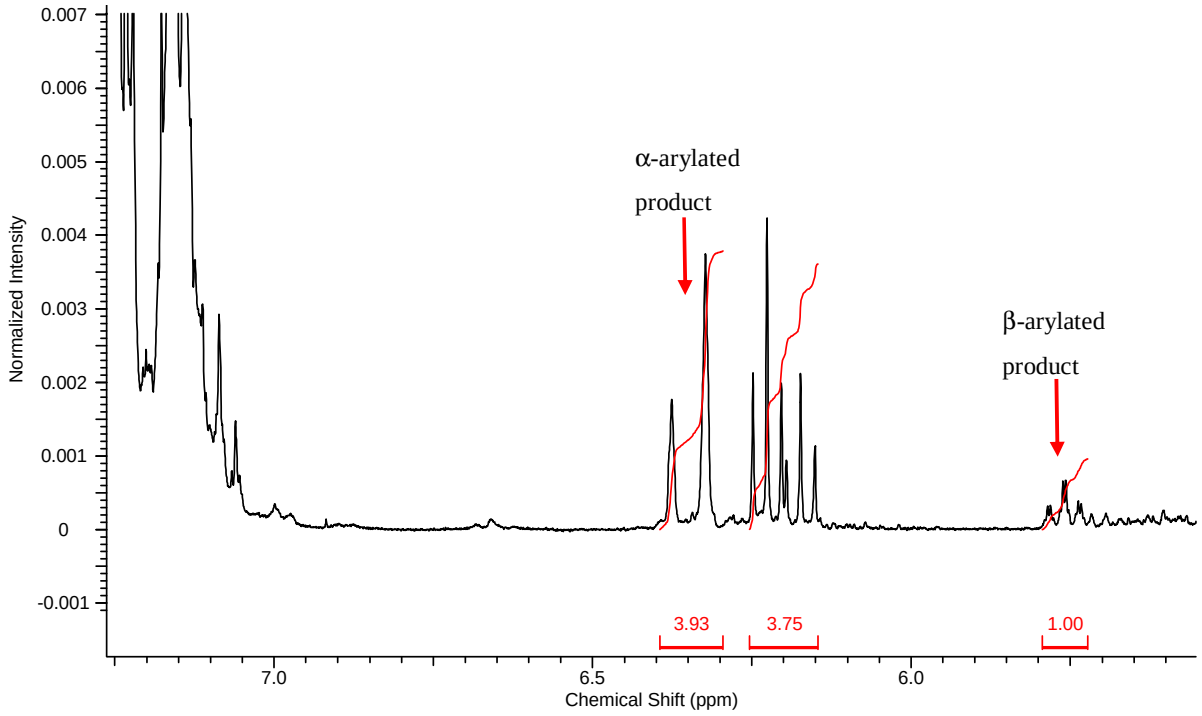

Fig. 4.11 ^{1}H NMR spectrum of crude product of arylation of 1-octene, after 24 hrs, catalysed by complex **C7**.

On the basis of these results the increase in regioselective formation of the α-arylated product when employing palladium metallodendrimers, can be rationalised by the absence of monodentate phosphine. Conversely, the lower regioselective formation of the α-arylated product when employing mononuclear palladacycles may be rationalised by the presence of monodentate phosphine, albeit in catalytic amounts.

4.3 Isomerisation of α-olefins.

The chemistry of olefins has always occupied centre stage in all branches of chemistry due to their presence as key structural features in polymeric materials through to natural products. The ease of chemical transformation of C-C double bonds has expanded the field of organic chemistry. Their substrate applicability is evidenced by the award of a number of Nobel Prizes in Chemistry for the chemical transformation of olefinic substrates.

The isomerisation of olefins, via interconversion of *E*- and *Z*-alkenes, provides a means of placing an unsaturation (C=C) in a predefined position without loss of stereochemical control.[35] Traditionally the selective isomerisation of terminal alkenes to 2-alkenes have been mediated by ruthenium complexes.[36-38] In recent years there have been a number of reports of palladium complexes which catalyse this transformation. A few examples will be discussed below.

4.3.1 Isomerisation of α-olefins catalysed by palladium complexes.

RajanBabu and co-workers reported the application of Ni(II) and Pd(II) salts of the type $[(allyl)MX]_2$ (M = Ni, Pd; X = Br, Cl) as catalysts in the isomerisation of mono- and 2,2'-disubstituted alkenes.[39] The palladium salt, in the presence of tri-(*o*-tolyl)-phosphine and silver triflate, was observed to be more catalytically efficient than the Ni-system and could facilitate the isomerisation of a wide range of allylic substrates. In general the observed *E*:*Z* selectivity was very low and sterically demanding substrates failed to undergo isomerisation. They proposed that the active species in the catalytic cycles was a metal hydride species (Fig. 4.12) and that alkene insertion was followed by β-hydride elimination under thermodynamic control. This also explained the propensity, albeit slight, for the formation of the *E*-isomer.

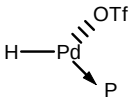

Fig. 4.12 A schematic representation of the proposed active species in the isomerisation of alkenes.[39]

Gauthier *et. al.* reported the application of a catalyst system derived from $Pd(dba)_2$, $P(^tBu)_3$ and *iso*-butyryl chloride (1:1:1 ratio) in the isomerisation of a variety of olefins. Internal olefins (*Z*-isomers) were observed to isomerise to their *E*-isomers and terminal olefins underwent selective isomerisation to 2-alkenes with a significant propensity for the formation of the *E*-isomers. The substrate scope encompassed allylbenzenes, heteroatom-substituted allyl groups bearing various functional groups as well as homoallylic alcohols and amines. It was found that the catalytically active species was a sterically bulky Pd(II)-hydride species (Fig. 4.13, **a**) with the catalytic activity being enhanced by bulky monodentate phosphine ligands capable of forming tricoordinate Pd(II) complexes.

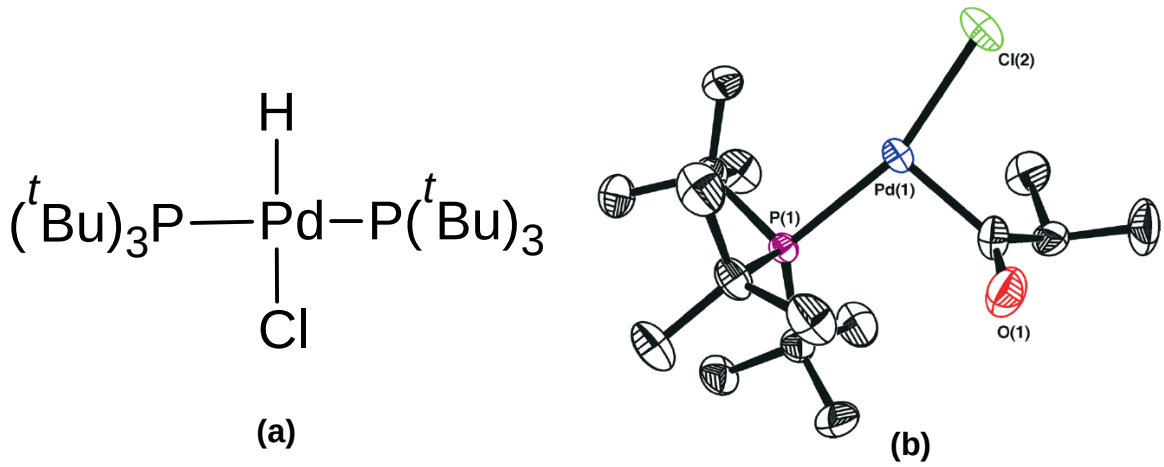

Fig. 4.13 The catalytically active Pd(II)-hydride species (**a**) and the tricoordinated acylpalladium(II) complex (**b**).

Mechanistic studies also revealed the formation of a tricoordinated acylpalladium(II) complex (Fig. 4.13, **b**) which is related to the catalytically active Pd(II)-hydride species.

4.3.2 Results and Discussion: Isomerisation of 1-hexene, catalysed by mononuclear palladacycles, C5-C8.

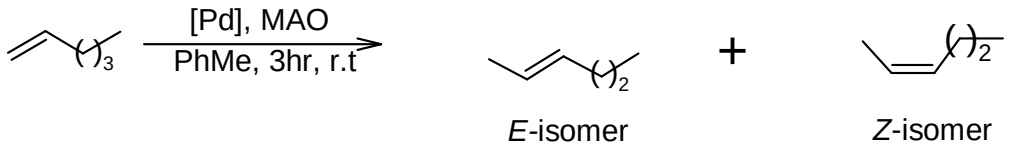

Scheme 4.4 A general scheme for the isomerisation of 1-hexene, catalysed by mononuclear palladacycles.

The mononuclear palladacycles, **C5-C8** (Scheme 4.4), were evaluated as catalyst precursors in the presence of methyl aluminoxane (MAO) in the isomerisation of 1-hexene (Fig. 4.14). A series of optimisation runs, employing complex **C5**, were performed in an attempt to increase both activity and selectivity (Table 4.1)

Table 4.1 Series of optimisation runs performed, for the isomerisation of 1-hexene employing complex **C5**.

Entry	mol Pd (%)	Substrate (mol)	Total Vol (ml)	Al:Pd	Time (hrs)	Conversion (%)[a]	Selectivity (%)[b]	
							E-isomer	*Z*-isomer
1	0.10	9.55	10	50:1	3	43	75	25
2	0.10	9.55	10	50:1	24	43	74	26
3	0.10	9.55	10	100:1	3	73	73	27
4	0.10	19.1	10	50:1	3	46	76	24
5	0.20	9.55	10	50:1	3	79	76	24

[a] Determined by GC-FID analysis of sample with *o*-xylene as internal standard. [b] Each isomer was identified by injection of a pure sample.

The base reaction showed 43 % conversion of 1-hexene (Entry 1) with a selectivity of 75 % for the formation of the *E*-isomer. Extending the reaction (Entry 2) had no affect on conversion or selectivity. Increasing the amount of co-catalyst (Entry 3) resulted in an

increase in conversion to 73 %. An increase in substrate concentration (Entry 4) had a negligible effect on both conversion and selectivity. An increase in catalyst concentration (Entry 5) showed the highest conversion and these reaction conditions were employed to evaluate complexes, **C6-C8**.

The mononuclear palladacycles in the presence of MAO were efficient catalysts for the isomerisation of 1-hexene as determined by GC-FID analysis of the reaction mixture employing *o*-xylene as internal standard (Fig. 4.14). The 2-alkene isomers were identified by injecting pure samples of *cis*- and *trans*-2-hexene.

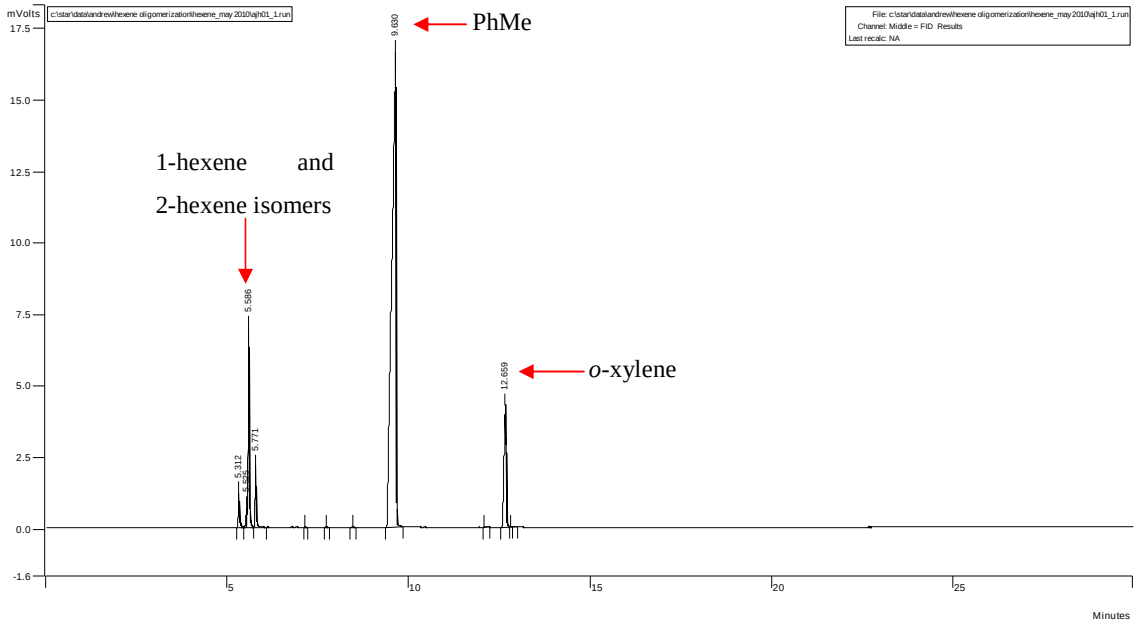

Fig. 4.14 GC-chromatogram of the reaction mixture, after 3hrs, during the isomerisation of 1-hexene catalysed by complex **C5**.

The activity and selectivity of the mononuclear palladacycles, **C5-C8**, in the isomerisation of 1-hexene are shown in Fig. 4.15. The catalyst precursors may be arranged in decreasing order of activity:

C7 > **C6** > **C5** > **C8**

As was observed for the Heck coupling reaction, the difference in catalytic activity may be attributed to increased stability of the mononuclear palladacycles bearing halogen substituents in the 2-position:

2-Br > **2-Cl** > **H** > **4-Me**

It should be noted that regardless of the catalyst precursor no significant change in the selectivity of the catalytic systems were observed. This may be attributed to the thermodynamic stability associated with the *E*-isomer. This observation also suggested that the catalytically active species was the same in all cases.

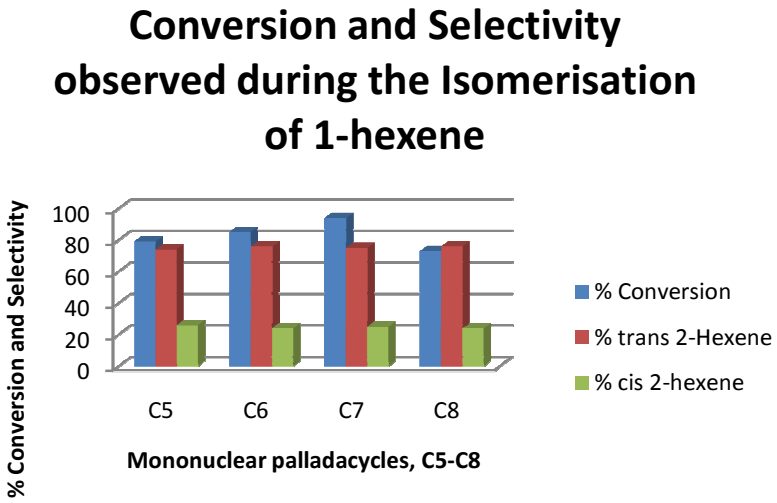

Fig. 4.15 A plot of the observed conversion and selectivity for the isomerisation of 1-hexene, employing complexes **C5**-**C8** as catalyst precursors.

Nozaki and co-workers reported experimental and theoretical studies of ethylene polymerisation reactions catalysed by palladium phosphine-sulphonate complexes in the

absence of a co-catalyst.[40] During the course of their investigations it was observed that the methylpalladium complex (Fig. 4.16) facilitated the isomerisation of 1-hexene in the absence of ethylene (when complex and olefin was placed in an NMR tube). Furthermore, the formation of a Pd-hexyl complex was also observed by $^{31}\{^{1}H\}$ NMR spectroscopy.

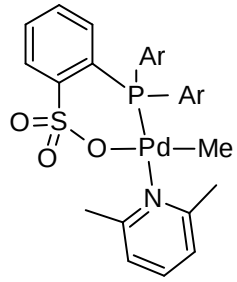

Ar: *o*-$MeOC_6H_4$

Fig. 4.16 The methylpalladium complex which facilitates the isomerisation of 1-hexene in the absence of ethylene.[40]

DFT studies showed that, in the absence of ethylene, the isomerisation reaction may be catalysed by a Pd(olefin)-hydride species formed during the polymerisation process. On the basis of these results it is possible that the catalytically active species which facilitated the isomerisation of 1-hexene in our study is a Pd-hydride species which formed from a Pd-alkyl complex, generated by activation of the catalyst precursor with MAO.

A plausible catalytic cycle for the isomerisation of 1-hexene is given in Scheme 4.5. The Pd-hydride species is formed bearing a vacant coordination site and subsequent olefin coordination and 1,2-insertion occurs as the kinetically controlled step. A 1-hexyl Pd complex is formed which undergoes thermodynamically controlled isomerisation to the 2-hexyl Pd complex (where 1- and 2- denotes the C-atom to which palladium is bound).

C2-C3 bond rotation forms both *E*- and *Z*-hexyl isomeric palladium complexes, with preferential formation of the *E*-form. Subsequent β-hydride elimination generates the (olefin)Pd-hydride species. Olefin dissociation results in the formation of the catalytically active Pd-hydride species.

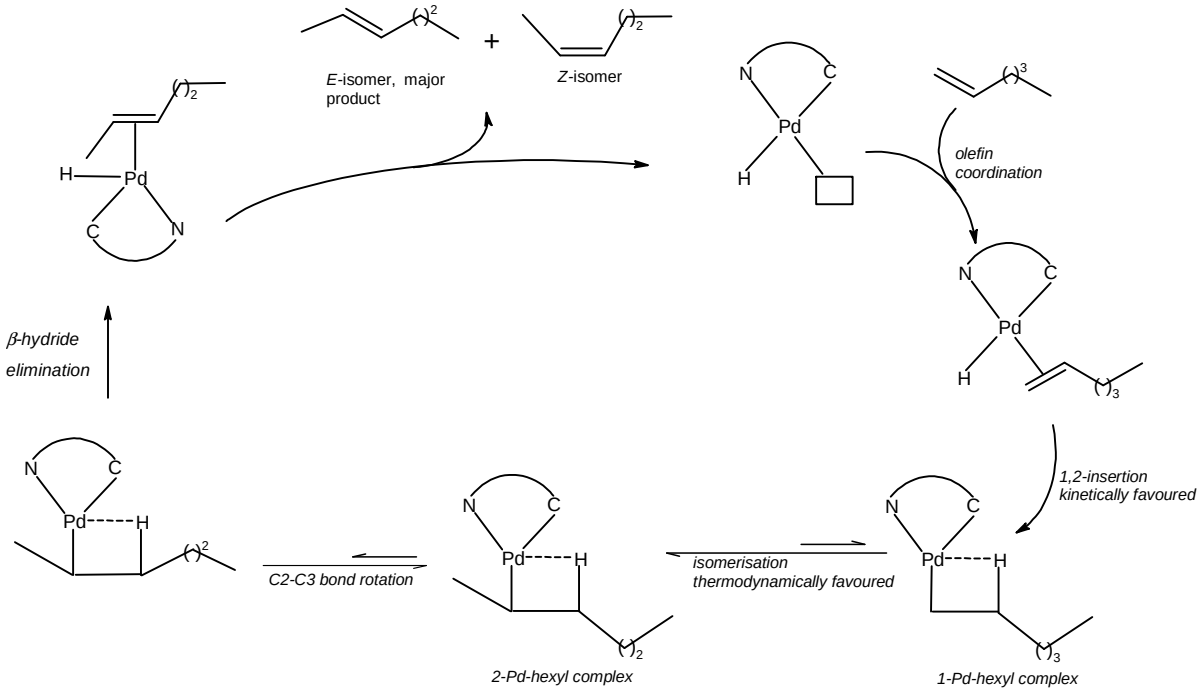

Scheme 4.5 A plausible catalytic cycle for the isomerisation of 1-hexene, catalysed by a Pd(II)-hydride species.[41]

4.4 Conclusions.

Both mononuclear palladacycles and palladium metallodendrimers were applied as catalyst precursors in the Heck coupling of iodobenzene and 1-octene. The dendritic catalysts displayed greater catalytic efficiency than the mononuclear palladacycles, both in activity and selectivity. The 2-Br palladacycle, complex **C7**, displayed the highest activity which was attributed to increased thermal stability of the halogen-bearing complexes. The effect of

thermal stability was less pronounced in the dendritic complexes. Observations made during the catalytic reaction suggest that the active species, for both types of catalyst precursors, may be palladium nanoparticles.

The mononuclear palladacycles, **C5-C8**, in the presence of MAO as activator effectively catalysed the isomerisation of 1-hexene to *E*- and *Z*-2-hexene with a propensity for the formation of the *E*-isomer. Again, the effect of thermal stability on conversion was observed, with complex **C7**, showing the highest conversion under the employed reaction conditions. Based on previous reports on palladium-catalysed alkene isomerisation reactions, the catalytically active species in this reaction was postulated to be a Pd(II)-hydride species. A plausible catalytic cycle was presented.

4.5 Materials and Methods

Catalytic runs were performed using a 12-place high temperature parallel reactor equipped with a cooling system or by employing standard Schlenk line techniques under an inert atmosphere of nitrogen. All solvents employed in the isomerisation reactions were distilled prior to use and all other reagents were employed as received. ^{1}H NMR (300 and 400 MHz) spectra were recorded on Varian VNMRS (300 MHz) and Varian Unity Inova (400 MHz) spectrometers and reported in δ ppm values. Proton resonances were referenced relative to the residual protons of the deuterated solvent and tetramethyl silane as internal standard. GC analysis was performed on a Varian CP-3800 instrument equipped with a flame ionisation detector (FID) and an Agilent HP-PONA column (50 m x 0.20 mm x 0.50 μm). The internal standard employed for all analyses was *o*-xylene.

4.5.1 General procedure for the Heck coupling of iodobenzene and 1-octene.

To a slurry of the requisite amount of palladium catalyst precursor (normalised to 1 mol % Pd regardless of precursor) in acetonitrile (10 ml) was added iodobenzene (10 mmol), triethylamine (10 mmol) and 1-octene (10 mmol). The reaction mixture was stirred while heating at 90 °C. Samples of approximately 1.5 ml were withdrawn periodically, filtered through 45 μm syringe filters (Anatech) and analysed by GC-FID. The conversion of iodobenzene was calculated based on *o*-xylene as internal standard.

4.5.2 General procedure for the isomerisation of 1-hexene, employing complexes C5-C8 as precursors.

To a stirring solution of the requisite amount of 1-hexene and catalyst precursor in toluene under an inert atmosphere, was added the requisite amount of co-catalyst. The reaction was stirred under N_2 and after the reaction period was quenched with 2M HCl solution (10ml). The organic layer was separated, dried over K_2CO_3 and filtered through 45 μm syringe filters (Anatech). A 1ml sample containing a known amount of *o*-xylene as internal standard was analysed by GC-FID. The conversion of 1-hexene was calculated based on *o*-xylene as internal standard. The selectivity was determined from the response factors of pure samples of the *E*- and *Z*-isomers.

References.

1. I. P. Beletskaya and A. V. Cheprakov, *J. Organomet. Chem.*, 2004, **689**, 4055-4082.
2. L. F. Tietze, H. Ila and H. P. Bell, *Chem. Rev.*, 2004, **104**, 3453-3516.

3. K. C. Nicolaou, P. G. Bulger and D. Sarlah, *Angew. Chem. Int. Ed.*, 2005, **44**, 4442-4489.

4. Nobelprize.org, The Nobel Prize in Chemistry 2010, http://nobelprize.org/nobel_prizes/chemistry/laureates/2010/, Accessed 22 November 2010.

5. R. F. Heck and J. P. Nolley, *J. Org. Chem.*, 1972, **37**, 2320-2322.

6. I. P. Beletskaya and A. V. Cheprakov, *Chem. Rev.*, 2000, **100**, 3009-3066.

7. A. S. Gruber, D. Pozebon, A. L. Monteiro and J. Dupont, *Tetrahedron Lett.*, 2001, **42**, 7345-7348.

8. C. S. Consorti, M. L. Zanini, S. Leal, G. Ebeling and J. Dupont, *Organic Letters*, 2003, **5**, 983-986.

9. D. E. Bergbreiter and S. Furyk, *Green Chem.*, 2004, **6**, 280-285.

10. D. E. Bergbreiter, J. Tian and C. Hongfa, *Chem. Rev.*, 2009, **109**, 530-582.

11. C. Amatore, A. Jutand and M. A. M'Barki, *Organometallics*, 1992, **11**, 3009-3013.

12. C. Amatore, E. Carre, A. Jutand and M. A. M'Barki, *Organometallics*, 1995, **14**, 1818-1826.

13. M. Ioele, G. Ortaggi, M. Scarsella and G. Sleiter, *Polyhedron*, 1991, **10**, 2475-2476.

14. F. Ozawa, A. Kubo and T. Hayashi, *Chem. Lett.*, 1992, **11**, 2177.

15. J. Dupont, C. S. Consorti and J. Spencer, *Chem. Rev.*, 2005, **105**, 2527-2572.

16. A. L. Casado and P. Espinet, *Organometallics*, 1998, **17**, 954-959.

17. F. Ozawa, A. Kubo and T. Hayashi, *J. Am. Chem. Soc.*, 1991, **113**, 1417-1419.

18. W. Cabri, I. Candiani, S. DeBernardinis, F. Francalanci, S. Penco and R. Santo, *J. Org. Chem.*, 1991, **56**, 5796-5800.

19. W. Cabri, I. Candiani, A. Bedeschi and R. Santi, *J. Org. Chem.*, 1990, **55**, 3654-3655.

20. W. Cabri, I. Candiani, A. Bedeschi and R. Santi, *Tetrahedron Lett.*, 1991, **32**, 1753-1756.

21. W. Cabri, I. Candiani, A. Bedeschi and R. Santi, *J. Org. Chem.*, 1992, **57**, 3558-3563.

22. W. Cabri, I. Candiani, A. Bedeschi, S. Penco and R. Santi, *J. Org. Chem.*, 1992, **57**, 1481-1486.

23. W. Cabri, I. Candiani, A. Bedeschi and R. Santi, *J. Org. Chem.*, 1993, **58**, 7421-7426.

24. M. Ludwig, S. Stromberg, M. Svensson and B. Akermark, *Organometallics*, 1999, **18**, 970-975.

25. K. Albert, P. Gisdakis and N. Rosch, *Organometallics*, 1998, **17**, 1608-1616.

26. R. J. Deeth, A. Smith, K. K. Hii and J. M. Brown, *Tetrahedron Lett.*, 1998, **39**, 3229-3232.

27. T. R. Krishna and N. Jayaraman, *Tetrahedron*, 2004, **60**, 10325-10334.

28. P. Servin, R. Laurent, A. Romerosa, M. Peruzzini, J.-P. Majoral and A.-M. Caminade, *Organometallics*, 2008, **27**, 2066-2073.

29. G. Jayamurugan and N. Jayaraman, *Adv. Synth. Catal.*, 2009, **351**, 2379-2390.

30. G. S. Smith and S. F. Mapolie, *J. Mol. Catal. A: Chem.*, 2004, **213**, 187-192.

31. C. Amatore and A. Jutand, *J. Organomet. Chem.*, 1999, **576**, 254-278.

32. C. Amatore and A. Jutand, *Acc. Chem. Res.*, 2000, **33**, 314-321.

33. M. R. Eberhard, *Organic Letters*, 2004, **6**, 2125-2128.

34. C.-L. Chen, Y.-H. Liu, S.-M. Peng and S.-T. Liu, *Organometallics*, 2005, **24**, 1075-1081.

35. D. Gauthier, A. T. Lindhardt, E. P. K. Olsen, J. Overgaard and T. Skrydstrup, *J. Am. Chem. Soc.*, 2010, **132**, 7998-8009.

36. B. M. Trost, F. D. Toste and A. B. Pinkerton, *Chem. Rev.*, 2001, **101**, 2067-2096.

37. B. Alcaide, P. Almendros and A. Luna, *Chem. Rev.*, 2009, **109**, 3817-3858.

38. T. J. Donohoe, T. J. C. O'Riordan and C. P. Rosa, *Angew. Chem. Int. Ed.*, 2009, **48**, 1014-1017.

39. H. J. Lim, C. R. Smith and T. V. RajanBabu, *J. Org. Chem.*, 2009, **74**, 4565-4572.

40. S. Noda, A. Nakamura, T. Kochi, L. W. Chung, K. Morokuma and K. Nozaki, *J. Am. Chem. Soc.*, 2009, **131**, 14088-14100.

41. J. Zhang, H. Gao, Z. Ke, F. Bao, F. Zhu and Q. Wu, *J. Mol. Catal. A: Chem.*, 2005, **2231**, 27-34.

Chapter 5: Conclusions and Future Prospects

5.1 General Conclusions

In summary, this thesis investigated the synthesis and catalytic applications of mono- and multinuclear palladacycles. The monofunctional benzylaldimine ligands, **L1-L4**, allowed for facile electrophilic C-H activation producing dinuclear μ-Cl palladacycles, **C1-C4**. Their reactivity toward mono- and bidentate tertiary phosphines were examined and produced the corresponding mononuclear palladacycles (**C5-C11**), non-cyclometallated palladium complexes (**C12-13**) as well as dinuclear μ-phosphine palladacycles (**C14-C20**). In all these complexes the metal centre adopted a slightly distorted square planar geometry as evidenced by SCD analysis.

An investigation into the synthesis of dendrimer-supported palladacycles was undertaken. Commercially available 1st generation DAB-PPI dendrimer was peripherally modified via Schiff base condensation producing multifunctional benzylaldimine ligands, **DL1-DL4**. An analogous synthetic method to that employed for the preparation of palladacycles, **C1-C4**, proved unsuccessful in isolating dendrimer-supported palladacycles. Upon closer inspection it was found that the starting materials and reaction conditions employed facilitated the isolation of 1st generation Pd(II) metallodendrimers, **DC1-DC4**. These metallodendrimers displayed a coordination mode in which the imine N-atom on the periphery of the dendrimer ligand coordinates to the palladium centre via two arms of the ligand. This was evidenced by a range of analytical techniques.

The mononuclear palladacycles, **C5-C8**, and 1st generation Pd(II) metallodendrimers, **DC1-DC4**, were evaluated in a comparative study as catalysts in the Heck coupling of iodobenzene and 1-octene. Both the palladacycles and metallodendrimers were efficient catalysts in this C-C coupling reaction. The Pd(II) metallodendrimers displayed significantly

higher catalytic efficiency than the mononuclear palladacycles, both in activity and selectivity. The catalytically active species was postulated to be palladium nanoparticles for both mono- and multinuclear complexes and the dendrimer support had a significant influence on the stability of the catalytically active species.

In addition, the mononuclear palladacycles, **C5-C8**, were evaluated as catalyst precursors in the isomerisation of 1-hexene. These complexes proved to be efficient catalysts in this process, after activation with MAO, with moderate activity and selectivity for the formation of *trans*-2-hexene. A mechanism was postulated involving the formation of a catalytically active Pd(II)-hydride species.

5.2 Future Prospects

A number of issues have arisen out of this study which may be addressed in future. Firstly, reaction conditions employed during the attempted synthesis of dendrimer-supported palladacycles may be appropriately modified to facilitate the isolation of the desired product. Employing $Pd(OAc)_2$ as the palladium salt may allow the electrophilic C-H activation to proceed by bringing the proton abstractor (acetate group) sufficiently close to the phenyl ring. This may serve to overcome the problems associated with the inherent flexibility of the dendritic ligand.

Secondly, even though the palladium metallodendrimers were highly efficient catalysts in the Heck coupling of iodobenzene and 1-octene, their separation and recyclability may also be investigated. Furthermore, the exact nature of the catalytically active species could be elucidated by employing appropriate microscopy techniques.

The mononuclear palladacycles were efficient catalysts, when activated with MAO, in the isomerisation of 1-hexene. The need for a co-catalyst may be circumvented by introducing a Pd-C bond, via methylation, in the coordination sphere of the palladium centre which does not form part of the metallacycle framework. Also, introducing electron-donating and withdrawing substituents at appropriate positions on the benzylidene ring may enhance both the activity and selectivity of the complexes in this catalytic process. A range of substrates may be evaluated to determine the scope and applicability of the isomerisation reaction. Mechanistic insight may be gained by employing DFT studies to identify possible catalytic intermediates and rationalise the observed catalytic activity and selectivity.

Lastly, the palladium metallodendrimers, **DC1-DC4**, may be evaluated as catalyst precursors in the oligo- and polymerisation of α-olefins and their activity and selectivity compared to that previously observed for the mononuclear palladacycles. The effect of dendrimer generation of the catalytic processes may be evaluated by preparing higher generation metallodendrimer analogues.